CALIFORNIA INSTITUTE OF TECHNOLOGY

DYNAMICS LABORATORY

TRANSMISSION MATRICES AND LUMPED PARAMETER MODELS FOR CONTINUOUS SYSTEMS

by

Richard D. Rocke

A report on research conducted under auspices of the Doctoral Fellowship Program, Hughes Aircraft Company

Pasadena, California

1966

TRANSMISSION MATRICES AND LUMPED PARAMETER MODELS FOR CONTINUOUS SYSTEMS

Thesis by

Richard Dale Rocke

In Partial Fulfillment of the Requirements
for the Degree of
Doctor of Philosophy

California Institute of Technology
Pasadena, California
1966

(Submitted May 16, 1966)

ACKNOWLEDGMENTS

The author desires to gratefully acknowledge the guidance and encouragement given by his former advisor, the late Professor C. E. Crede, during the early phases of graduate work.

The many ideas and suggestions provided by Dr. Sheldon Rubin during the entire course of this investigation have been sincerely appreciated.

The author is especially grateful to Professor D. E. Hudson, his present advisor, for the guidance, encouragement, and valuable suggestions provided during the course of this work and the preparation of this manuscript.

The author is further indebted to the Hughes Aircraft Company for the Doctoral Fellowship and other generous financial aids provided, to the California Institute of Technology, and to the National Aeronautics and Space Administration for partial support of this work under Contract No. NAS 8-2451.

No acknowledgment would be complete without the author's expressed appreciation to his wife for the understanding and sacrifices which were willingly given to make the completion of graduate work possible. Thanks, too, are given to those various colleagues who provided help during the preparation of this manuscript.

ABSTRACT

The use of transmission matrices and lumped parameter models for describing continuous systems is the subject of this study. Non-uniform continuous systems which play important roles in practical vibration problems, e.g., torsional oscillations in bars, transverse bending vibrations of beams, etc., are of primary importance.

A new approach for deriving closed form transmission matrices is applied to several classes of non-uniform continuous segments of one dimensional and beam systems. A power series expansion method is presented for determining approximate transmission matrices of any order for segments of non-uniform systems whose solutions can not be found in closed form. This direct series method is shown to give results comparable to those of the improved lumped parameter models for one dimensional systems.

Four types of lumped parameter models are evaluated on the basis of the uniform continuous one dimensional system by comparing the behavior of the frequency root errors. The lumped parameter models which are based upon a close fit to the low frequency approximation of the exact transmission matrix, at the segment level, are shown to be superior. On this basis an improved lumped parameter model is recommended for approximating non-uniform segments. This new model is compared to a uniform segment approximation and error curves are presented for systems whose areas vary quadratically and linearly. The effect of varying segment lengths is investigated for one dimensional systems and results indicate very little improvement in

comparison to the use of equal length segments. For purposes of completeness, a brief summary of various lumped parameter models and other techniques which have previously been used to approximate the uniform Bernoulli-Euler beam is given.

TABLE OF CONTENTS

NOMENCLATURE

$[A]$ = matrix $(n \times n)$ which characterizes a system

$A(x)$ = cross sectional area expressed as a function of x

A_o = cross sectional area at the input end of a segment

A_ℓ = cross sectional area at the output end of a segment

B = $N\beta$

b = width of a rectangular cross section

C = variable used to control segment lengths

C_k^i = constants in the transmission matrix for a beam $i,\ k = 1, 2, 3, 4$

c = velocity of sound

$D_i(x)$ = i^{th} differential operator with the independent variable x

$[E]$ = transmission matrix $(n \times n)$ for a uniform continuous system

E = Young's modulus

$EI(x)$ = beam bending stiffness expressed as a function of x

EI_o = beam bending stiffness at the input end of a segment

$e_{\nu N}$ = non-dimensional frequency root error for the ν^{th} mode with N segments

F = force

f = $1/\xi$

g = $1 + f$

G = shearing modulus

h = height of a rectangular cross section

i = $\sqrt{-1}$

$I_{\pm n}$ = modified Bessel function of the first kind, of order n

$J_{\pm n}$ = Bessel function of the first kind, or order n

$K_{\pm n}$ = modified Bessel function of the second kind, of order n

k_i = i^{th} spring constant

$[L]$ = transmission matrix ($n \times n$) for lumped parameter models

L = length of an element composed of N segments

ℓ = length of one segment (or increment)

$[M]$ = transmission matrix ($n \times n$) derived by power series expansion method

M = point mass (except where noted in Appendix D)

N = number of segments

n = constant for controlling cross sectional variation of beams

p = constant for controlling cross sectional area variation

r = radius of circular cross sections

$\overline{r}$ = radius of gyration

$[T]$ = transmission matrix ($n \times n$) for non-uniform continuous systems

u = rectilinear displacement

v = rectilinear velocity

$Y_{\pm n}$ = Bessel functions of the second kind, of order n

$\overline{Y}(x)$ = admittance type element in the $[A]$ matrix expressed as function of x

α = $f\beta$

β_1 = $\omega \sqrt{\rho / E}$

ϵ = matrix norm

ϵ_{ij} = error term for matrix norm

η = subdividing parameter for lumped parameter models

ξ = slope parameter

ρ = mass density

σ = stress (force/area)

$\hat{\mu}$ = $2\left(\frac{\ell}{\xi}\right)\left(\frac{g}{f}\right)^{\frac{1}{2}}\left[\frac{\rho A_o}{EI_o}\right]^{\frac{1}{4}}$

ν = mode number

ψ = state vector (column vector)

ω = circular frequency

Ω = $\ell\left[\frac{\omega^2 \rho A_o}{EI_o}\right]^{\frac{1}{4}}$

CHAPTER I

INTRODUCTION

A general theory for vibration problems involving continuous systems has existed for many years. However, the number of problems which are exactly solvable analytically is very small, e.g., uniform and some simple non-uniform systems. Therefore, other techniques, which give approximate solutions to continuous systems, have been extensively investigated. These methods provide solutions to many practical vibration problems which do not fit into the category of being exactly solvable.

One method, which has been especially emphasized since the advent of large computers, is the lumped parameter approximation whereby the continuum is replaced by a finite N degree of freedom system composed of lumped elements, i.e., massless springs, point masses, etc. This technique was first applied by Lagrange[1] and Rayleigh[2] in studying the vibrating string. Duncan[3], using a lumped parameter model attributed to Lagrange, was one of the first to study the behavior of errors resulting from lumped parameter approximations. Livesley[4], Gladwell[5], and others[6,7,8] have evaluated lumped parameter approximations of uniform continuous beams using many different models.

Transmission matrices, which have been applied to mechanical vibration problems only in recent years, provide another approach for describing continuous systems in either an exact or approximate manner. The earliest application of this method was the steady state

description of four terminal electrical networks in which case the method is commonly designated "four pole parameters". Molloy[9] was one of the first to systematically apply four pole parameters to acoustical, mechanical, and electromechanical vibration problems. Pestel and Leckie[10] have catalogued transmission matrices for uniform elastomechanical elements up to twelfth order. Rubin[11] has extended the application of transmission matrices through a completely general treatment.

1.1 Contents of Thesis

The objective of the present study is to investigate more thoroughly several aspects of the application of lumped parameter and transmission matrix approaches to vibration problems, in particular, those problems which involve non-uniform continuous systems.

In Chapter II transmission matrices and their derivation are briefly discussed.

One dimensional systems are treated in Chapter III. Results from this chapter can be applied to the following practical problems: acoustical oscillations in air conditioning ducts, torsional oscillations in gear trains, propagating wave effects in vibration isolators, and longitudinal vibration of shell sections in missiles. A recent example of the last problem is the unstable oscillation resulting from interaction between a longitudinal structure mode of vibration and the propulsion system which occurred in several Gemini missile

flights[12]. Models based on the one dimensional wave equation similar to those to be treated in Chapter III were used to describe structural components and fluid lines in the analysis of this missile vibration problem.

Chapter III also contains a presentation of transmission matrices for three classes of non-uniform continuous cross sections and the transmission matrix technique is used to evaluate the error behavior of four types of lumped parameter models used to approximate the uniform continuous system. A new lumped parameter model is proposed for non-uniform systems and for one particular case, the linear taper model, the lumped parameters are defined. In addition, the effect of varying segment lengths is studied.

Chapter IV includes a summary of various lumped parameter models which have been used to approximate uniform beams. Transmission matrices for three groups of non-uniform continuous beams are derived.

A power series expansion method for obtaining transmission matrices which are low frequency approximations for non-uniform continuous systems of any order is presented in Chapter V.

Finally a summary of the work presented herein, and appropriate conclusions are contained in Chapter VI.

CHAPTER II

TRANSMISSION MATRICES

2.1 Description

The transmission matrix describes the manner in which sinusoidal forces and motions are transmitted through a linear elastic element during steady state conditions. All consideration of the differential equations describing the element is contained within the derivation of the transmission matrix and the approach is equally applicable to lumped parameter or continuous systems.

A general transmission element is shown in Fig. 2.1.1. The state vector, denoted by ψ, is a column vector consisting of forces and velocities or displacements. The transmission matrix relates the state vector at the input to that at the output of the element. The form of the transmission matrix which will be used herein is:

$$\{\psi\}_{input} = [T]\{\psi\}_{output} \qquad (2.1.1)$$

where $[T]$ is commonly designated the "forward transmission matrix". The sign convention to be used, see arrows in Fig. 2.1.1, has positive directions for forces applied by the output the same as those for forces applied to the input.

When a line of elements or segments are in an end-to-end or chain like arrangement, which is the situation for which this approach is best suited, the transmission matrices for the individual segment are:

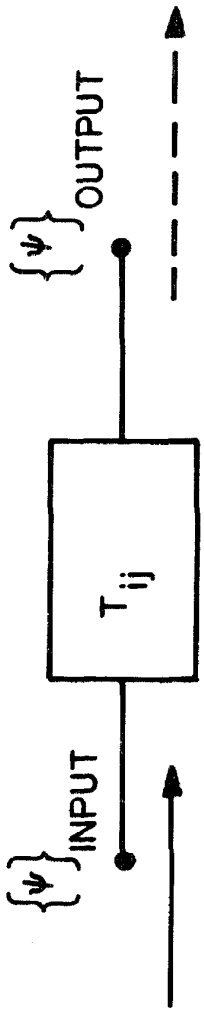

GENERAL REPRESENTATION OF A TRANSMISSION ELEMENT

FIG. 2.1.1

$$\{\psi_1\} = [T_1]\{\psi_2\}$$

$$\{\psi_2\} = [T_2]\{\psi_3\}$$

$$\vdots$$

$$\{\psi_{N-1}\} = [T_{N-1}]\{\psi_N\}$$

and for the total chain of segments:

$$\{\psi_1\} = [T_1][T_2] \ldots\ldots [T_{N-1}]\{\psi_N\} \quad . \qquad (2.1.2)$$

This simple result is obtained because the state vector at the input of any given segment is equal to the state vector delivered by the output of the preceding segment. This result will be used in the following chapters to obtain the overall transmission matrix for a system composed of N segments.

Another way to write the state vector and transmission matrix is in partitioned form where the state vector becomes:

$$\{\psi\} = \begin{Bmatrix} F_p \\ \hline V_p \end{Bmatrix} \qquad (2.1.3)$$

and the transmission matrix is:

$$[T] = \left[\begin{array}{c|c} A & B \\ \hline C & D \end{array}\right] \qquad (2.1.4)$$

For one dimensional systems, e.g., the longitudinally vibrating rod, F_p is the force, V_p is the velocity, and the submatrices in Eq. (2.1.4) reduce to scalar quantities. For the simple transverse bending beam, however, the transmission matrix is fourth-order,

$$\{F_p\} = \begin{Bmatrix} V \\ M \end{Bmatrix} \begin{matrix} \text{shear force} \\ \text{bending moment} \end{matrix}$$

$$\{V_p\} = \begin{Bmatrix} \dot{w} \\ \dot{\phi} \end{Bmatrix} \begin{matrix} \text{rectilinear velocity} \\ \text{rotational velocity} \end{matrix} ,$$

and the submatrices in Eq. (2.1.4) are 2×2 matrices. Pestel and Leckie[10] have catalogued transmission matrices for various uniform elastomechanical elements which have transmission matrices up to twelfth-order (12×12).

The elements of the transmission matrix are not independent and as a consequence of reciprocity it has been shown[11] that the square submatrices of Eq. (2.1.4) must satisfy:

$$[A]^T[D] - [C]^T[B] = [I] \qquad (2.1.5)$$

where:

$[I]$ = the identity matrix, and

$[A]^T$ = the matrix transpose of $[A]$.

Equation (2.1.5) provides an excellent means of checking the validity of derivations of transmission matrices.

Normal mode frequencies, which will be used to evaluate

lumped parameter models in Chapter III, are important characteristics of undamped linear elastic systems which can be obtained through the use of transmission matrices. The transmission matrix, by definition, is independent of boundary conditions and is a function of frequency, ω. Upon substituting the appropriate boundary conditions for a system into the input and output state vectors of Eq. (2.1.1), a frequency determinant can be obtained. A simply supported beam, for example, with the boundary conditions included in the state vectors is described by:

$$\begin{Bmatrix} V_i \\ 0 \\ 0 \\ \dot{\phi}_i \end{Bmatrix} = \begin{bmatrix} & & & \\ & T_{ij} & & \\ & & & \end{bmatrix} \begin{Bmatrix} V_o \\ 0 \\ 0 \\ \dot{\phi}_o \end{Bmatrix}$$

which gives:

$$0 = V_o T_{21} + \dot{\phi}_o T_{24} \tag{2.1.6}$$

$$0 = V_o T_{31} + \dot{\phi}_o T_{34} \quad . \tag{2.1.7}$$

For a nontrivial solution of Eqs. (2.1.6) and (2.1.7) the determinant of the T_{ij} coefficients must be zero, that is,

$$\begin{vmatrix} T_{21} & T_{24} \\ T_{31} & T_{34} \end{vmatrix} = 0 \quad .$$

Other boundary conditions give similar second-order determinants

which define the natural frequencies. To obtain normal mode frequencies of one dimensional systems which are described by second-order (2×2) transmission matrices the above process reduces to finding zeros of single T_{ij} elements, e.g., the natural frequencies of a free-free rod are given by the zeros of the T_{12} term.

Having determined the natural frequencies, the corresponding normal mode shapes can also be obtained. This is accomplished by relating the nonzero components of the input state vector to one reference component. Then the state vectors are determined at other points through the system, in terms of the one reference component, by applying the transmission matrix which relates the input to the point in question. The determination of normal mode frequencies and mode shapes in this manner has been demonstrated by Molloy[9], Pestel and Leckie[10], Rubin[13], and others in their application of transmission matrices to mechanical vibration problems.

2.2 Direct Derivation of Transmission Matrices

Methods used in finding transmission matrices, in the past, have varied according to the preferences of the users. These methods have proven satisfactory for simple lumped parameter or lower-order uniform continuous systems, but become cumbersome when used for non-uniform and higher-order systems because of the required algebraic manipulations. Recently, however, Rubin[14] has formulated a systematic approach which eliminates much of the

algebra and results directly in differential equations for the elements of the transmission matrix. This approach will be summarized in this section and its application demonstrated in Appendices A, B, and D.

In general, the state vector is usually known[10] to satisfy a differential equation of the form:

$$\frac{d}{dx}\{\psi(x)\} = [A(x)]\{\psi(x)\} \quad . \tag{2.2.1}$$

The $[A(x)]$ matrix is entirely determined by the differential equations which govern a dx increment of the system (see Appendix A or D). By definition of the forward transmission matrix:

$$\{\psi(0)\} = [T(x)]\{\psi(x)\} \quad . \tag{2.2.2}$$

Differentiating Eq. (2.2.2) with respect to x gives:

$$0 = [T'(x)]\{\psi(x)\} + [T(x)]\{\psi(x)\}' \quad . \tag{2.2.3}$$

However, $\{\psi(x)\}'$ can be replaced using Eq. (2.2.1); hence, reducing Eq. (2.2.3) to:

$$0 = [T'(x)]\{\psi(x)\} + [T(x)][A(x)]\{\psi(x)\}$$

which upon elimination of $\{\psi(x)\}$ gives:

$$\frac{d}{dx}[T(x)] = -[T(x)][A(x)] \quad . \tag{2.2.4}$$

Therefore, the transmission matrix is given directly by Eq. (2.2.4). By shrinking $\Delta x \to 0$ in Eq. (2.2.2) the first initial condition

becomes:

$$[T(0)] = I \quad , \quad \text{the identity matrix.} \qquad (2.2.5)$$

Substituting this result into Eq. (2.2.4) gives:

$$[T'(0)] = -[A(0)] \quad . \qquad (2.2.6)$$

Differentiating Eq. (2.2.4) with respect to x and using Eqs. (2.2.5) and (2.2.6) results in $[T''(0)]$. This process can be continued to obtain as many initial conditions as required to evaluate constants which arise in solving Eq. (2.2.4); hence, the formulation of the derivation is complete.

CHAPTER III

SYSTEMS GOVERNED BY THE ONE DIMENSIONAL WAVE EQUATION

3.1 Comparison of the Different Physical Systems

The one-dimensional wave equation mathematically describes a group of uniform continuous systems. The following three vibration problems have this identical mathematical formulation with suitable interpretation of properties.

1. longitudinal vibration of rods,
2. torsional vibration of bars, and
3. acoustical vibrations in tubes.

Another system belonging to this category is the electrical transmission line, which has been treated rather extensively by Pipes [15,16,17]. The transmission line will not be specifically included herein, but some of the resulting transmission matrices and lumped parameter models could be directly applied to this problem.

When considering the cross sectional properties of the above systems to be non-uniformly distributed, the governing differential equations in each case are all similar; and each system under steady-state sinusodial conditions is described by a similar second-order (2×2) transmission matrix of the following form.

$$\left\{ \begin{matrix} \psi \\ \end{matrix} \right\}_{\text{input}} = \begin{bmatrix} T_{11} & T_{12} \\ T_{21} & T_{22} \end{bmatrix} \left\{ \begin{matrix} \psi \\ \end{matrix} \right\}_{\text{output}} \qquad (3.1.1)$$

In each case the transmission matrix is determined by the same governing matrix, [A], as follows:

$$\frac{d[T]}{dx} = -[T][A] \tag{3.1.2}$$

where

$$[A] = \begin{bmatrix} 0 & -\bar{Z}(x) \\ -\bar{Y}(x) & 0 \end{bmatrix} .$$

Table (3.1.A) compares the $\bar{Z}(x)$ and the $\bar{Y}(x)$ functions and the non-dimensional frequency constant for the systems of interest. The differential equations used to formulate the governing matrix, [A], are given in Appendix A. For conciseness only the case of the longitudinal rod will be used throughout this work. However, the other cases follow immediately by interchanging the symbols as shown in Table (3.1.A); thus, rendering the transmission matrices and lumped parameter models to follow to be applicable in describing all three systems.

Attention should be given to the assumptions used in deriving the governing [A] matrix. These are listed for each case in Appendix A, and in general are those used in the most elementary theory; i.e., plane sections remain plane, density and elastic properties remain constant, etc. Transmission matrices can be used equally well with higher order theory. The intent here is to present some new transmission matrices of general value for

TABLE 3.1.A

Comparison of Physical Properties for One Dimensional Systems

Vibrating System	Non-Dimensional Freq. Parameter	State Vector	$\overline{Z}(x)^*$	$\overline{Y}(x)^*$
Longitudinal Bar	$\beta = \omega L \sqrt{\rho/E}$	$\psi = \begin{Bmatrix} F \\ v \end{Bmatrix}$ Force; Velocity (rectilinear)	$i\omega\rho A(x)$	$\frac{i\omega}{EA(x)}$
Torsional Rod	$\beta = \omega L \sqrt{\rho/G}$	$\psi = \begin{Bmatrix} T \\ \dot{\theta} \end{Bmatrix}$ Torque; Velocity (angular)	$i\omega\rho\overline{r}^2 A(x)$	$\frac{i\omega}{G\overline{r}^2 A(x)}$
Acoustical Tube	$\beta = \frac{\omega L}{c}$	$\psi = \begin{Bmatrix} F \\ v \end{Bmatrix}$ Force; Velocity (particle)	$i\omega\rho A(x)$	$\frac{i\omega}{\rho_o c^2 A(x)}$

* See Appendix A for details of formulation.

describing non-uniform systems and in particular to use them to improve lumped parameter modeling of continuous systems. These principles can be sufficiently demonstrated using the elementary theory.

3.2 Transmission Matrices for Continuous Systems

The parameter describing the spatial dependence in the governing matrix, [A], is the area, A(x). To obtain a transmission matrix useful for describing many non-uniform systems requires selection of a general function to represent the variable area. This function must be general to represent many useful cases but of a form which will lead to closed form solutions. One such function is:

$$A(x) = A_o(1+ax)^{2p-1} \qquad (3.2.1)$$

where

a = some suitable constant and

p = an integer or non-integer.

Another useful function for exponentially tapered sections is:

$$A(x) = A_o e^{2(x/x_o)} \qquad (3.2.2)$$

where

x_o = some suitable constant.

Equation (3.2.1) with a convenient coordinate transformation leads to differential equations for the transmission matrix elements of the following form:

$$x^2 \frac{d^2 T_{ij}}{dx^2} + ax \frac{dT_{ij}}{dx} + bx^2 T_{ij} = 0 \quad .$$

It is well known that this equation with variable coefficients has solutions in terms of Bessel functions. The exponential taper leads to second-order differential equations with constant coefficients of the form:

$$\frac{d^2 T_{ij}}{dx^2} + a \frac{dT_{ij}}{dx} + bT_{ij} = 0$$

which can be easily solved.

Using the two area functions given in Eq. (3.2.1) and (3.2.2) and following the basic approach outlined in Section 2.2, general transmission matrices can be derived for a broad group of non-uniform continuous elements. The derivation of the general matrix elements for three specific cases (p = an integer, p ≠ an integer, and the exponential taper) is given in Appendix B. The resulting transmission matrices for these three cases are given below:

Case I $\qquad A(x) = A_o(1+ax)^{2p-1} \qquad p = 0$ or an integer

$$T_{11}(\ell) = \left(\frac{g}{f}\right)^{1-p} \frac{1}{X} \{Y_{-p}(f\beta)J_{1-p}(g\beta) - J_{-p}(f\beta)Y_{1-p}(g\beta)\}$$

$$T_{12}(\ell) = \frac{\beta}{i\omega}\left[\frac{EA_o}{\ell}\right]\left(\frac{g}{f}\right)^{p} \frac{1}{X} \{Y_{p}(f\beta)J_{p}(g\beta) - J_{p}(f\beta)Y_{p}(g\beta)\}$$

$$T_{21}(\ell) = -\frac{i\omega}{\beta}\left[\frac{\ell}{A_o E}\right]\left(\frac{g}{f}\right)^{1-p} \frac{1}{X} \{Y_{p-1}(f\beta)J_{p-1}(g\beta) - J_{p-1}(f\beta)Y_{p-1}(g\beta)\}$$

$$T_{22}(\ell) = \left(\frac{g}{f}\right)^{p} \frac{1}{X} \{Y_{p-1}(f\beta)J_{p}(g\beta) - J_{p-1}(f\beta)Y_{p}(g\beta)\}$$

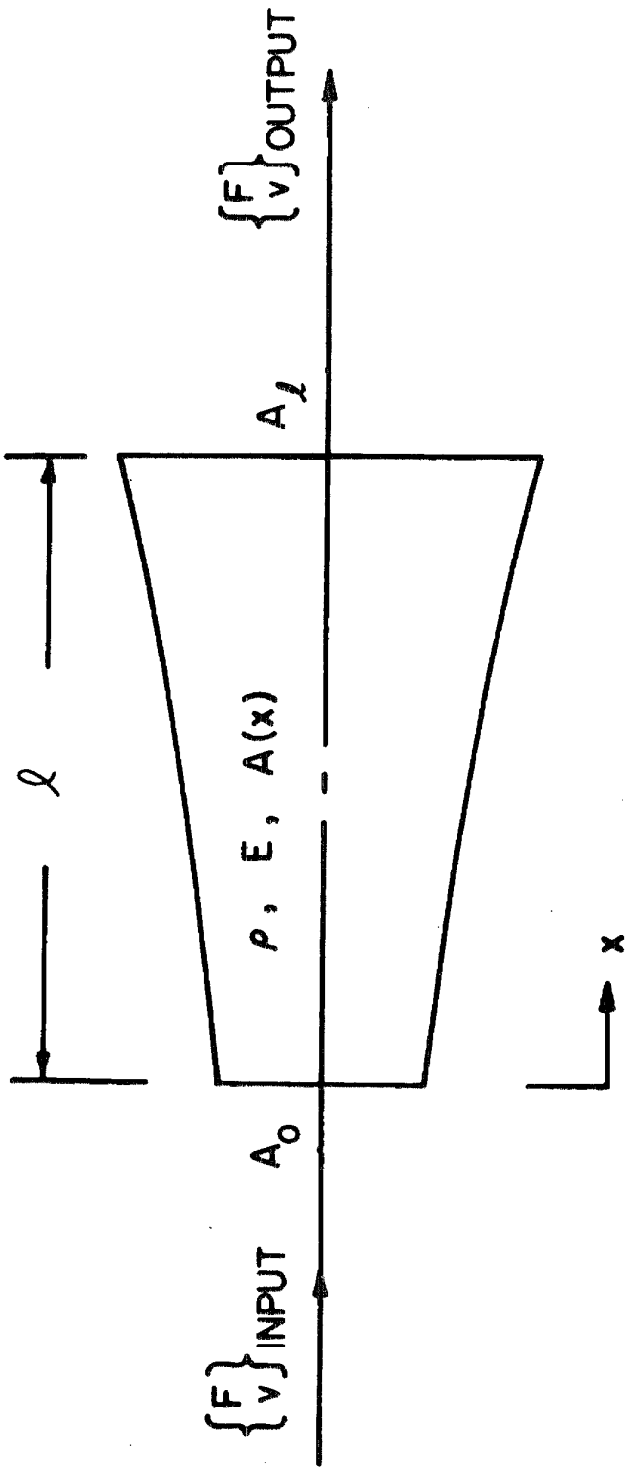

NON-UNIFORM ELASTIC ELEMENT

FIG. 3.2.1

$X = 2/\pi f\beta$ independent of "p" in this case.

Case II $\quad A(x) = A_o(1+ax)^{2p-1} \quad p \neq 0$ or an integer

$$T_{11}(\ell) = \left(\frac{g}{f}\right)^{1-p} \frac{1}{X} \{J_p(f\beta)J_{1-p}(g\beta)+J_{-p}(f\beta)J_{p-1}(g\beta)\}$$

$$T_{12}(\ell) = \frac{\beta}{i\omega}\left[\frac{EA_o}{\ell}\right]\left(\frac{g}{f}\right)^{p} \frac{1}{X} \{J_p(f\beta)J_{-p}(g\beta)-J_{-p}(f\beta)J_p(g\beta)\}$$

$$T_{21}(\ell) = -\frac{i\omega}{\beta}\left[\frac{\ell}{A_oE}\right]\left(\frac{g}{f}\right)^{1-p} \frac{1}{X} \{J_{1-p}(f\beta)J_{p-1}(g\beta)-J_{p-1}J_{1-p}(g\beta)\}$$

$$T_{22}(\ell) = \left(\frac{g}{f}\right)^{p} \frac{1}{X} \{J_{1-p}(f\beta)J_p(g\beta)+J_{p-1}(f\beta)J_{-p}(g\beta)\}$$

$$X = \frac{2}{\pi f\beta} \sin(p\pi) \quad .$$

In Cases I and II the following definitions are appropriate (see Fig. 3.2.1).

$$\xi = \text{a slope parameter} = \frac{\sqrt{A_\ell} - \sqrt{A_o}}{\sqrt{A_o}}$$

A_o = area at the input end of the element

A_ℓ = area at the output end of the element

$f = 1/\xi$; $a = \xi/\ell$; $g = f + 1$; and $\beta = \omega\ell\sqrt{\rho/E}$.

For systems with circular cross sections:

$$\xi = (r_\ell - r_o)/r_o$$

where r_o and r_ℓ are the radii at the input and output ends, respectively.

Case III $\quad A(x) = A_o e^{2(x/x_o)}$

$$T_{11}(\ell) = e^{-\ell/x_o}\left(\cos(\gamma\ell) + \frac{1}{\gamma x_o}\sin(\gamma\ell)\right)$$

$$T_{12}(\ell) = -\frac{e^{\ell/x_o}}{i\omega}(A_o E)\left(\frac{\beta_1^2}{\gamma}\right)\sin(\gamma\ell)$$

$$T_{21}(\ell) = -\frac{e^{-\ell/x_o}}{i\omega}\left(\frac{\beta_1^2}{\rho A_o \gamma}\right)\sin(\gamma\ell)$$

$$T_{22}(\ell) = e^{\ell/x_o}\left(\cos(\gamma\ell) - \frac{1}{\gamma x_o}\sin(\gamma\ell)\right)$$

where

$$\gamma = \sqrt{\beta_1^2 - 1/x_o^2}$$

and the other terms are identical to those used in Cases II and III. This element exhibits a cut-off frequency, $\beta_1^2 = 1/x_o^2$. When $\beta_1^2 < 1/x_o^2$, oscillations do not occur in the element; and when $\beta_1^2 > 1/x_o^2$, mechanical oscillations do exist. Thus, this element behaves as a high pass mechanical filter.

3.3 Investigation of Lumped Parameter Models

The determination of eigenvalues and eigenfunctions for continuous systems is generally a difficult problem. The approach of using transmission matrices to piecewise describe a continuous system has been previously discussed in Section 2.1, and a general group of transmission matrices for the non-uniform, one dimensional

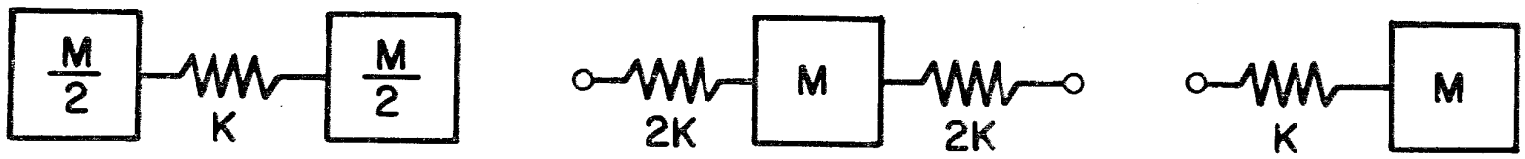

(a) (b) (c)

LUMPED PARAMETER MODELS

FIG. 3.3.1

systems has been given in Section 3.2. Another more commonly used approach is to replace the continuum by a discrete N degree of freedom system composed of lumped parameters. It has been shown[2] that the behavior of the discrete N degree system approaches that of the continuous system in the limit as $N \rightarrow \infty$, and it is on this basis that this method is justified. However, the degree to which the finite system approximates the continuous is often uncertain even though this technique is widely used. The main goal in this and the following sections is to formulate some generalizations as to which lumped parameter models should be used, how they should be employed, and what accuracies can be expected upon using the models.

Three models that have been used previously are given in Fig. (3.3.1). In the first model, which was first used by Rayleigh[2], the total mass of each of the N increments into which the rod has been segmented is further divided into two equal masses concentrated at each end of a spring which represents the stiffness of the increment. The second model, which has been attributed in the literature[18] to Lagrange, has been investigated to some extent by Duncan[3] and is some times referred to as Duncan's model. This model has the mass of the increment concentrated at the center and equal springs on each side. The third model, which is used to a large extent in practice, has the mass concentrated at one end of a spring.

To critically examine the usefulness of these models requires a mathematical approach which allows the formulation of the problem on the incremental level and provides a means of evaluating the overall

system representation as a function of the number of increments. A method commonly used by some is the finite difference approach. The approach used herein is that of the transmission matrix, which was chosen for the following reasons:

1. This method allows complete freedom to choose incremental models in any form.
2. This method provides a means of determining how well the models represent the continuum at the incremental level. Also, the accuracy of representing a total element by N increments of a given model can be evaluated.
3. The method allows for an analytic treatment of uniform systems and is easily extended to include non-uniform systems.

3.3.1 Model Comparison on the Incremental Level

The first comparison for the models shown in Fig. (3.3.1) is to determine how well the transmission matrix for each agrees with that of the continuous uniform system for one increment of length ℓ. This should give some insight into what model will best describe an overall continuous uniform element composed of N increments. Using the state vector form involving force and displacement, the transmission matrix for the continuous uniform rod is (see Appendix B):

$$[E] = \begin{bmatrix} \cos(\beta) & -\frac{A_o E}{\ell}\beta\sin(\beta) \\ \frac{\ell}{A_o E}\frac{\sin(\beta)}{\beta} & \cos(\beta) \end{bmatrix} . \quad (3.3.1)$$

This represents the exact description of a uniform continuous incremental element of length ℓ (considering the elementary theory being used). The transmission matrices for the three lumped parameter models are:

$$[L_1] = \begin{bmatrix} 1 - \frac{M\omega^2}{2k} & -M\omega^2 + \frac{M^2\omega^4}{4k} \\ \frac{1}{k} & 1 - \frac{M\omega^2}{2k} \end{bmatrix} \quad (3.3.2)$$

$$[L_2] = \begin{bmatrix} 1 - \frac{M\omega^2}{2k} & -M\omega^2 \\ \frac{1}{k} - \frac{M\omega^2}{4k^2} & 1 - \frac{M\omega^2}{2k} \end{bmatrix} \quad (3.3.3)$$

$$[L_3] = \begin{bmatrix} 1 & -M\omega^2 \\ \frac{1}{k} & 1 - \frac{M\omega^2}{k} \end{bmatrix} \quad (3.3.4)$$

where $[L_i]$ is the matrix for the i^{th} model (see Fig. 3.3.1). Using the relationships $k = AE/\ell$, $\beta = \omega\ell\sqrt{\rho/E}$, $z_o = (AE/\ell)$ and $M = A\rho\ell$, expressions (3.3.2), (3.3.3), and (3.3.4) can be written in

terms of the constant z_o and the frequency parameter β.

$$[L_1] = \begin{bmatrix} 1-\beta^2/2 & -z_o(\beta^2 - \beta^4/4) \\ \frac{1}{z_o} & 1 - \beta^2/2 \end{bmatrix} \tag{3.3.5}$$

$$[L_2] = \begin{bmatrix} 1-\beta^2/2 & -z_o\beta^2 \\ \frac{1}{z_o}(1-\beta^2/4) & 1-\beta^2/2 \end{bmatrix} \tag{3.3.6}$$

$$[L_3] = \begin{bmatrix} 1 & -z_o\beta^2 \\ \frac{1}{z_o} & 1-\beta^2 \end{bmatrix} \tag{3.3.7}$$

To facilitate a comparison between the elements of the lumped parameter matrices and those of the matrix for the continuous element, series expansions for the trigonometric functions are used. The E_{ij} elements from Eq. (3.3.1) then become:

$$E_{11} = 1 - \beta^2/2 + \beta^4/24 - O(\beta^6) - - - -$$

$$E_{12} = -z_o\{\beta^2 - \beta^4/6 + O(\beta^6) - - - -\}$$

$$E_{21} = 1/z_o\{1 - \beta^2/6 + \beta^4/120 - O(\beta^6) - - - -\}$$

$$E_{22} = 1 - \beta^2/2 + \beta^4/24 - O(\beta^6) - - - - \quad .$$

A comparison of matrix terms indicates that the L_{ij} terms of model

(a) match the E_{ij} terms to almost the same degree as those of model (b). With models (a) and (b) the L_{11} and L_{22} elements are identically equal to the first two terms in the series for E_{11} and E_{22}. In model (a) the L_{12} term is almost the same as the two first terms in E_{12}, and L_{21} is equal only to the order unity term of E_{21}, the term of $O(\beta^2)$ is not present in L_{21}. In model (b) nearly the reverse of model (a) is true. The L_{21} term of model (b) is nearly equal to the first two terms of E_{21}, but the L_{12} term includes only the first term of the series for E_{12}, L_{12} in model (b) does not have any $O(\beta^4)$ term. Model (c) displays each of the deficiencies shown by models (a) and (b) when it is compared to E_{ij}. Also L_{11} of the matrix for model (c) has only the first term of the series for E_{11} and no $O(\beta^2)$ term. From this comparison at the incremental level it appears natural that model (c) would be inferior to models (a) and (b) when N increments are used to approximate a continuous element. This conclusion does hold true in most cases and some illustrative results are shown in Figs. (3.3.3) and (3.3.4).

The comparison between the L_{ij} and E_{ij} elements indicates why the finite lumped parameter system is only a low frequency approximation to the continuous system. The L_{ij} expressions, particularly for models (a) and (b), are similar to the first two terms of the series representations of the E_{ij} elements. If β, which is proportional to the product of frequency and length of the increment, is small, then these first two terms are good approximations to the trigonometric functions. This then implies that for good approximation the frequency must be small or the length of the increment short.

This same argument remains true when describing the total element because the transmission matrix for the total element is just the product of N incremental matrices. Although it is arbitrary how small β must be to achieve good approximations from a few terms of the trigonometric series, it follows directly that the approximations become poorer as the value of β increases; assuming the number of increments and the length remain constant. Thus, lumped parameter approximations are best for small values of β or low frequencies.

3.3.2 Model Comparison on the Basis of Total Element Representation

The conclusion obtained above in the incremental comparison was that models (a) and (b) should be superior to model (c) in describing an element composed of N such increments. The three models will now be compared on the basis of representing an entire uniform element. Figure (3.3.2) depicts an element subdivided into N equal length increments, each of which will be described by the appropriate transmission matrix as given in Eqs. (3.3.2), (3.3.3), or (3.3.4). However, to determine which model best approximates the dynamic behavior of the total element requires the adoption of some qualitative basis of comparison. Two criteria which are motivated by the method used herein and the classical method of superposition of normal modes are:

1. Compare the overall transmission matrix, which represents the N cascaded incremental matrices, to that for the continuous element.

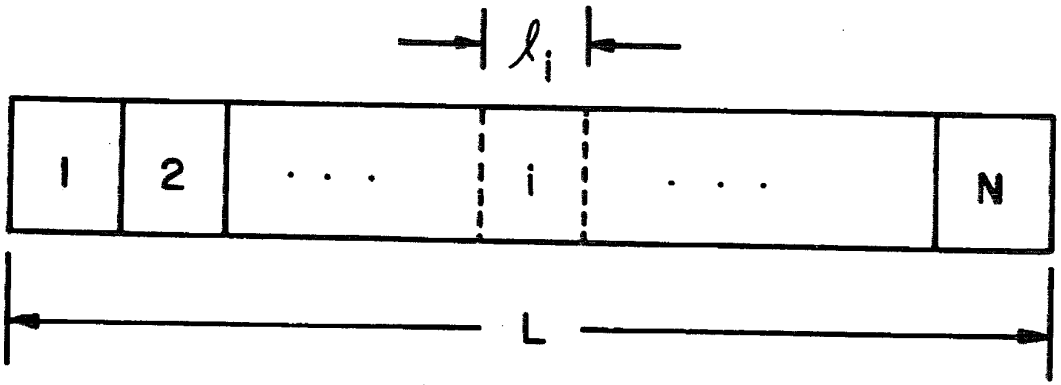

UNIFORM CONTINUOUS ELEMENT SUBDIVIDED INTO N INCREMENTS

FIG. 3.3.2

The model whose matrix best approximates the matrix of the continuum is the better model.

2. The model that produces eigenvalues (natural frequencies) closest to those of the continuous element with specific boundary conditions of free or fixed ends is the better model.

In the following it will be shown that the second choice is the more acceptable criterion.

The first step in evaluating the overall element representation by any of the models with either of the above criterion is to obtain the transmission matrix for the total element. For the uniform system this matrix is given by the product of N equal incremental transmission matrices.

$$[\bar{L}] = [L]_1 \; [L]_2 \; . \; . \; . \; . \; . \; . \; . \; . \; . \; [L]_N$$

or

$$[\bar{L}] = \begin{bmatrix} L_{11} & L_{12} \\ L_{21} & L_{22} \end{bmatrix}^N .$$

A square matrix can be raised to the N^{th} power by employing the Cayley Hamilton theorem[19] which states that any square matrix [M] satisfies its own characteristic equation. A direct result of this is that $[M]^N$ for any $(n \times n)$ matrix can be expressed as a polynomial P(M) of order n-1.

In this case the matrix [M] is the transmission matrix [L] and the order is two (n = 2). Therefore

$$[L]^N = C_o[I] + C_1[L] \tag{3.3.8}$$

$$\lambda_1^N = C_o + C_1\lambda_1 \tag{3.3.9}$$

$$\lambda_2^N = C_o + C_1\lambda_2 \tag{3.3.10}$$

where λ_1 and λ_2 are the characteristic values of [L]. Solving Eqs. (3.3.9) and (3.3.10) for the constants C_o and C_1 gives:

$$C_o = \frac{\lambda_2\lambda_1^N - \lambda_1\lambda_2^N}{\lambda_2 - \lambda_1} \tag{3.3.11}$$

and

$$C_1 = \frac{\lambda_1^N - \lambda_2^N}{\lambda_1 - \lambda_2} \quad . \tag{3.3.12}$$

The characteristic values of the incremental transmission matrix are defined by:

$$\text{Det.} \begin{Vmatrix} (L_{11}-\lambda) & L_{12} \\ L_{21} & (L_{22}-\lambda) \end{Vmatrix} = 0 \qquad \text{or}$$

$$\lambda^2 - \lambda(L_{11} + L_{22}) + (L_{11}L_{22} - L_{12}L_{21}) = 0 \quad .$$

It is well known that the second-order transmission matrix has the following property (see Eq. 2.1.5):

$$L_{11} L_{22} - L_{12} L_{21} = \text{Det. } |L_{ij}| = 1 \quad .$$

Therefore,

$$\lambda_{1,2} = \frac{(L_{11} + L_{22})}{2} \pm \sqrt{\left[\frac{L_{11} + L_{22}}{2}\right]^2 - 1} \quad .$$

From Eqs. (3.3.5), (3.3.6) and (3.3.7):

$$(L_{11} + L_{22})/2 = 1 - \beta^2/2$$

for all three models; hence,

$$\lambda_{1,2} = D_1 \pm iD_2$$

where

$$D_1 = (1 - \beta^2/2) \quad \text{and} \quad D_2 = \sqrt{(\beta^2 - \beta^4/4)} \quad \text{for} \quad 0 \leqslant \beta \leqslant 2 \quad .$$

Writing λ in polar form gives

$$\lambda_1 = \tilde{\lambda} e^{-i\theta} \quad \text{and} \quad \lambda_2 = \tilde{\lambda} e^{i\theta} \qquad (3.3.13)$$

where

$$\tilde{\lambda} = D_1^2 + D_2^2 = 1 \quad \text{and}$$

$$\theta = \tan^{-1}(D_2/D_1) \quad .$$

By combining Eqs. (3.3.11), (3.3.12), and (3.3.13) constants C_o and C_1 can be determined, whereby $[\bar{L}]$ is known. Denoting the elements from the transmission matrix to the N^{th} power as $\bar{L}_{ij}$ gives:

$$\bar{L}_{11} = \frac{L_{11}\sin(N\theta)-\sin(N-1)\theta}{\sin\theta} \qquad (3.3.14)$$

$$\bar{L}_{12} = \frac{L_{12}\sin(N\theta)}{\sin\theta} \qquad (3.3.15)$$

$$\bar{L}_{21} = \frac{L_{21}\sin(N\theta)}{\sin\theta} \qquad (3.3.16)$$

$$\bar{L}_{22} = \frac{L_{22}\sin(N\theta)-\sin(N-1)\theta}{\sin\theta} \quad . \qquad (3.3.17)$$

At the outset of the investigation the first criterion based on the matrix comparison appeared to offer attractive possibilities. First, the transmission matrix was available because it was the basic technique being used. Secondly, the matrix is independent of any boundary conditions on the element. However, this criterion is still not completely defined because there are several ways of comparing matrices. One possibility, which seems meaningful here, is to compare matrix norms. The definition of matrix norm used is,

$$\text{Matrix Norm} = \epsilon(L) = \sum_{i,j} |E_{ij}-\bar{L}_{ij}|$$

which is a measure of the total absolute difference between the elements of the two matrices being compared. The norm does have the advantage of independence of boundary conditions, but it also has the disadvantage of not being independent of cross sectional properties of the increment. Note that in Eqs. (3.3.15) and (3.3.16) $\bar{L}_{12}$ and $\bar{L}_{21}$

are directly proportional to L_{12} and L_{21}, respectively. These terms, however, are directly and inversely proportional to (AE/ℓ), respectively. Therefore, the magnitude of (AE/ℓ) will govern to some degree the importance of the $\bar{L}_{12}$ and $\bar{L}_{21}$ terms in the norm. Because of this difficulty the norm criterion was discarded; moreover, no other suitable matrix comparison was found and the second criterion of the non-dimensional frequency root comparison, which is independent of (AE/ℓ), was used.

To complete the three model comparison, the behavior of the non-dimensional frequency root errors was determined for each model. This was done for four sets of boundary conditions; fixed-fixed, free-free, fixed-free, and free-fixed.

The frequency roots for the free-free and fixed-fixed boundary conditions are determined by the zeros of the $\bar{L}_{12}$ and $\bar{L}_{21}$ terms, respectively. By inspection of Eq. (3.3.15) and (3.3.16) it is apparent that L_{12}, L_{21}, or $\sin(N\theta)$ must then be zero as $\sin\theta$ is a bounded function. Re-examining the L_{12} and L_{21} terms for all models shows that the L_{12} term in models (b) and (c) is the same and, similarly, the L_{21} term is the same in models (a) and (c). Equating these expressions to zero gives only the rigid body mode, $\beta = 0$, for $L_{12} = 0$ and in the other case L_{21} is a constant. In the L_{12} and L_{21} terms of models (a) and (b), respectively, there is an additional $1 - \beta^2/4$ factor. This factor contributes the non-rigid mode for model (a) and the free-free case when $N = 1$, and the first mode for the fixed-fixed case with model (b) when $N = 1$ where

$\sin N\theta/\sin\theta$ cannot be equal to zero. Consequently, the major term of interest for these two boundary conditions is $\sin(N\theta)$. The zeros of this function give the non-dimensional frequency roots for the lumped system. From the discussion above and the fact that $\sin(N\theta)$ is identical for all three models it becomes obvious that all three models must give the same frequency roots for the specific cases of free-free and fixed-fixed boundary conditions. Equating $\sin(N\theta)$ to zero then gives:

$$\sin(N\theta) = 0 \qquad \text{or} \qquad \theta = \frac{\nu\pi}{N}$$

where $\nu = 1, 2, 3, \ldots N$.

$$\tan\theta = \frac{\sin\theta}{\cos\theta} = \sqrt{\frac{1-a_1^2}{a_1}}$$

where

$$a_1 = \frac{L_{11} + L_{22}}{2} = 1 - \beta^2/2 \quad ,$$

$L = N\ell$ (length of total element), and

$B = \omega L \sqrt{\rho/E} = N\beta$.

Solving for the frequency roots of the total element gives:

$$B^2_{\nu N} = 2N^2\left(1 - \cos\frac{\nu\pi}{N}\right) \qquad (3.3.18)$$

where

$\nu = (1, 2, 3 \ldots N)$ mode number and

N = number of increments .

The frequency roots for the other two boundary conditions, fixed-free and free-fixed, are the same for models (a) and (b), but they are different than the ones for model (c). For models (a) and (b) $(L_{11})_a = (L_{11})_b = (L_{22})_a = (L_{22})_b = 1 - \frac{B^2}{2N^2}$; consequently, the frequency roots for these two models are given by:

$$(1-B^2/2N^2)\sin(N\theta) - \sin(N-1)\theta = 0$$

or

$$B^2_{\nu N} = 2N^2\left[1 - \cos\frac{(2\nu-1)\pi}{2N}\right]. \qquad (3.3.19)$$

For model (c) similar expressions can be obtained and are given by:

$$B^2_{\nu N} = 2N^2\left[1 - \cos\frac{(2\nu-1)\pi}{(2N\pm 1)}\right] \qquad (3.3.20)$$

where

(2N+1) ~ fixed-free boundaries, and

(2N-1) ~ free-fixed boundaries.

The behavior of the error in the frequency roots is obtained by subtracting Eqs. (3.3.18), (3.3.19), and (3.3.20) from the exact roots which are denoted as $B_{\nu e}$. For all three models with boundary conditions being free-free or fixed-fixed:

$$e_{\nu N} = (\text{error in the } \nu^{th} \text{ mode}) = B_{\nu e} - B_{\nu N}$$

$$e_{\nu N} = \nu\pi - 2N \sin\frac{\nu\pi}{2N} \quad .$$

Expanding $\sin(\nu\pi/2N)$ and retaining only the lower order terms for large N gives:

$$e_{\nu N} \approx \frac{(\nu\pi)^3}{24N^2} \quad . \tag{3.3.21}$$

The errors which occur when using models (a) or (b) with boundary conditions of fixed-free or free-fixed ends are:

$$e_{\nu N} = \left[\frac{(2\nu-1)}{2}\right]\pi \; - \; 2N \sin \frac{(2\nu-1)\pi}{4N}$$

or for large N:

$$e_{\nu N} \approx \frac{(2\nu-1)^3\pi^3}{192N^2} \quad . \tag{3.3.22}$$

For model (c) the results are:

$$e_{\nu N} = \left[\frac{(2\nu-1)}{2}\right]\pi \; - \; 2N \sin \frac{(2\nu-1)\pi}{2(2N\pm1)} \quad .$$

Expanding the sin term gives:

$$e_{\nu N} = \left[\frac{(2\nu-1)}{2}\right]\pi - \frac{N(2\nu-1)\pi}{(2N\pm1)} + \text{higher order terms,}$$

or

$$e_{\nu N} = \pm \frac{(2\nu-1)\pi}{4N(1\pm1/2N)} + \text{higher order terms.}$$

Thus, for large N ther error behaves as:

$$e_{\nu N} \approx \pm \frac{(2\nu-1)\pi}{4N} \quad . \tag{3.3.23}$$

In retrospect, two significant conclusions can be stated about the representation of the uniform system by the three models

used above. For reasonably large N the frequency root error is proportional to $1/N^2$, except for the cases of fixed-free and free-fixed rods when approximated by model (c). In these cases, the error is proportional to $1/N$. Duncan[3] has examined several of the cases described above. Using Rayleigh's principle, Duncan established a general inverse square law for model (b) which states that the error in the frequency of any normal mode of oscillation varies inversely as the square of the number of segments. The results presented here for model (b) agree with those of Duncan. Duncan also investigated briefly the case where the mass is moved away from the center of the increment and concluded that this always results in frequency root errors which behave as $1/N$ for large N. Model (c) is an example of this case and the results presented here verify Duncan's conclusion in part; however, they show that this conclusion does not hold true in every case, and in particular not for the free-free and fixed-fixed cases. Figure (3.3.3) and (3.3.4) show the non-dimensional frequency root errors for all three models with the four boundary conditions. Figure (3.3.4) gives the errors for only the fixed-free boundary condition. However, for models (a) and (b) these errors are identical to those for the free-fixed case. For model (c) the errors are of the same magnitude but negative because this model always gives frequency roots which are too large for the free-fixed condition.

Another interesting technique of modeling was also investigated for the two cases of fixed-fixed and free-free boundary conditions. The element was divided into N equal masses which

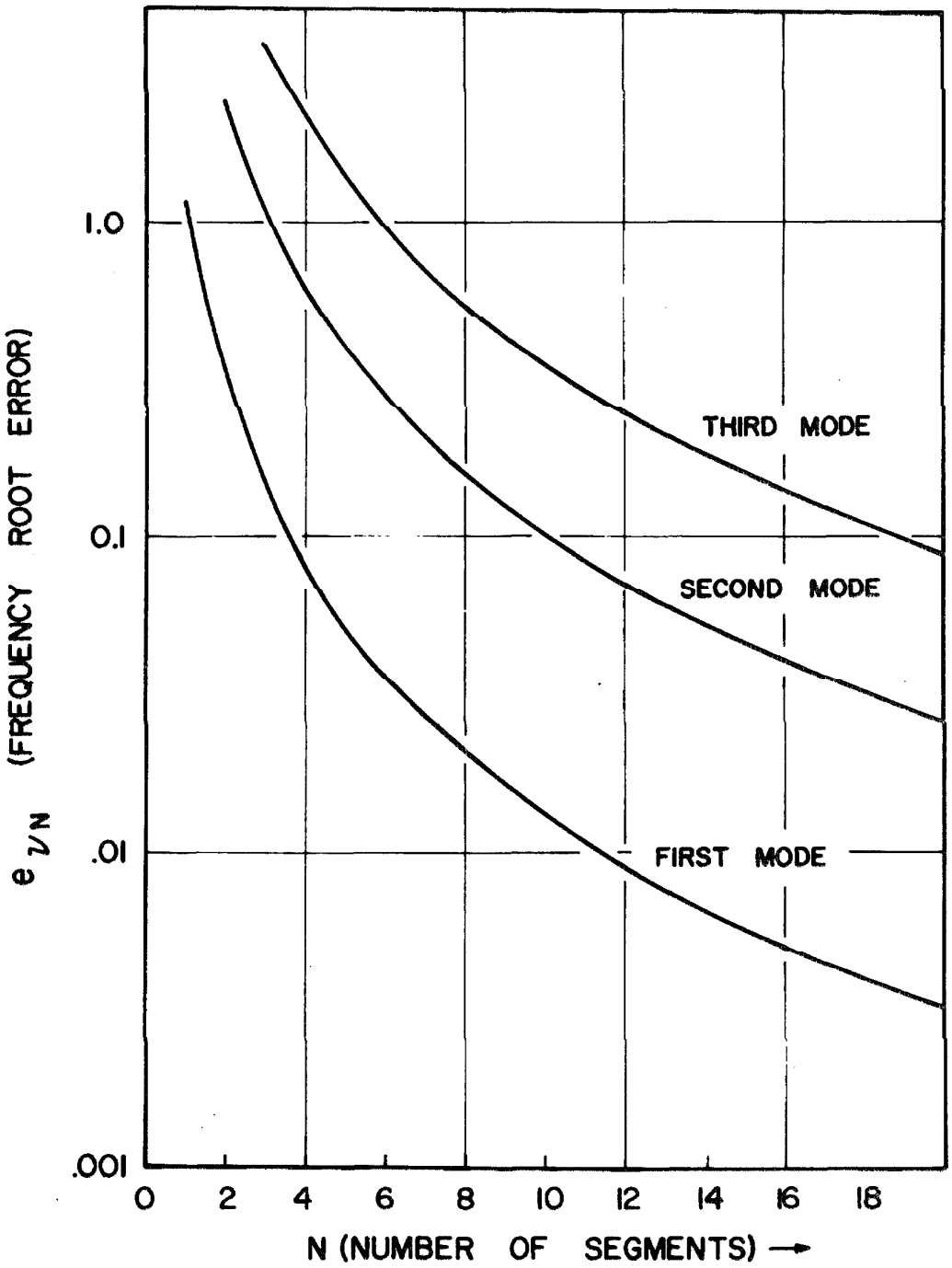

Fig. 3.3.3 Non-Dimensional Frequency Root Errors for Free-Free and Fixed-Fixed Elements when Approximated by Models (a), (b), and (c).

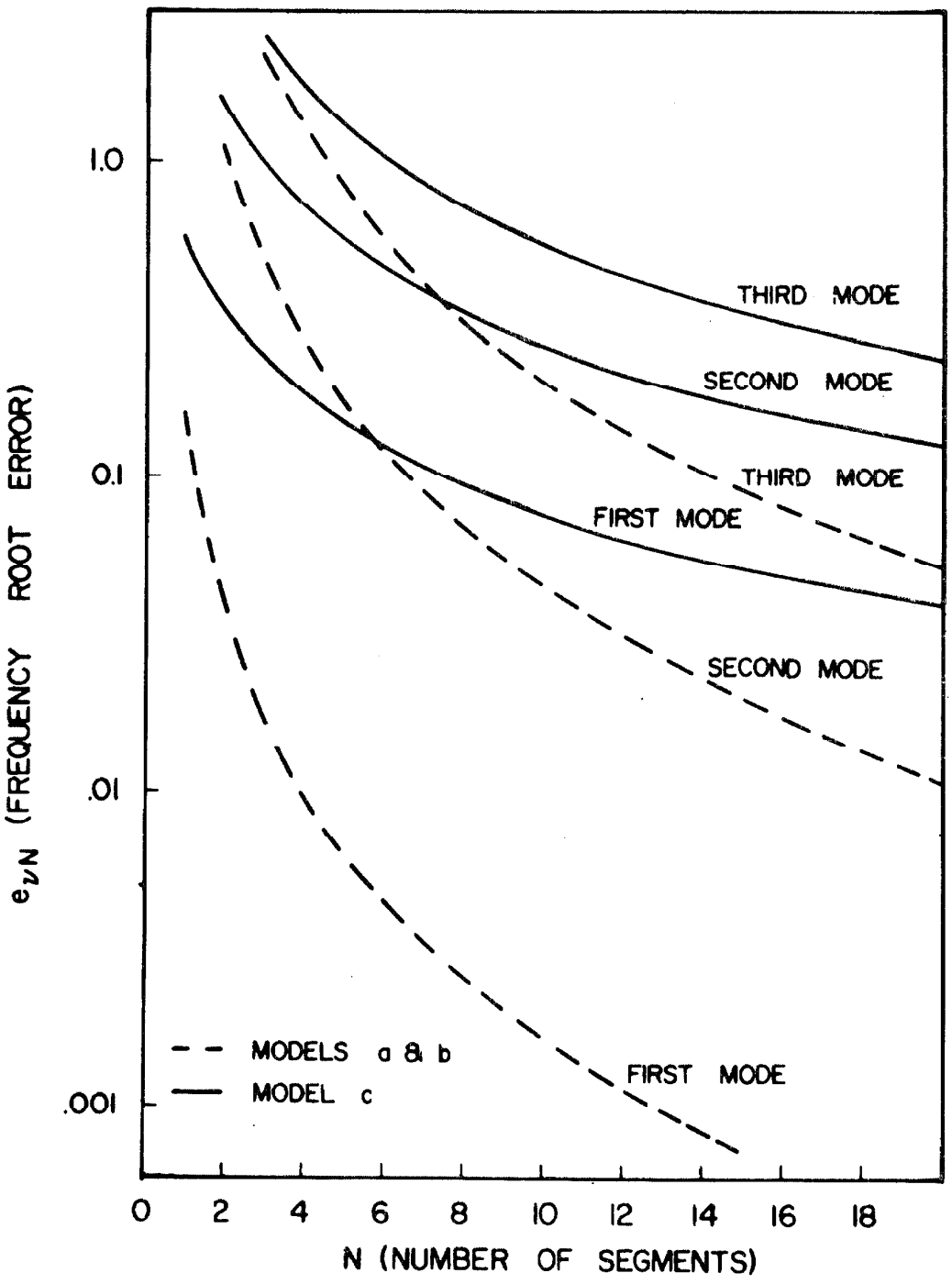

Fig. 3.3.4 Non-Dimensional Frequency Root Errors for Fixed-Free Elements.

represent the total mass and $N + 1$ or $N - 1$ equal springs which represent the total stiffness. If the boundary conditions are fixed-fixed, then $N + 1$ springs are used; in the other case only $N - 1$ springs are used. The motivation for this type of modeling comes from the following reasoning. When using models (a) or (b) the results for these two boundary conditions are the same. Moreover, if model (a) is used for the free-free case and model (b) is used for the fixed-fixed case, then the total mass and total stiffness of the element are always active in the models. In contrast to this, model (c) does not reflect the total mass of the element in the fixed-fixed case because the last mass is always inactivated by the boundary condition. Likewise, in the free-free case the total stiffness is not reflected by use of model (c). To determine if these deficiencies cause model (c) to be less effective than possible, the modeling technique described above was investigated.

To avoid confusion with models (a), (b), and (c), the modeling technique described above will be designated as model (d). Model (d) can be analyzed by the previous methods and the frequency roots can be found in the same manner. The $[\bar{L}]$ matrix for the free-free case is:

$$[\bar{L}] = \begin{bmatrix} 1 - \frac{B^2}{N(N+1)} & - \frac{B^2}{(N+1)} \left(\frac{EA}{L}\right) \\ \left(\frac{L}{AE}\right) \frac{1}{N} & 1 \end{bmatrix}^{N^*} \qquad (3.3.24)$$

and for the case of fixed-fixed ends:

$$[\bar{L}] = \begin{bmatrix} 1 - \frac{B^2}{N(N+1)} & - \frac{B^2}{N}\left(\frac{AE}{L}\right) \\ \left(\frac{L}{AE}\right)\frac{1}{N+1} & 1 \end{bmatrix}^{N^*} \qquad (3.3.25)$$

where

$$N^* = N + 1 \quad .$$

Using Eqs. (3.3.15) and (3.3.16) to determine $\bar{L}_{12}$ and $\bar{L}_{21}$ indicates that the frequency roots for both cases are determined by the zeros of $\sin(N^* \theta)$; therefore, the frequency roots are given by:

$$B_{\nu N} = 2\sqrt{N(N+1)} \quad \sin \frac{\nu\pi}{2(N+1)} \quad . \qquad (3.3.26)$$

The frequency root error is:

$$e_{\nu N} = (\nu\pi)\left[1 - \frac{N}{N+1}\right] + \sqrt{\frac{N(N+1)}{24}}\ \frac{\nu^3\pi^3}{(N+1)^3} + \text{higher order terms.}$$

Expanding this expression for large N and retaining the lowest order term gives:

$$e_{\nu N} \sim \left(\frac{\nu\pi}{2}\right)\frac{1}{N} \quad , \quad \text{for large } N \quad . \qquad (3.3.27)$$

The result, therefore, is that the errors in the frequency roots decrease as $1/N$ for large N. This is the same behavior as displayed in Fig. (3.3.4) for model (c). Figure (3.3.5) shows, in particular, how many increments are required by both models (d) and model (a) or (b) to achieve a specific percentage error in the non-dimensional frequency roots for the first three normal modes. For example, to

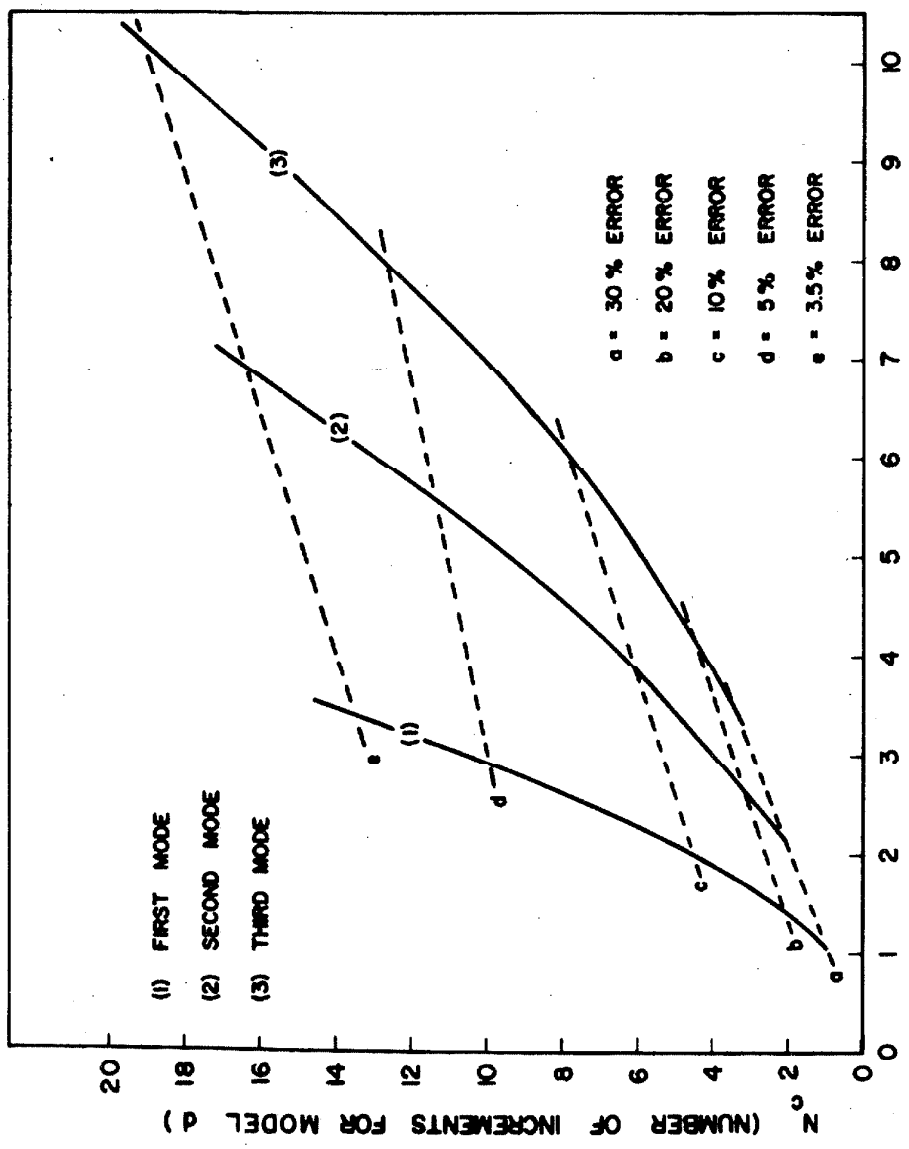

Fig. 3.3.5 Comparison of Model (d) to Models (a) and (b).

achieve a frequency root error of 5 per cent or less in the first normal mode three increments of model (a) or (b) and eleven increments of model (d) are required.

In summary, it has been shown that models (a) and (b) give consistent results when used to approximate the uniform system. The errors in the non-dimensional frequency roots for these two models decrease as $1/N^2$ for large N. Models (c) and (d) are less consistent in that for some boundary conditions their frequency root errors decrease as $1/N$ for large N; hence, model (d) has not, in general, shown any improvement over model (c). When considering the higher modes two additional trends are apparent (see Figs. 3.3.4 and 3.3.5). First, the overall error level increases as expected with higher modes for all models; and, second, the advantage of models (a) and (b) with respect to model (c) decreases in higher modes. The fact that the differences between these models decreases for higher modes is not surprising, since the higher modes are less sensitive to boundary conditions which is the main difference between model (a) or (b) and model (c). Model (b) is slightly more efficient than model (a) because it achieves the same accuracy in frequency roots with one less mass, which in turn means that the number of differential equations is, in general, one less when using model (b).

3.4 Linear Taper Model

Exact solutions for non-uniform one dimensional systems are available when the system is made up of segments which can be

described by exact transmission matrices (see Section 3.2). Systems which are not susceptible to exact solution can be treated in several alternative ways. A commonly recommended approach[10] is to use a piecewise uniform segment representation as shown in Fig. (3.4.1) A second approach, which should obviously be better, is to approximate each segment by some best fit non-uniform segment for which the exact transmission matrix is known. Approximate transmission matrices can also be obtained more directly as discussed in Chapter V. A third approach is to subdivide the continuous system into N segments and then represent each of these segments by lumped parameters. In this section the lumped parameter approach will be of primary concern.

The standard way of representing the N non-uniform segments by lumped parameters is to base the parameters on some mean or average uniform section for that particular segment, which is a further approximation to the first case mentioned above, (see Fig. (3.4.1). Duncan[3] derived a general error law for a particular model, which is similar to the model in Fig. (3.4.3) except ℓ_1 always equals ℓ_2, that is used with equal segment lengths to approximate linear non-uniform systems. The goal here is to investigate the lumped parameter representation of a non-uniform segment in a more general manner in an attempt to improve upon Duncan's model and to determine if other models are more appropriate. The work herein will be compared to Duncan's model and the uniform segment approximation.

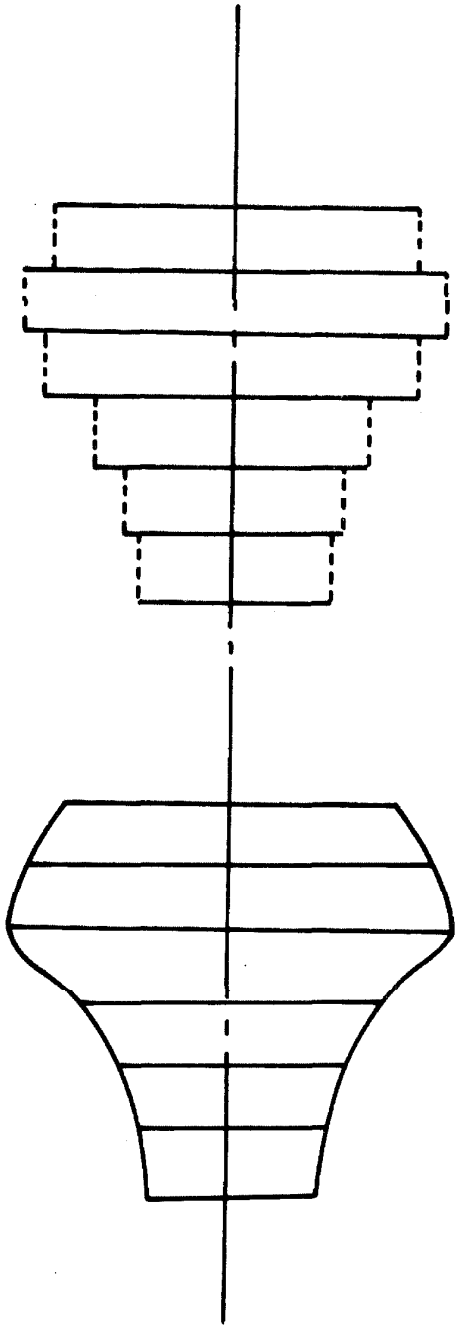
NON-UNIFORM CONTINUOUS ELEMENT
PIECEWISE UNIFORM APPROXIMATION

FIG. 3.4.1

From the investigation of the uniform system, model (b) and model (a) of Fig.(3.3.1)were found to be about equivalent with model (b) being slightly more efficient; therefore, a model similar to model (b) will be employed in this section. When considering how to improve the standard lumped parameter approximation based upon uniform equivalent segments, a natural extension would be to use variable segments of prescribed variation for which simple and accurate lumped parameters are known. For example, in one dimensional non-uniform systems where cross sections are circular the variable radius could be best fitted on a piecewise basis with segments that have a linearly varying radius. Once a general segment with a linearly varying radius is well approximated in terms of lumped parameters, this model could be applied just as the uniform segments are used and improved results would be anticipated. Figure(3.4.2) indicates how the piecewise linear approximation can be employed geometrically for the case of non-uniform, circular cross sectional systems. For convenience the following development treats specifically circular cross sectional systems, but it will be emphasized later that the results apply to much more general systems.

Figure (3.4.3) shows how a linearly tapered increment will be represented by a spring-mass-spring model. This lumped parameter model is essentially the same as model (b), but for the non-uniform segment the springs are not equal; k_1 and k_2 represent the stiffness of the portions of length ℓ_1 and ℓ_2, respectively. The transmission matrix for this lumped model is:

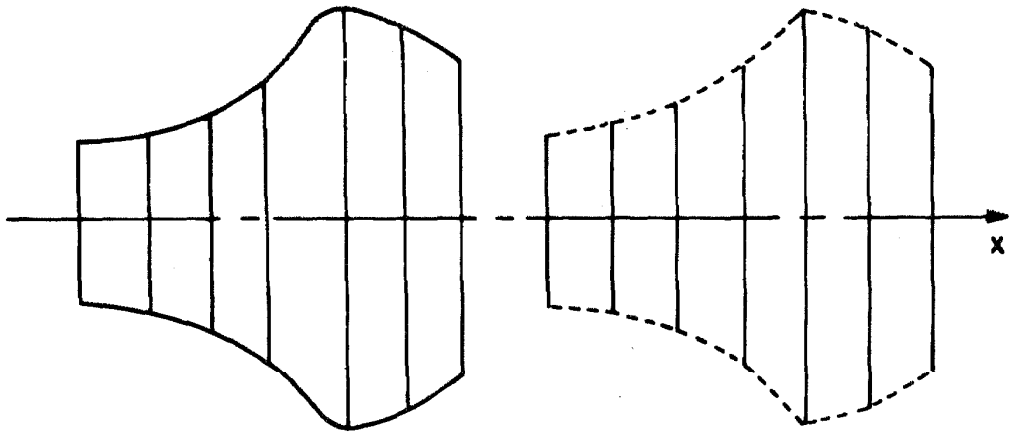

NON-UNIFORM SYSTEM

PIECEWISE LINEAR TAPER APPROXIMATION

FIG. 3.4.2

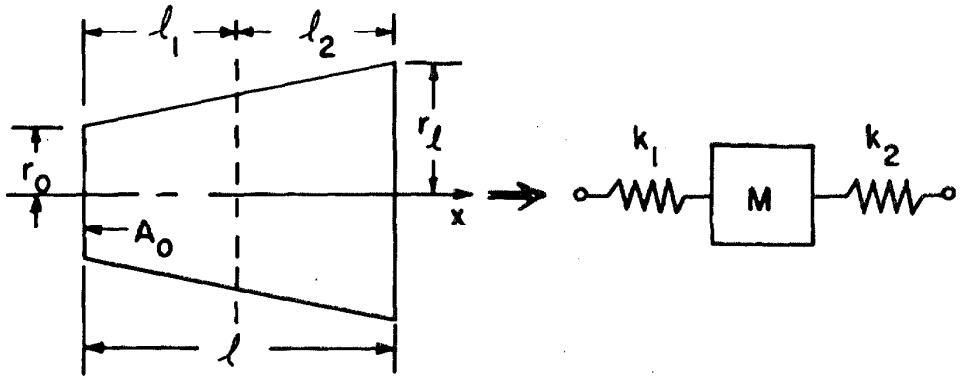

LINEARLY TAPERED SEGMENT

LUMPED PARAMETER REPRESENTATION OF A SEGMENT WITH A LINEAR TAPER

FIG. 3.4.3

$$[L] = \begin{bmatrix} 1 - \frac{M\omega^2}{k_2} & -M\omega^2 \\ \frac{1}{k_1} + \frac{1}{k_2} - \frac{M\omega^2}{k_1 k_2} & 1 - \frac{M\omega^2}{k_1} \end{bmatrix} . \quad (3.4.1)$$

It will be shown that the L_{12} term and the first part of L_{21}, $(1/k_1 + 1/k_2)$, are fixed for any given increment. The L_{11} and L_{22} terms are functions of ℓ_1 and ℓ_2, however, and they can be adjusted by the choice of these lengths. To define a criterion for choosing ℓ_1 and ℓ_2, the lumped parameter matrix will be compared and adjusted to approximate the exact transmission matrix for a continuous linearly tapered segment.

Several types of tapered systems commonly encountered in practical vibration problems can be included in the two following groups:

Group I: Cross sectional area which varies quadratically with the spatial variable. A common example is the solid circular cross section with a linearly varying radius. Another is the solid rectangular cross section where height and width both vary linearly.

Group II: Cross sectional area which varies linearly with the spatial variable. Examples are: circular, thin wall,

cross sections where radius varies linearly, and solid or thin wall rectangular cross sections where one lateral dimension remains constant and the other varies linearly.

Recalling that the area function was given in Section 3.2 as:

$$A(x) = A_o \left(1 + \frac{\xi x}{\ell}\right)^{2p-1}$$

it can be observed that Group I is characterized by $p = 1.5$ and Group II by $p = 1.0$ where the definition of ξ was given as:

$$\xi = \frac{\sqrt{A_\ell} - \sqrt{A_o}}{\sqrt{A_o}}$$

where:

A_ℓ = area at the output end of a segment

A_o = area at the endput end of a segment.

As mentioned above the following development is specifically for circular cross sectional systems, but with the above definition of ξ there is no loss of generality and the results apply equally well to all other systems belonging to Groups I or II. The name "linear taper model" comes only from the geometrical fact that the radius does vary linearly for circular cross sectional systems of the two groups to be considered.

Group I is defined by $p = 3/2$; therefore, the exact transmission matrix can be obtained from Case II in Section 3.2. Using the following relationships:

$$J_{1/2}(y) = \sqrt{\frac{2}{\pi y}} \sin y$$

$$J_{-1/2}(y) = \sqrt{\frac{2}{\pi y}} \cos y$$

$$J_{3/2}(y) = \sqrt{\frac{2}{\pi y}} \left[\frac{\sin y}{y} - \cos y\right]$$

$$J_{-3/2}(y) = \sqrt{\frac{2}{\pi y}} \left[\frac{\cos y}{y} + \sin y\right]$$

and the T_{ij} expressions from Case II, the transmission matrix terms for the continuous, linearly tapered element for Group I can be written in terms of trigonometric functions as:

$$T_{11}(\ell) = \frac{f}{g}\left(\frac{\sin\beta}{f\beta} + \cos\beta\right) \tag{3.4.2}$$

$$T_{12}(\ell) = -\left(\frac{g}{f}\right) z_o(\beta)\left(\sin\beta + \frac{\sin\beta}{(fg)\beta^2} + \frac{(f-g)}{fg}\cos\beta\right) \tag{3.4.3}$$

$$T_{21}(\ell) = \left(\frac{f}{g}\right)\frac{1}{z_o}\left(\frac{\sin\beta}{\beta}\right) \tag{3.4.4}$$

$$T_{22}(\ell) = \left(\frac{g}{f}\right)\left(\cos\beta - \frac{\sin\beta}{g\beta}\right) \tag{3.4.5}$$

The transmission matrix which describes Group II, $p = 1$, is obtained from Case I in Section 3.2. The terms for this matrix remain in Bessel function form.

$$T_{11}(\ell) = \beta\{Y_o(g\beta)J_1(f\beta) - Y_1(f\beta)J_o(g\beta)\} \tag{3.4.6}$$

$$T_{12}(\ell) = z_o \left(\frac{g}{2\pi}\right) \beta^2 \{Y_1(f\beta)J_1(g\beta) - Y_1(g\beta)J_1(f\beta)\} \qquad (3.4.7)$$

$$T_{21}(\ell) = -\frac{1}{z_o} \left(\frac{f}{2\pi}\right) \{Y_o(f\beta)J_o(g\beta) - Y_o(g\beta)J_o(f\beta)\} \qquad (3.4.8)$$

$$T_{22}(\ell) = \left(\frac{g}{2\pi}\right) \beta\{Y_o(f\beta)J_1(gB) - Y_1(g\beta)J_o(f\beta)\} \quad . \qquad (3.4.9)$$

Equations (3.4.2) through (3.4.9) must be expanded in series form to be compared to the matrix elements in expression (3.4.1). For the first group the trigonometric series can be used which immediately gives:

$$T_{11}(\ell) = 1 - \beta^2 \left[\frac{(\xi+3)}{6(1+\xi)}\right] + O(\beta^4) \qquad (3.4.10)$$

$$T_{12}(\ell) = -\frac{A_o E}{\ell} \{1+\xi+\xi^2/3\}\beta^2 + O(\beta^4) \qquad (3.4.11)$$

$$T_{21}(\ell) = \frac{\ell}{A_o E} \left(\frac{1}{1+\xi}\right) \{1-\beta^2/6\} + O(\beta^4) \qquad (3.4.12)$$

$$T_{22}(\ell) = 1 - \beta^2 \left[\frac{2\xi+3}{6}\right] + O(\beta^4) \quad . \qquad (3.4.13)$$

To expand the second group for lower order terms in β is somewhat more difficult because of the behavior of $Y_o(\beta)$. For small arguments $Y_o(\beta) \sim \frac{2}{\pi} \ell n(\beta)$; therefore, $Y_o(\beta) \to \infty$ as $\beta \to 0$ and $Y_o(\beta)$ can not be expanded directly in a power series of the form:

$$a_o + a_1 x + a_2 x^2 + \ldots\ldots\ldots + a_n x^n \quad .$$

The approach used to obtain a converging power series, valid for small β, is to expand the T_{ij} functions directly in a Maclaurin's series. This may, in general, be done for any continuous function

that possesses finite derivatives.

Applying the Maclaurin series:

$$T_{ij}(\beta) = T_{ij}(o) + \beta T'_{ij}(o) + \frac{\beta^2}{2!} T''_{ij}(o) + \ldots + \frac{\beta^N}{N!} T^N_{ij}(o) + R_N$$

and using l'Hospital's rule to evaluate indeterminate forms gives:

$$T_{11}(\ell) = 1 + \frac{\beta^2}{2}\left[\frac{f^2-g^2}{2} + f^2 \ell n(g/f)\right] + O(\beta^4) \qquad (3.4.14)$$

$$T_{12}(\ell) = \frac{EA_o}{\ell}\left[\left(\frac{\beta^2}{2}\right)\frac{f^2-g^2}{f}\right] + O(\beta^4) \qquad (3.4.15)$$

$$T_{21}(\ell) = \frac{\ell}{A_o E} f\, \ell n(g/f)\left[1 - \left(\frac{\beta^2}{2}\right)\frac{f^2+g^2}{2}\right] + O(\beta^4) \qquad (3.4.16)$$

$$T_{22}(\ell) = 1 - \frac{\beta^2}{2}\left[\frac{f^2-g^2}{2} + g^2 \ell n(g/f)\right] + O(\beta^4) \quad . \qquad (3.4.17)$$

To check the validity of the series expansions in Eq. (3.4.10) through (3.4.17) the condition that $\xi \to 0$, which is the uniform rod in the limit, can be imposed. Completing this for both groups above gives expressions which agree with the lower order terms in the series for the E_{ij} elements which were given in Section 3.2.1.

As mentioned earlier the L_{12} term and the first part of the L_{21} term, $(1/k_1 + 1/k_2)$, from expression (3.4.1) are fixed for any given increment. This can be illustrated by using the appropriate relationships for M and ω which shows that the lower order terms in Eqs. (3.4.11) and (3.4.15) are always identical to L_{12}. Likewise, by using the appropriate k_1 and k_2 expressions from Appendix C, it can be shown that the order unity term in Eqs. (3.4.12) and (3.4.16) is always equal to $(1/k_1 + 1/k_2)$. The two remaining terms

which can be used to define the subdivision of a segment are L_{11} and L_{22}. The choice of ℓ_1 and ℓ_2 is based upon minimizing the difference between the lower order terms in T_{11} and T_{22} and those in expressions for L_{11} and L_{22}, respectively. Proceeding in this manner gives:

$$\eta = \ell_1/\ell \qquad \text{and} \qquad \ell_1 + \ell_2 = \ell \quad .$$

For Group I:

$$k_1 = (1+\xi\eta)\ \frac{A_o E}{\ell_1}$$

$$k_2 = (1+\xi)(1+\xi\eta)\ \frac{A_o E}{\ell_2}$$

$$M\omega^2 = \frac{A_o E}{\ell}\ \{1 + \xi + \xi^2/3\}\beta^2 \quad .$$

Therefore,

$$L_{11} = 1 - \frac{M\omega^2}{k_2} = 1 - \frac{(1-\eta)}{(1+\xi)(1+\xi\eta)}\ (1+\xi+\xi^2/3)\beta^2$$

$$L_{22} = 1 - \frac{M\omega^2}{k_1} = 1 - \frac{\eta}{(1+\xi\eta)}\ \{1+\xi+\xi^2/3\}\beta^2 \quad .$$

Consequently, for ϵ_{11} and ϵ_{22} (where $\epsilon_{ij} = T_{ij} - L_{ij}$):

$$\epsilon_{11} = \left[\frac{(1-\eta)(1+\xi+\xi^2/3)}{(1+\xi)(1+\xi\eta)} - \frac{\xi+3}{6(1+\xi)}\right]\beta^2$$

$$\epsilon_{22} = \left[\frac{\eta}{(1+\xi\eta)}\ (1+\xi+\xi^2/3) - \frac{2\xi+3}{6}\right]\beta^2 \quad .$$

Then setting $\epsilon_{ij} = 0$ to equate the coefficient of the $O(\beta^2)$ term in L_{11} and L_{22} to that in T_{11} and T_{22} respectively, gives the following expression in both cases.

$$\eta_I = \frac{2\xi+3}{3(\xi+2)} \quad . \tag{3.4.18}$$

For Group II:

$$k_1 = \frac{A_o E}{\ell_1} \frac{\eta\xi}{\ell n(1+\eta\xi)}$$

$$k_2 = \frac{EA_o}{\ell_2} \frac{\xi(1-\eta)}{\ell n[(1+\xi)/(1+\eta\xi)]}$$

$$M\omega^2 = \frac{A_o E}{\ell} (1+\xi/2)\beta^2 \quad .$$

Setting ϵ_{11} and ϵ_{22} equal to zero as before gives an expression, which is the same in both cases, for η_{II}.

$$\eta_{II} = \frac{1}{\xi}\left[\left((1+\xi)^b e^{-c}\right)^{1/a} - 1\right] \tag{3.4.19}$$

where:

$$b = 2(1+\xi)^2$$

$$c = \xi(2+\xi)$$

$$a = 2\xi(2+\xi) \quad .$$

A check on both η_I and η_{II} for $\xi \to 0$, which again is the uniform case, shows that $\eta_{I,II} \to 1/2$ as $\xi \to 0$ in the limit. This is exactly the condition used for model (b) in representing the uniform system. Figure (3.4.4) shows how η_I and η_{II} vary as a function of ξ, the slope parameter for a given linearly tapered segment.

Having defined a basic procedure for determining the lumped parameters of the linear taper model, the second step is to evaluate this model. This was accomplished by comparing the non-dimensional

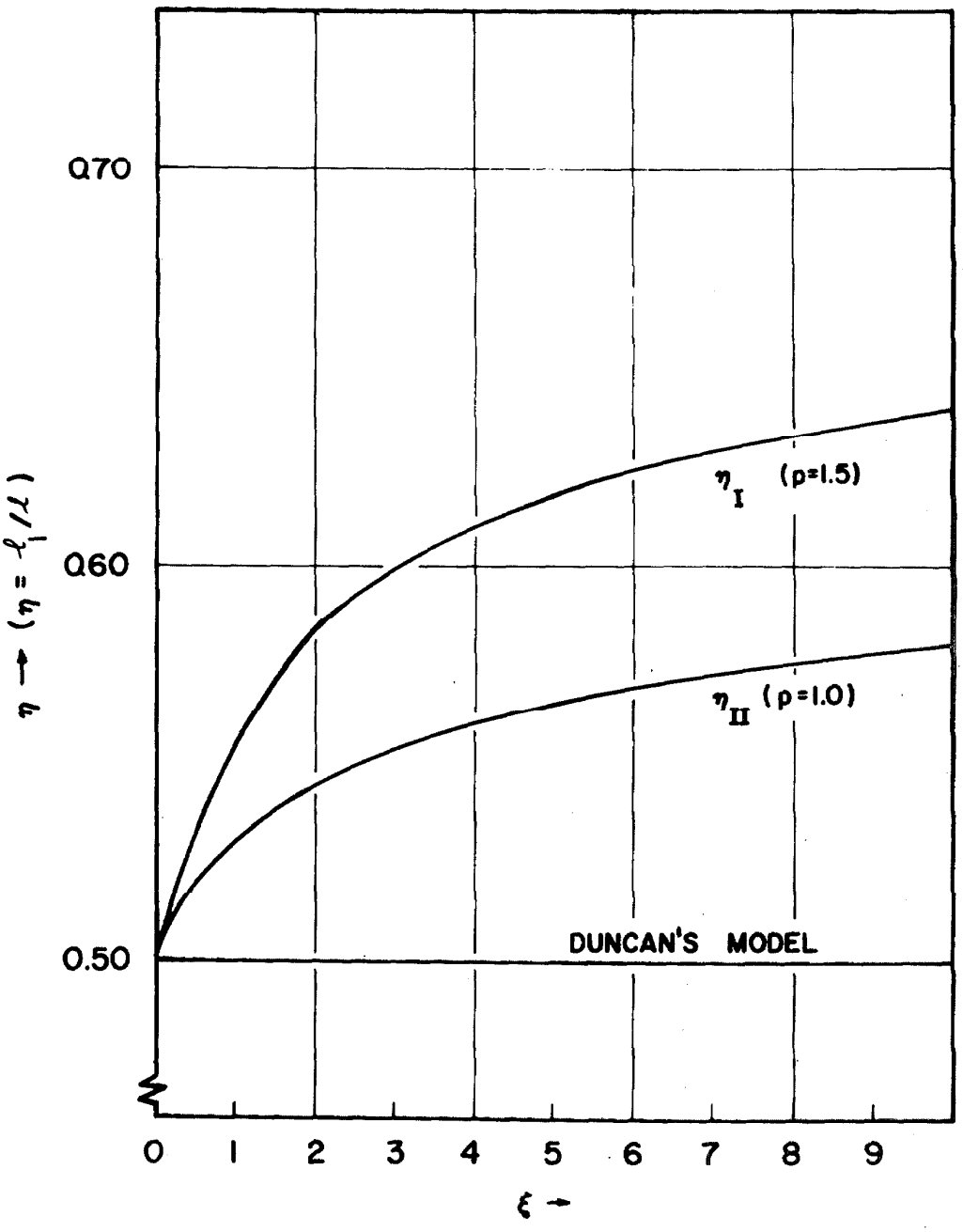

Fig. 3.4.4 Subdividing Parameter for the Linear Taper Model.

frequency root errors obtained by this model with those of Duncan's model and those from the piecewise uniform approximation. A continuous linearly tapered system with various boundary conditions as used in Section 3.3 was used as a basis for this comparison. Duncan's model uses $\eta = 1/2$ independent of the slope parameter but is otherwise similar to the linear taper model. Model (b), as described in Section 3.3, was used to describe the parameters in the piecewise uniform approximation, and the mean area of each segment was used in expressions involving area. The first two normal modes for all four boundary conditions of various linearly tapered elements subdivided into N equal length segments were used in the comparison of the frequency root errors. This comparison was accomplished numerically because the incremental transmission matrices are not functionally interrelated so that a single expression could be formulated for the product of N such matrices. An investigation into the use of unequal length segments is presented in Section 3.5.

The basic recurrence relationships that follow apply to Fig. (3.4.5) which depicts a general linearly tapered element divided into N segments. The i^{th} segment is further subdivided as shown in Fig. (3.4.3) and the parameters are calculated on the basis of Eqs. (3.4.18) and (3.4.19) for cases in Group I or Group II, respectively. If the following recurrence relationships are used:

$$\ell_i = L/N \quad ; \quad r_i = r_o \left(1 + i \frac{\xi}{N}\right) \quad i = 1, 2, 3, \ldots N-1$$

$$A_i = A_o \left(1 + \frac{i\xi}{N}\right)^2 \quad ; \quad \xi = \frac{r_N - r_o}{r_o} \quad ; \quad \beta_i = B/N \quad ;$$

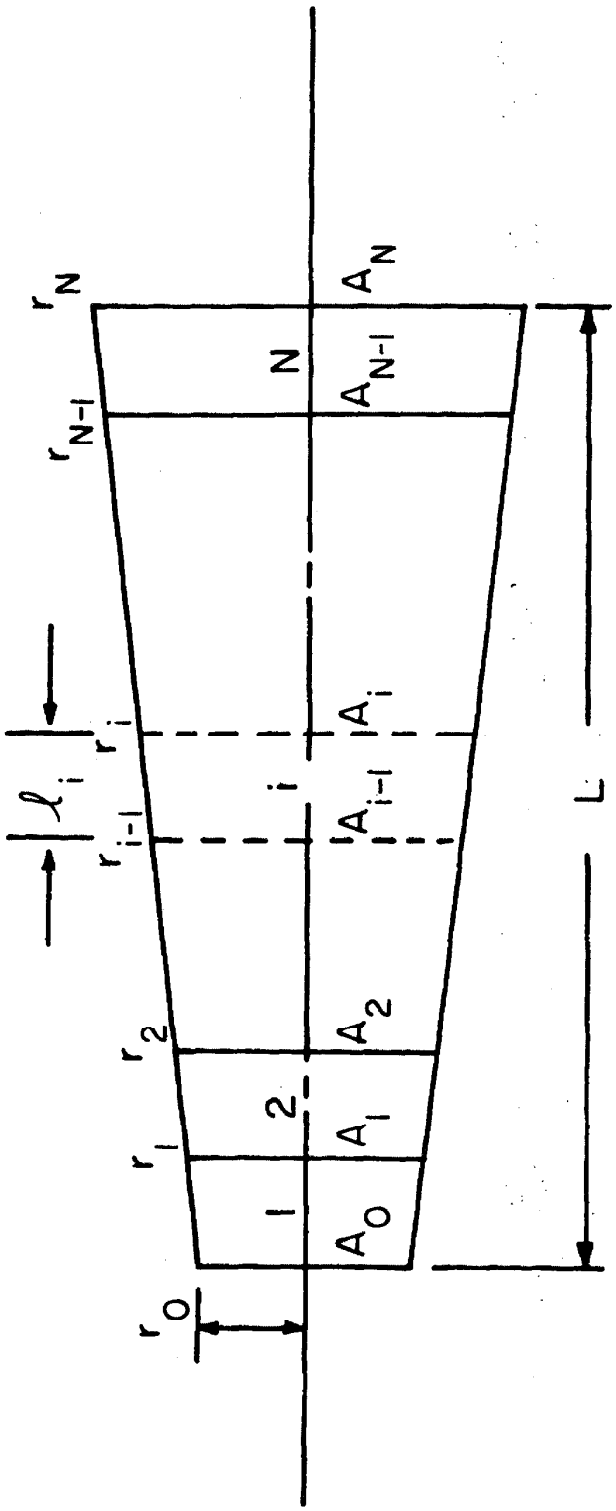

LINEARLY TAPERED ELEMENT SUBDIVIDED INTO N SEGMENTS

FIG. 3.4.5

$$\xi_i = \frac{r_i - r_{i-1}}{r_{i-1}} \quad ; \quad g_i = 1 + f_i \quad ; \quad \text{and} \quad f_i = 1/\xi_i$$

then for Group I the lumped parameters for the i^{th} segment are:

$$\left.\begin{aligned} k_{i_1} &= (1+\xi_i\eta_i)\ \frac{A_{i-1}E}{\ell_{i_1}} \\ k_{i_2} &= (1+\xi_i)(1+\xi_i\eta_i)\ \frac{A_{i-1}E}{\ell_{i_2}} \\ M_i\omega^2 &= \frac{A_{i-1}E}{\ell_i}\left(1+\xi_i+\frac{\xi_i^2}{3}\right)\beta_i^2 \end{aligned}\right\} \quad . \qquad (3.4.20)$$

For Group II the lumped parameters for the i^{th} segment become:

$$\left.\begin{aligned} k_{i_1} &= \frac{\eta_i\xi_i}{\ell n(1+\eta_i\xi_i)}\ \frac{A_{i-1}E}{\ell_{i_1}} \\ k_{i_2} &= \frac{\xi_i(1-\eta_i)}{\ell n[(1+\xi_i)/(1+\eta_i\xi_i)]}\ \frac{EA_{i-1}}{\ell_{i_2}} \\ M_i\omega^2 &= \frac{EA_{i-1}}{\ell_i}\left(1+\frac{\xi_i}{2}\right)\beta_i^2 \end{aligned}\right\} \quad . \qquad (3.4.21)$$

For both Group I and Group II the following relationships with appropriate terms from expressions (3.4.20) and (3.4.21) become applicable for the L_{ij} terms of the incremental transmission matrices.

$$\left.\begin{aligned} L_{11}(\ell_i) &= 1 - \frac{M_i\omega^2}{k_{i_2}} \quad ; \quad L_{12}(\ell_i) = -M_i\omega^2 \\ L_{21}(\ell_i) &= \frac{1}{k_{i_1}} + \frac{1}{k_{i_2}} - \frac{M_i\omega^2}{k_{i_1}k_{i_2}} \quad ; \quad \text{and} \\ L_{22}(\ell_i) &= 1 - \frac{M_i\omega^2}{k_{i_1}} \end{aligned}\right\} \quad . \qquad (3.4.22)$$

The numerical procedure used to evaluate the frequency root errors was similar to that used in Section 3.3 for the uniform system. Using the recurrence relationships in (3.4.20) or (3.4.21) and, subsequently, those in (3.4.22), the overall lumped parameter transmission matrix for the element was determined. The frequency roots for the four various boundary conditions were found iteratively and substracted from the roots obtained using Eqs. (3.4.2) through (3.4.5) or Eqs. (3.4.6) through (3.4.9), which represent the continuous linearly tapered systems for Group I and II, respectively. The round-off error which occurs when N incremental transmission matrices are numerically multiplied together was also determined. This was accomplished by using the T_{ij} matrix for the continuous system at the incremental level, numerically multiplying these N matrices, and comparing the elements of the resulting matrix to those of the T_{ij} matrix as expressed for the total element. This evaluation indicated a negligible difference between the elements of the respective matrices. In the iterative solution for the frequency roots the Aitken algorithm[20] was used for interpolation of the zeros. Three points about the zero crossings were used in conjunction with this interpolation algorithm and the increments in the independent variable, β, were chosen to obtain good resolution within the region containing the zero.

The results for the frequency root evaluation are shown in Figs. (3.4.6) through (3.4.12). When plotting the errors $(e_{\nu N})$ directly as functions of N, the behavior was found to be similar to

model (b) in the uniform case. For large N the error decreases as α/N^2, where α is some constant. To compress the data into a more usable form the constant α, which has been designated the error constant, is plotted as a function of ξ which is the slope parameter for the overall element. To find the percentage error of any given frequency root the following relationship applies to these figures:

$$\alpha(\text{error constant}) \times \frac{100}{N^2} = \text{percentage error.} \qquad (3.4.23)$$

To use Figs. (3.4.6) through (3.4.12) in determining the percentage error in the non-dimensional frequency root, one proceeds as follows:

1. Determine ξ for the overall element,
2. from the figures obtain the error constant, and
3. use Eq. (3.4.23) to calculate the percentage error.

These figures apply to any system belonging to Groups I or II which are subdivided into N equal length segments which are, in turn, described by the various lumped parameter models. Results for Duncan's model and the piecewise uniform model are given only in Figs. (3.4.6) through (3.4.10)for comparison with the linearly tapered model in Group I. It should be emphasized that all three models have the same error constant in the limit where $\xi = 0$. Because of its definite improvement, only the results for the linearly tapered model are shown for Group II in Figs. (3.4.11) and (3.4.12). The error constants in these figures are based on large N. When using these figures for small N (N = 4 or 5) the error constant will differ from the correct

value by as much as one to five per cent.

Several general conclusions can be reached after reviewing the results on the linearly tapered model. In the first mode, the linearly tapered model is better than Duncan's model except in the fixed-free condition, and it is considerably better than the piecewise uniform approximation in all instances except the free-free condition. A comparison of these three approaches for the second normal mode shows similar results. In addition, the error constant for the linear taper model varies much less than the other two models as ξ, the slope parameter, changes. Although the error level still varies somewhat between the various boundary conditions used, the linear taper model minimizes these variations for any given ξ value, providing some assurance of better results with this model under arbitrary boundary conditions. Table(3.4.A), which shows the number of segments required by each model to insure an error equal to or less than one per cent for the first model with the four boundary conditions, clearly shows the efficiency of the linearly tapered model in comparison to the other models. For this illustration, a slope parameter of four ($\xi = 4.0$) was chosen.

TABLE 3.4.A*

	Number of Segments Required		
Boundary Conditions	Linear Taper Model	Duncan's Model	Piecewise Uniform Model
Fixed-Free	4	7	11
Free-Free	8	9	12
Free-Fixed	7	8	5
Fixed-Fixed	2	2	14

The basic idea involved in defining the lumped parameters for the linearly tapered segment can be extended further to describe segments with other area variations. It is anticipated that this idea would continue to produce improved lumped parameter models. Moreover, using the linearly tapered model to describe non-uniform elements on a best fit basis should always be superior to the piecewise uniform approximation.

* Based on a non-dimensional frequency root error $\leqslant 1.0\%$ in the first model and a slope parameter of 4.0 for the element.

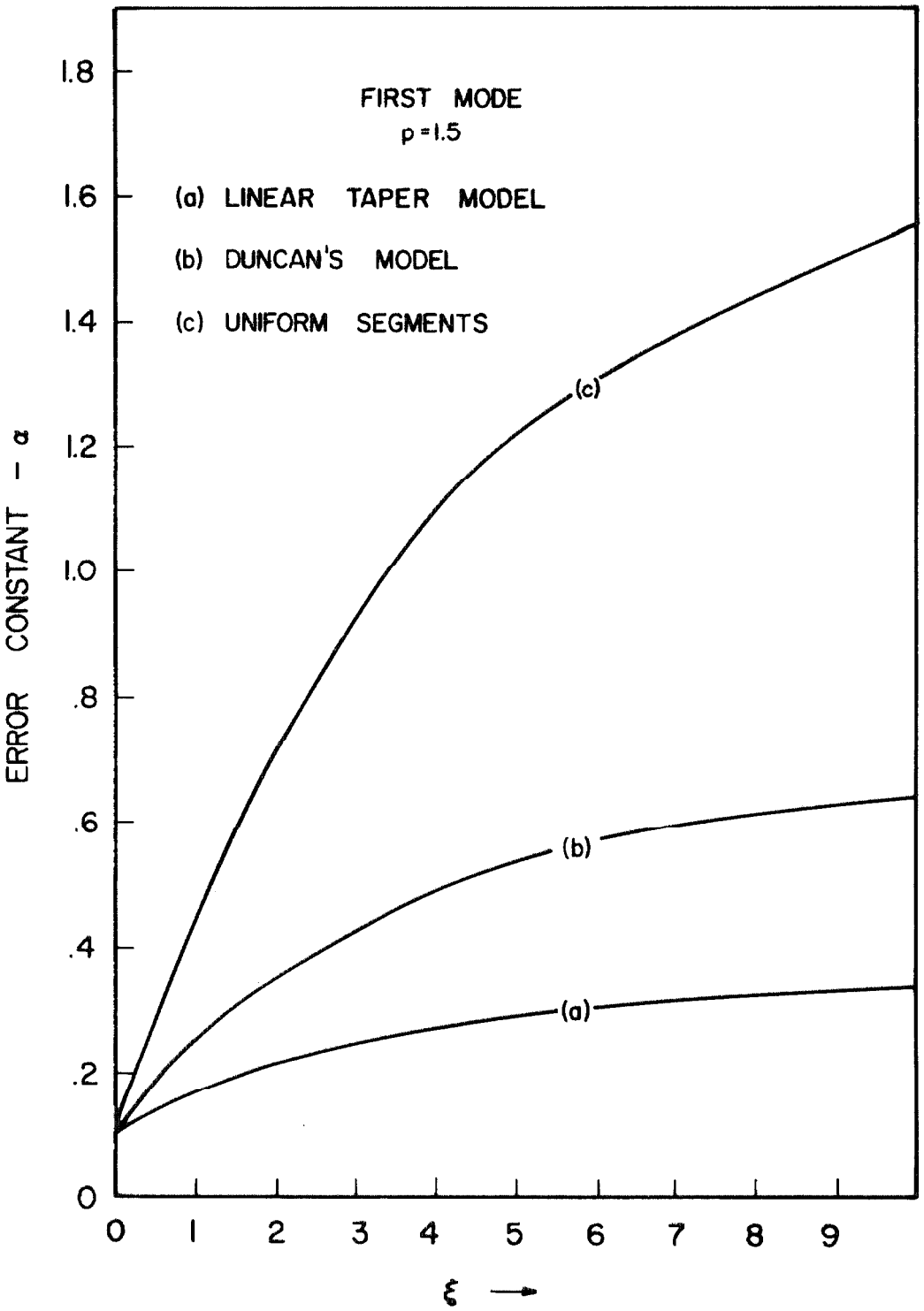

Fig. 3.4.6 Frequency Root Error Constants for Free-Fixed Elements, Group I.

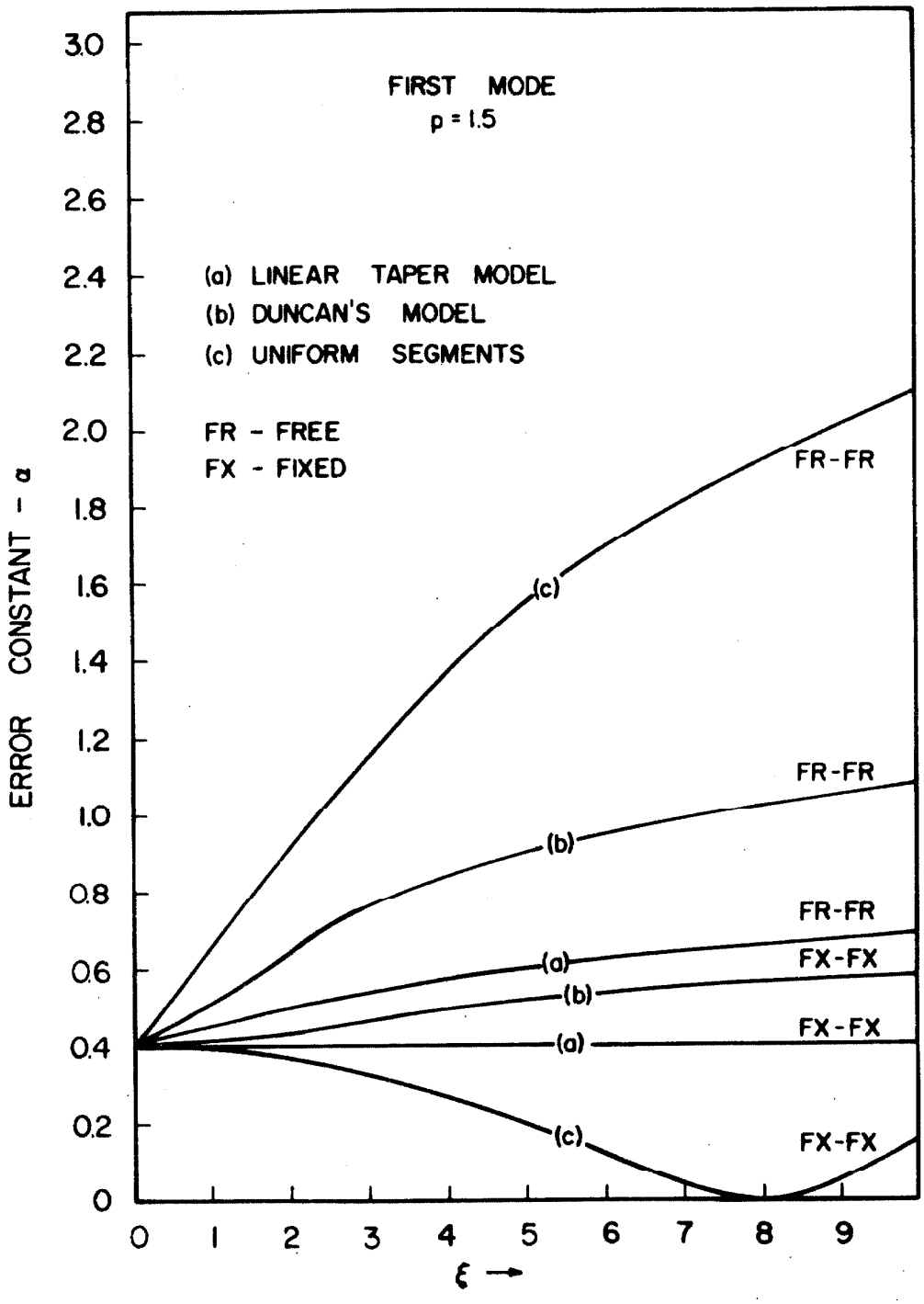

Fig. 3.4.7 Frequency Root Error Constants for Free-Free and Fixed-Fixed Elements, Group I.

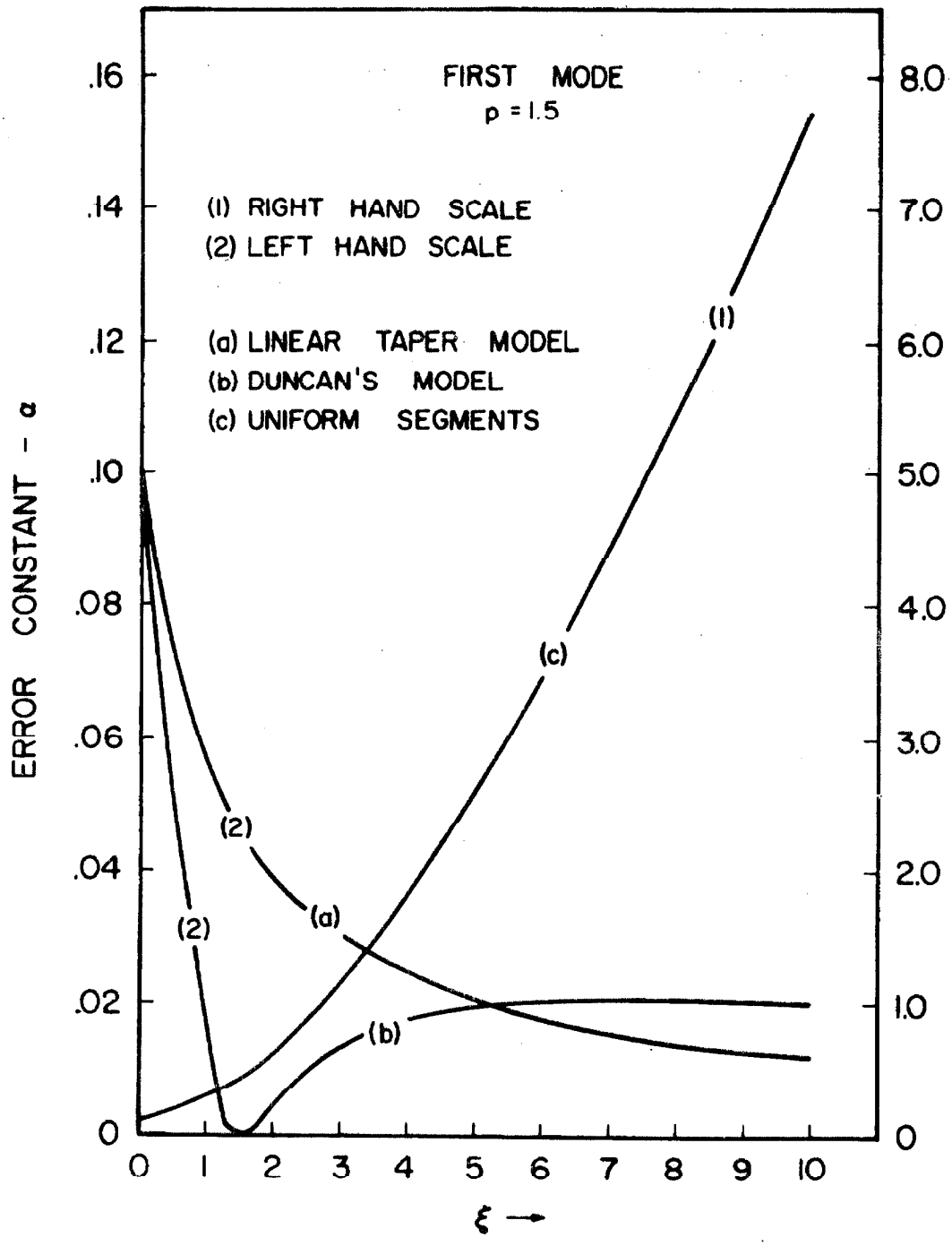

Fig. 3.4.8 Frequency Root Error Constants for Fixed-Free Elements, Group I.

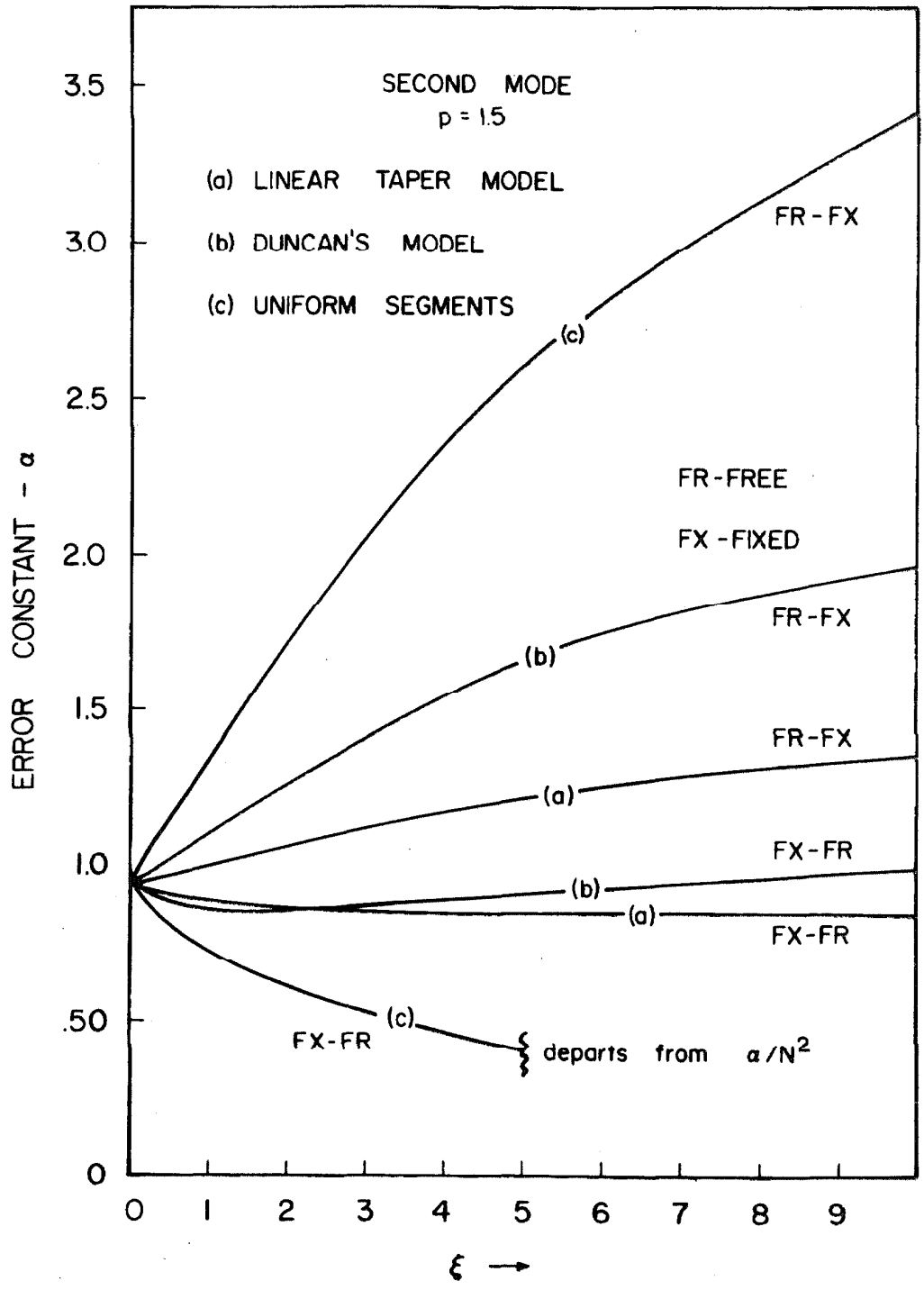

Fig. 3.4.9 Frequency Root Error Constants for Free-Fixed and Fixed-Free Elements, Group I.

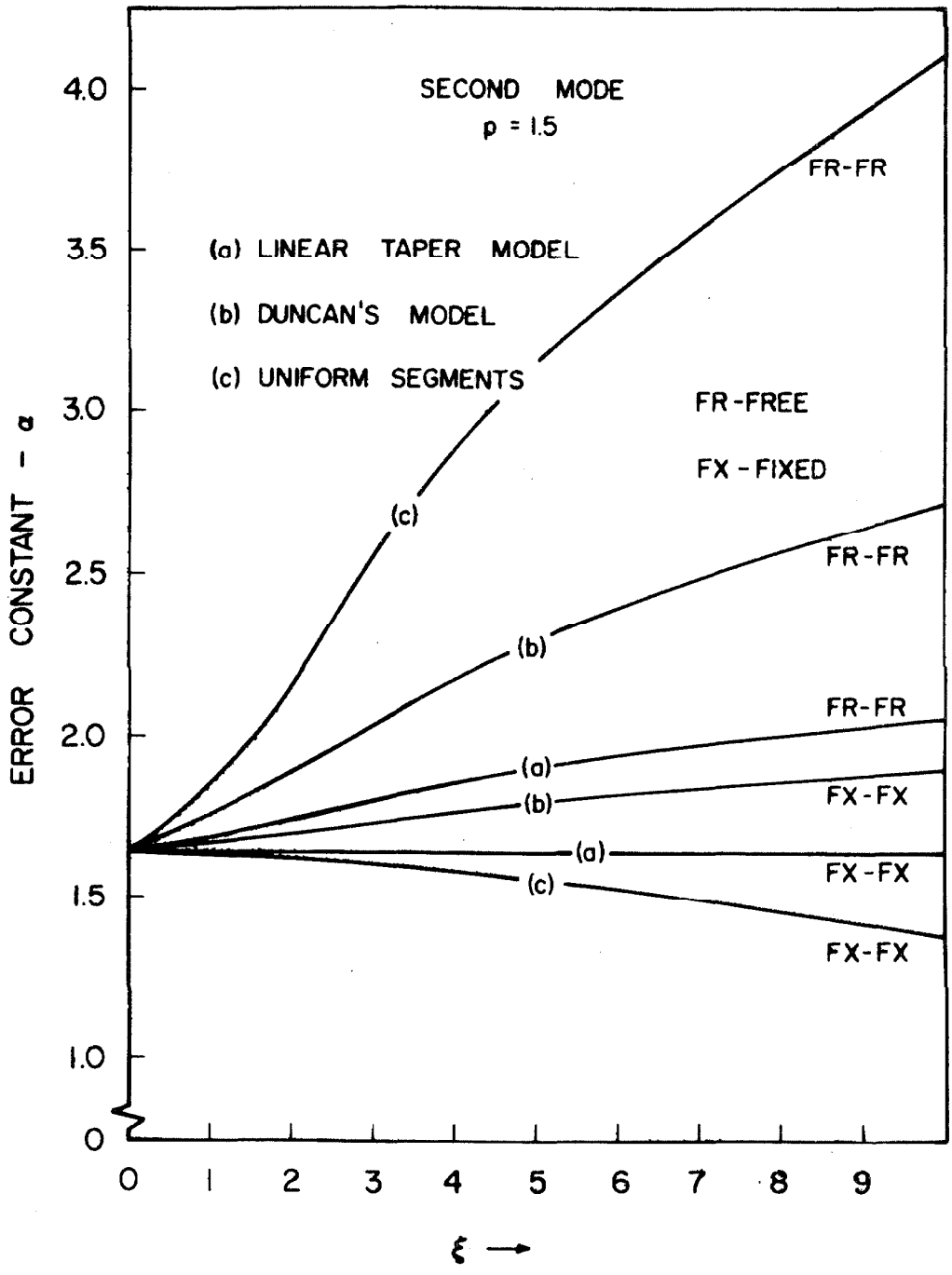

Fig. 3.4.10 Frequency Root Error Constants for Free-Free and Fixed-Fixed Elements, Group I.

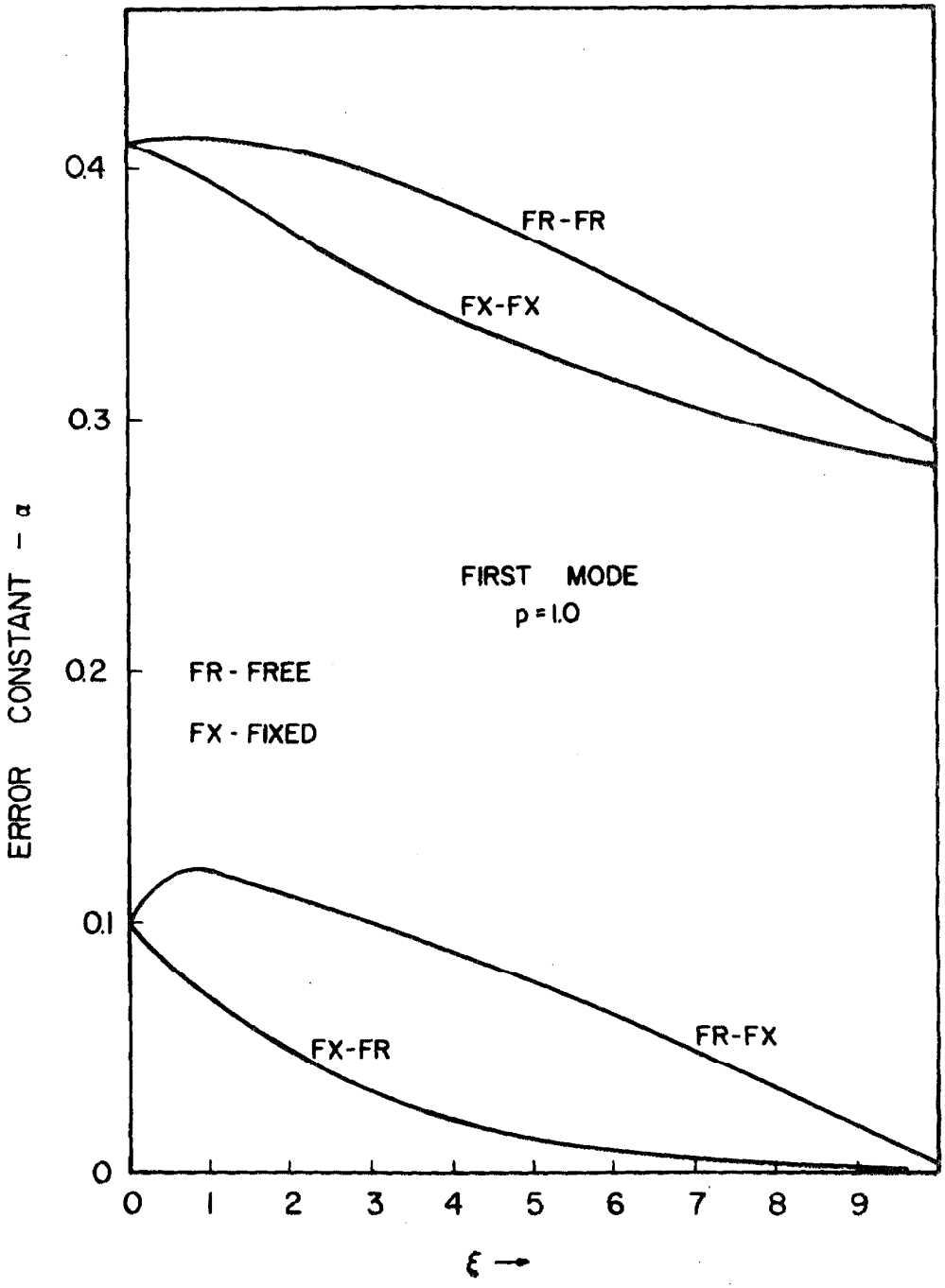

Fig. 3.4.11 Frequency Root Error Constants for Elements from Group II, Linear Taper Model.

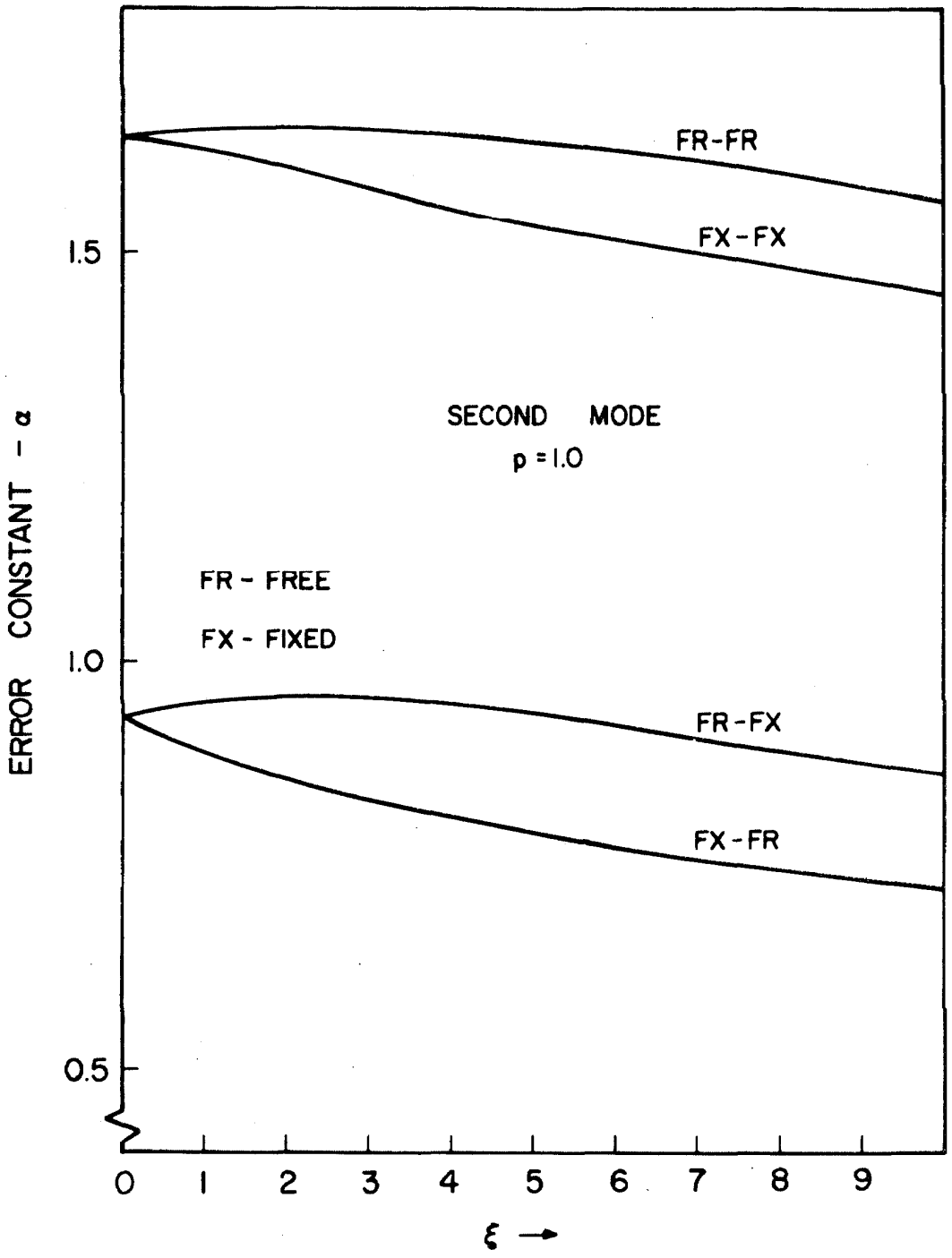

Fig. 3.4.12 Frequency Root Error Constants for Elements from Group II, Linear Taper Model.

3.5 Optimum Segmenting with the Linear Taper Model

The conventional manner in which elements are segmented is to choose N equal length segments. Intuitively, it seems that this may not constitute the most efficient employment of N segments. Thus, the effect of the segment length should be examined.

At the outset, it was hypothesized that there are three other approaches which might yield better results when approximating a linearly tapered continuous element by N segments of the linear taper model. These three approaches correspond to segment lengths, ℓ_i, established on the basis of:

1. Equal segment mass,
2. equal segment stiffness, and
3. linear variation of ℓ_i with respect to position along the element.

The first approach causes segment lengths to decrease as the radius increases, and the second has the opposite effect.

Further investigation of the numerical calculations required for comparing all three approaches indicated that the third hypothesis could be described by recurrence relationships more easily than either the first or second one. Therefore, an investigation based upon the linear variation was completed first with the thought that if definite improvement could be shown by either increasing or decreasing the segment lengths linearly, then further investigation into the effect of the other approaches would be justified.

To evaluate the linear variation in segment lengths a numerical approach similar to that of Section 3.4 was used. A systematic means was devised for selecting the lengths of the N segments being used to approximate a linearly tapered continuous element with a given slope parameter, ξ. The relationships used in determining these segment lengths are (see Fig. 3.4.5):

$$\left.\begin{aligned} \Delta_N &= \left[\frac{1 - \frac{C}{1+\xi}}{N-1}\right] \\ \ell_N\left[1 + \frac{(N-1)C}{1+\xi} + \sum_{j=1}^{N-2} (j)\ \Delta_N\right] &= L \\ \ell_{N-1} &= (1-\Delta_N)\ell_N \\ &\vdots \\ \ell_i &= [1-(N-i)\Delta_N]\ell_N \\ &\vdots \\ \ell_1 &= \left(\frac{C}{1+\xi}\right)\ell_N \end{aligned}\right\} \qquad (3.5.1)$$

where:

N = number of segments

$\xi = \dfrac{r_n - r_o}{r_o}$ for the total element, and

C = a control constant which determines the linear variation of the segment lengths.

When $C = (1+\xi)$ the segment lengths are equal which is equivalent to the case investigated in Section 3.4. When $C < (1+\xi)$ the lengths decrease linearly as the radius increases, and for $C > (1+\xi)$ the lengths increase linearly as the radius increases. In addition, it can be seen that $C < (1+\xi)$ tends in the direction of equal mass segments, and $C > (1+\xi)$ tends to selection of segments with equal stiffnesses.

After determining the segment lengths, ℓ_i, for any particular case, expressions (3.4.20), (3.4.21), and (3.4.22) are used to determine the lumped parameters and the incremental transmission matrices. The final step is determining the non-dimensional frequency root errors as a function of length variation.

The frequency root errors again behaved as α/N^2, and the data can be presented in a form similar to that used previously. Figures(3.5.1) through(3.5.8)illustrate how the error constants vary as segment lengths change. These figures describe the error constants for the first and second normal modes of cases included previously in Groups I and II of Section 3.4 for all four boundary conditions. The solid lines in the figures represent the error constants for equal length segments. To determine if the equal segment length approach is nearly optimum the minimum error constants obtainable through the use of the linear variation process were determined for specific ξ values of 1, 2, 5, 8, and 10. These minimum C values are shown as points in each of the following figures and they are labeled appropriately.

Upon reviewing Figs. (3.5.1) through (3.5.8), several conclusions can be formulated. For the linearly varying segment lengths,

there is a definite trend which minimizes the error constants in most cases. This trend is caused by linearly increasing the segment length as the radius increases, $C > (1+\xi)$. The two main exceptions are the first mode error constants for the fixed-free and the free-fixed boundary conditions. For the free-fixed case, the error constant decreases as $C > (1+\xi)$ and in the other case, fixed-free, the error constant decreases for $C < (1+\xi)$. Although the values of C which minimize the error constants appear in some cases to be appreciably greater than those for the equal length cases, the error constant in these instances is really not greatly improved. In most instances the minimum error constants deviate from those for the equal length segments by an amount of six per cent or less which corresponds to a very small improvement in the frequency root. In one instance, the first mode for the fixed-fixed rod, the error constant could be improved by fifteen per cent by using unequal length segments. In addition, the second mode error constants appear to be less affected than those of the first mode, and Group II is much less affected than Group I by the change to unequal segment lengths.

The basic conclusion or generalization to be made from this investigation is that some improvement can be made by use of unequal segment lengths. When considering the ease and mechanical advantages of using equal length segments, however, as compared to the small gain in improvement with other techniques, it seems that the use of equal length segments is quite satisfactory. If for geometrical or other reasons it is advantageous in some particular instances with

specific boundary conditions to use unequal segment lengths, then these figures are appropriate, and the basic rule of using $C > (1+\xi)$, with an increasing radius, should be observed. In retrospect, it seems that a physical explanation for the behavior of equal length segments could be that the governing relationship for varying cross sections is to keep the mass to stiffness ratio constant as opposed to the suppositions proposed earlier.

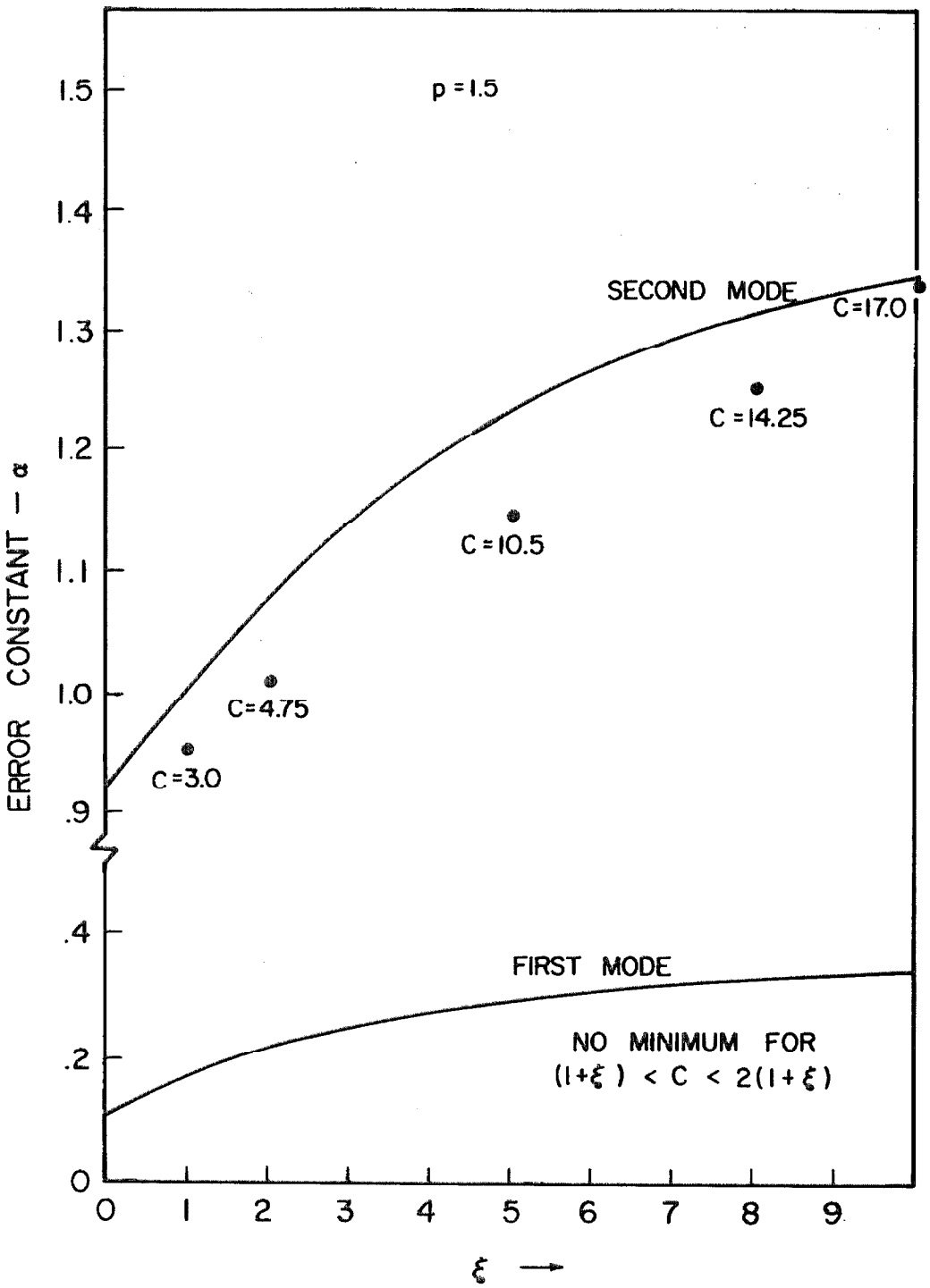

Fig. 3.5.1 Comparison of Frequency Root Error Constants for Free-Fixed Elements with Variable Segment Lengths.

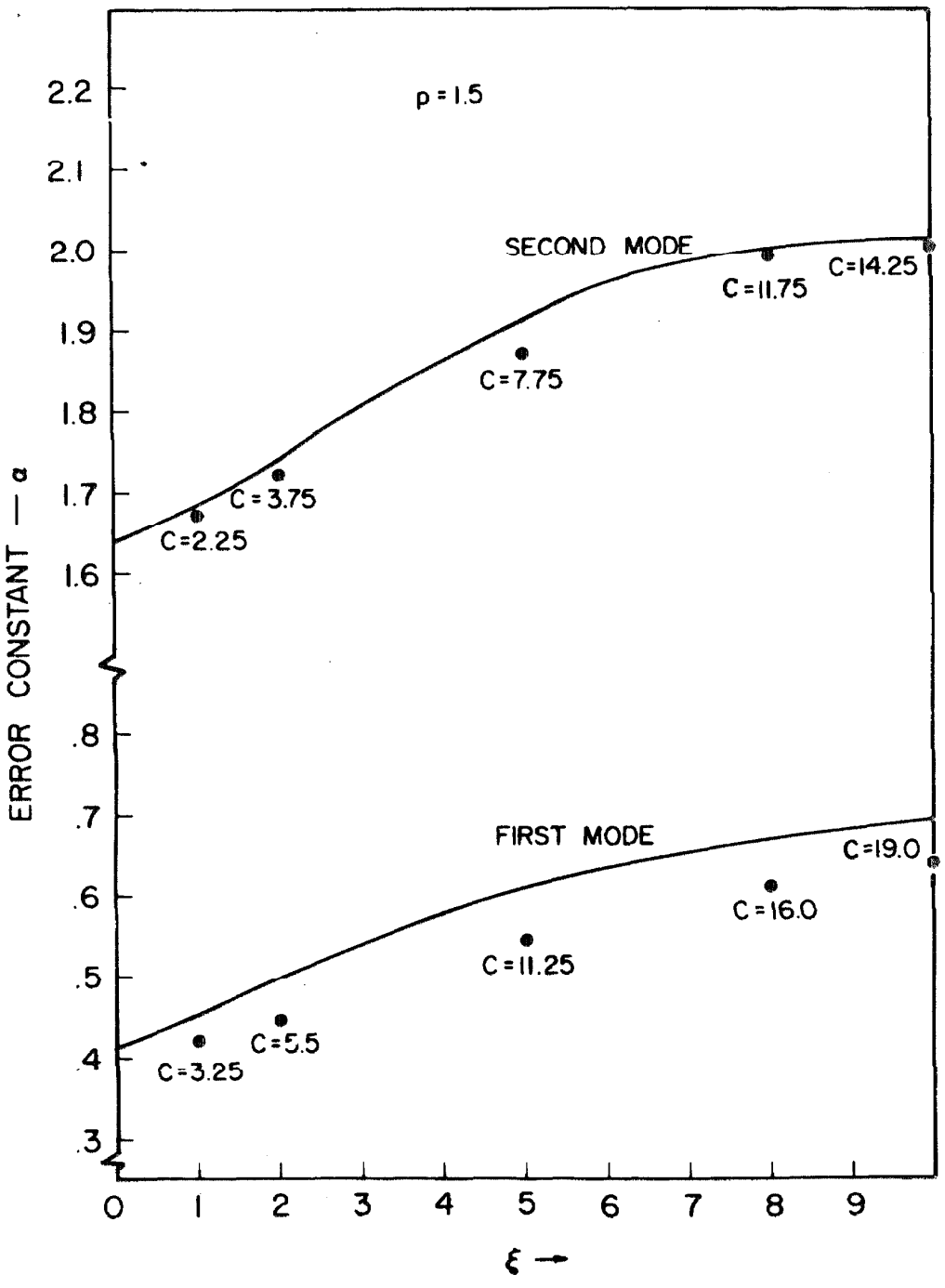

Fig. 3.5.2 Comparison of Frequency Root Error Constants for Free-Free Elements with Variable Segments Lengths.

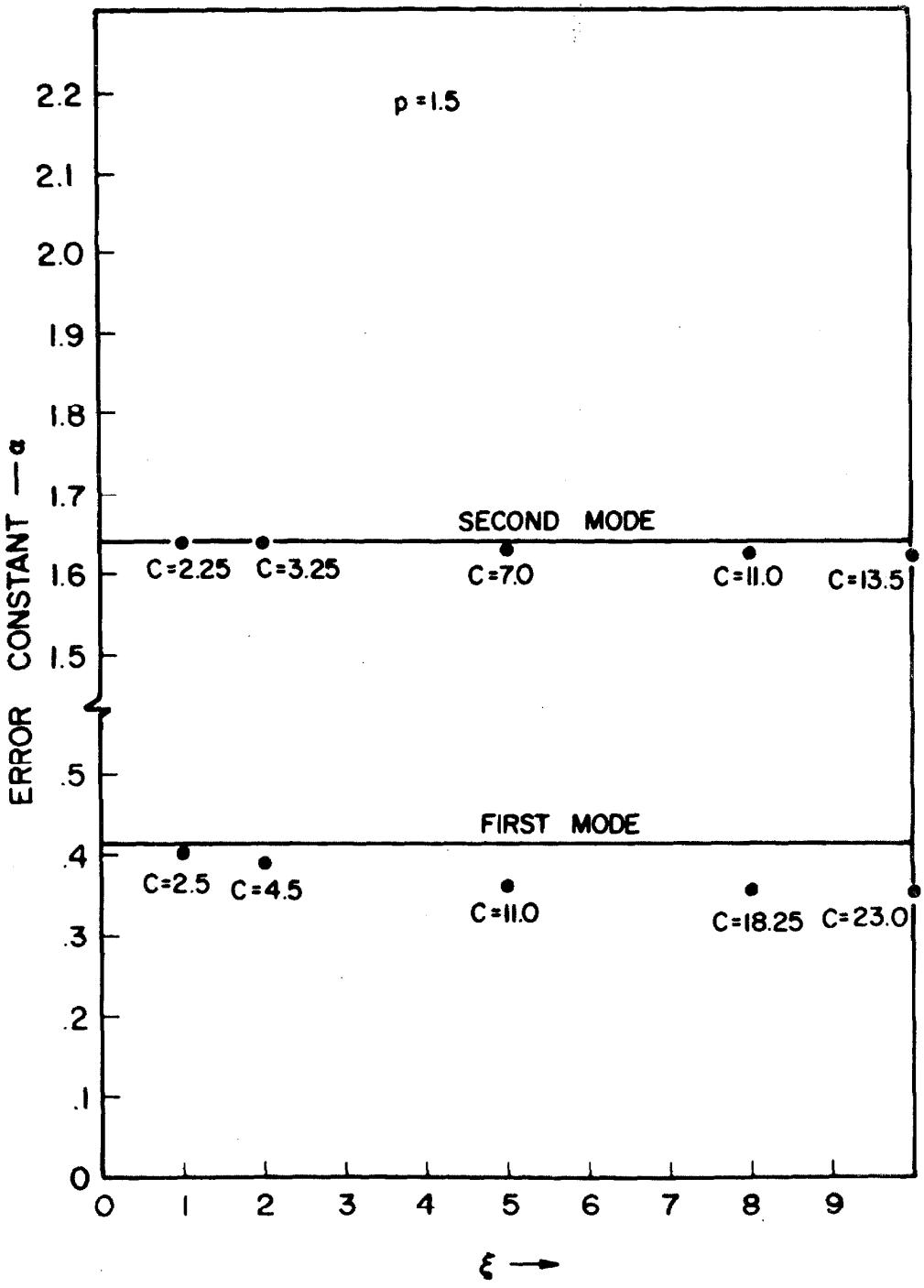

Fig. 3.5.3 Comparison of Frequency Root Error Constants for Fixed-Fixed Elements with Variable Segment Lengths.

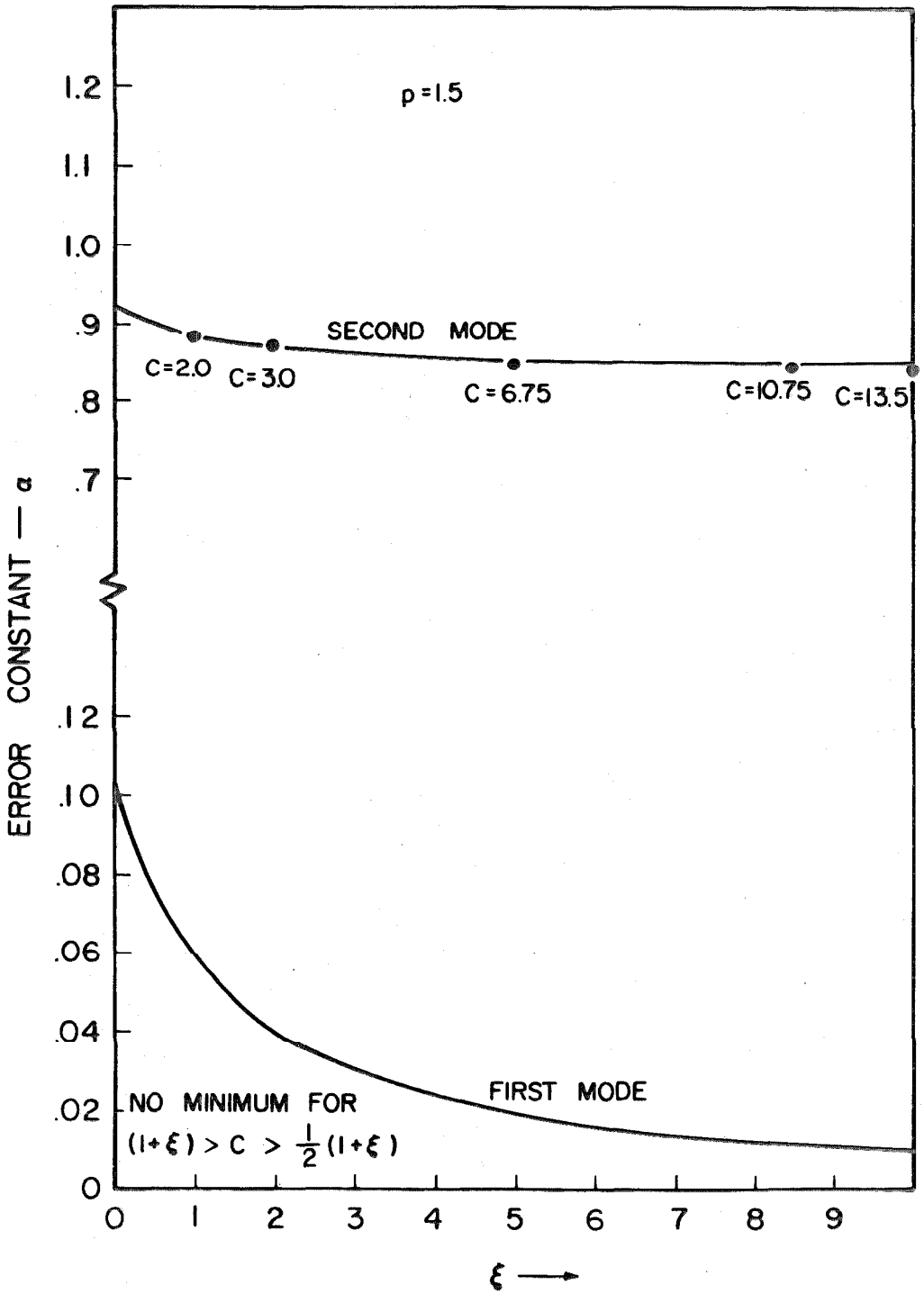

Fig. 3.5.4 Comparison of Frequency Root Error Constants for Fixed-Free Elements with Variable Segment Lengths.

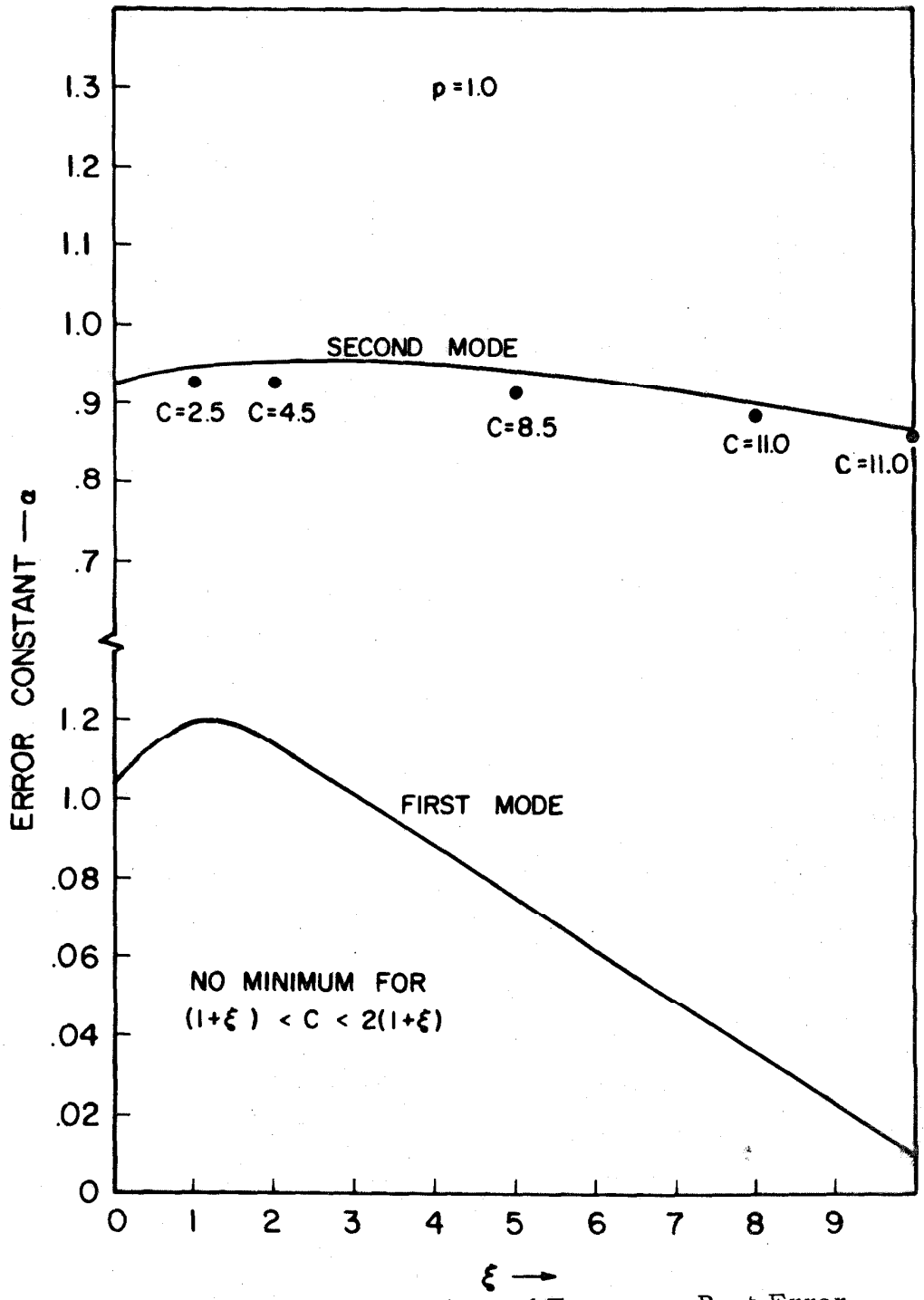

Fig. 3.5.5 Comparison of Frequency Root Error Constants for Free-Fixed Elements with Variable Segment Lengths.

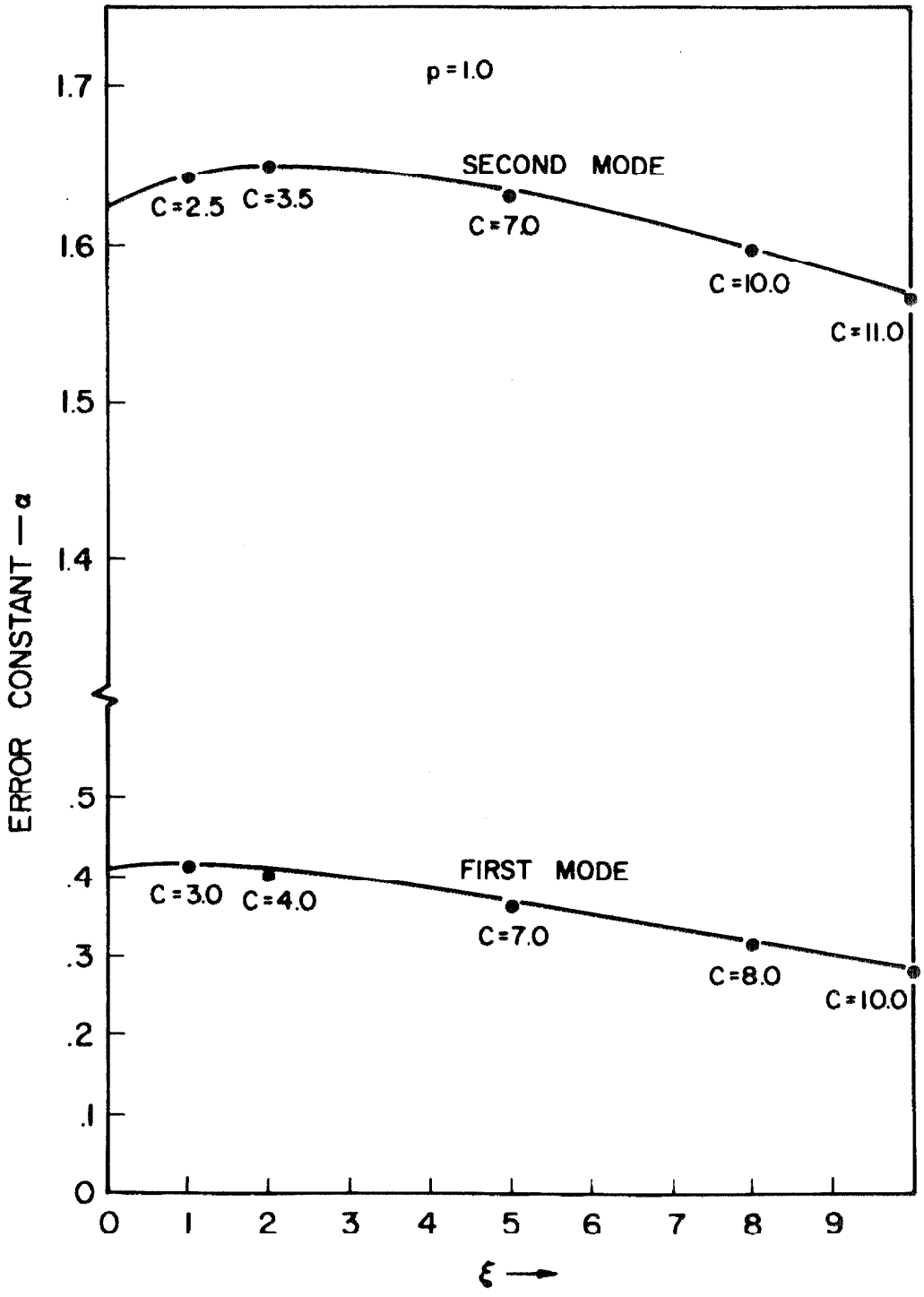

Fig. 3.5.6 Comparison of Frequency Root Error Constants for Free-Free Elements with Variable Segment Lengths.

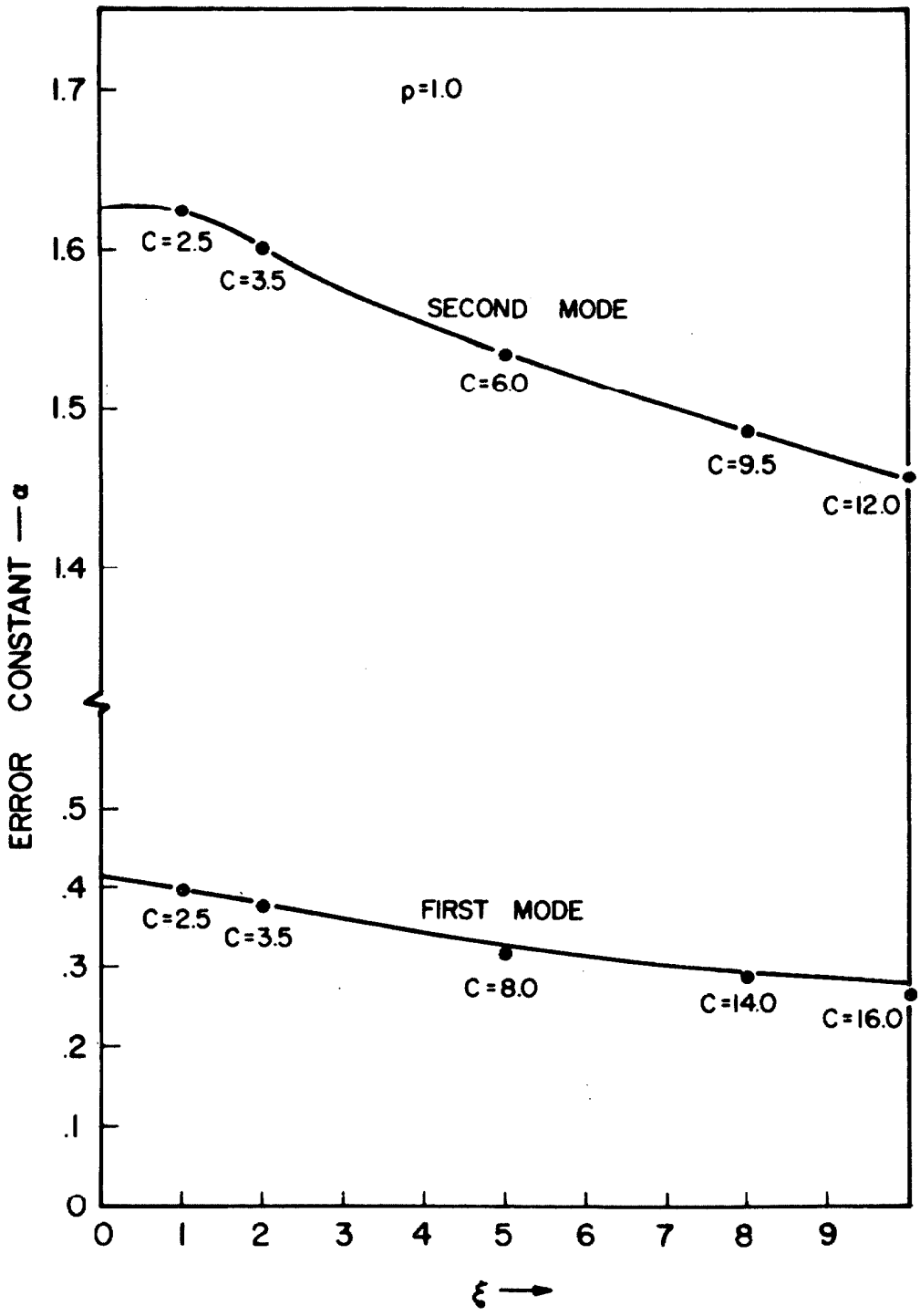

Fig. 3.5.7 Comparison of Frequency Root Error Constants for Fixed-Fixed Elements with Variable Segment Lengths.

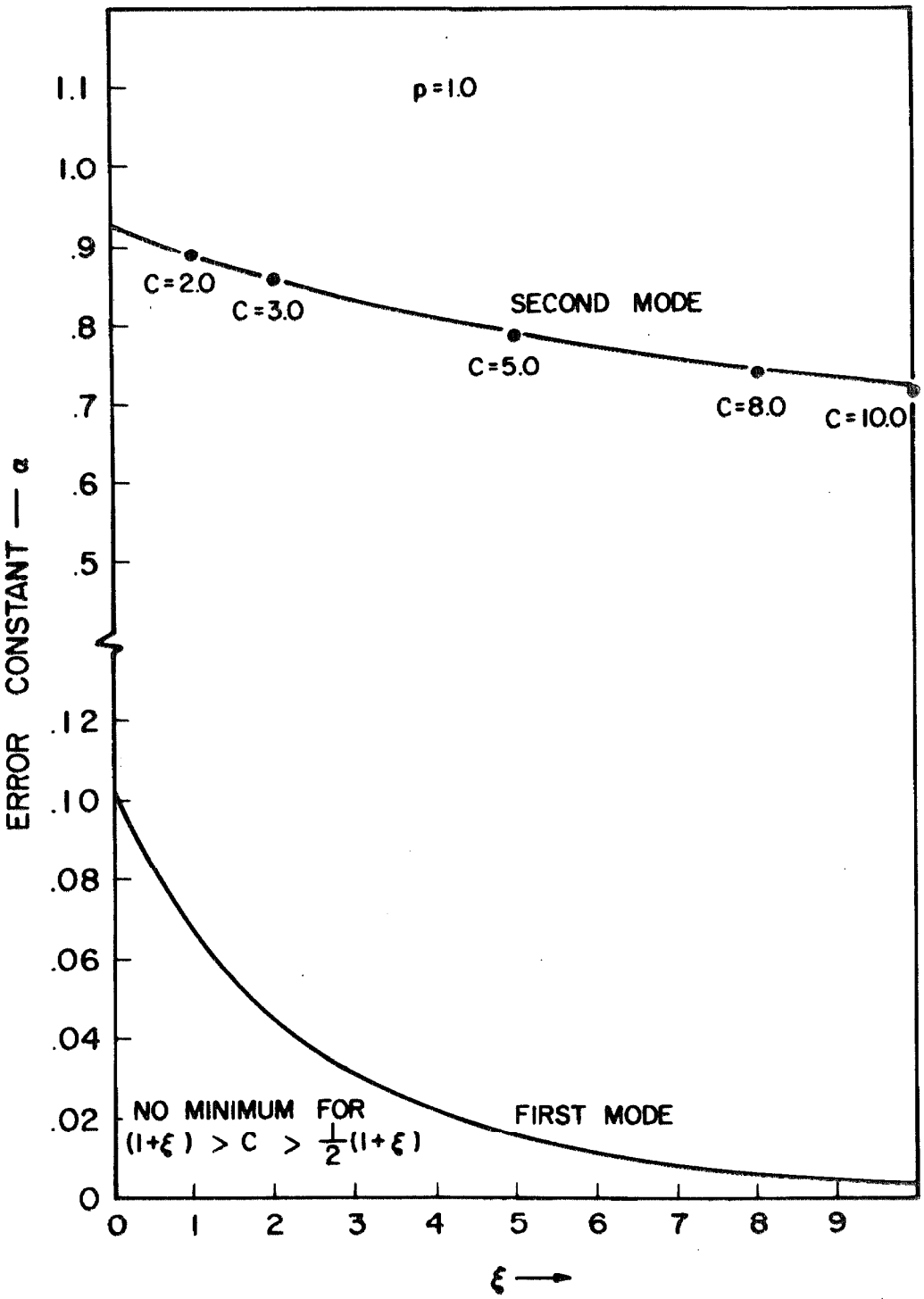

Fig. 3.5.8 Comparison of Frequency Root Error Constants for Fixed-Free Elements with Variable Segment Lengths.

CHAPTER IV

BEAM ELEMENTS

4.1 Lumped Parameter Models for Uniform Continuous Beams

Because beams are the primary elements used in forming structures, evaluation of lumped parameter approximations for the uniform Bernoulli-Euler beam has received much more attention than the one dimensional systems previously discussed. It is, therefore, appropriate that a summary of this work be given in this section before extending the theory to non-uniform beams.

One of the first investigators to record his findings was Duncan[3] who studied the lumped parameter representation of a uniform cantilever beam using the spring-mass-spring model and numerical techniques, see Fig. (4.1.1). Later, Livesley[4] formed an exact expression for the frequency root error involved when representing a simply supported (i.e. pinned-pinned) beam by the Rayleigh model, see Fig. (4.1.1). Gladwell[5] has found analytical expressions for the errors in the natural frequencies with other end conditions using both the Duncan and Rayleigh model, and he established two classifications for frequency root errors in uniform beam approximations.

1. If neither end is free the errors are proportional to $1/N^4$ for large N, and for both models the errors are given by:

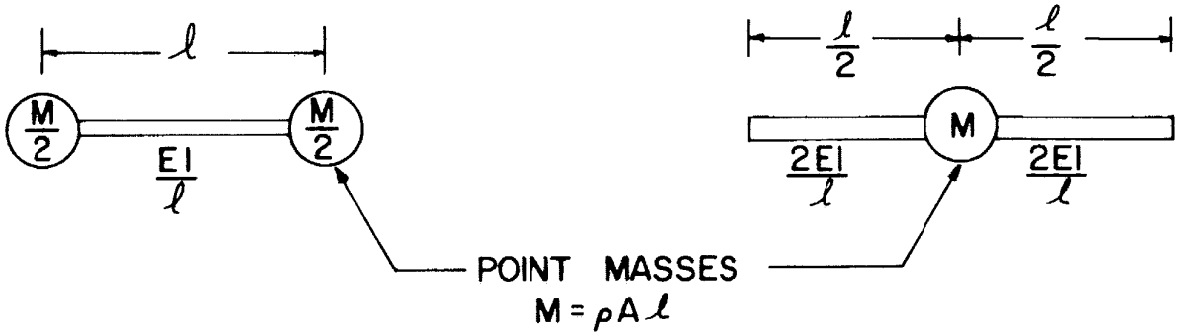

RAYLEIGH'S MODEL

DUNCAN'S MODEL

LUMPED PARAMETER MODELS FOR UNIFORM BEAMS

FIG. 4.1.1

$$e_{\nu N} = \frac{\omega_\nu - \omega_{\nu N}}{\omega_\nu} \approx \frac{(\Omega_\nu)^4}{1440N^4}$$

where Ω_ν denotes the exact ν^{th} mode frequency root. Note that the error is positive which means the approximate frequency roots are always less than the exact ones.

2. In cases where one or both ends are free the errors are proportional to $1/N^2$ for large N, and Rayleigh's model always gives errors which are positive. For Rayleigh's model with one end free the errors are:

$$e_{\nu N} \sim \frac{(\Omega_\nu)}{3N^2}$$

and the error is twice this value when both ends are free. Moreover, for this category the errors associated with Duncan's model are always negative and given by:

$$e_{\nu N}(\text{Duncan}) = -\frac{1}{2} e_{\nu N}(\text{Rayleigh}).$$

Lindberg and Leckie[6] have extended the study by using several other types of models (see Fig. 4.1.2). They refer to model (b) as the Myklestad model instead of Duncan's model as denoted here. Using finite difference equations for model (b) they confirm the results of Gladwell for three specific boundary conditions: pinned-pinned, clamped-clamped, and free-free. In addition, they have determined that the other models in Fig. (4.1.2) give larger errors than Duncan's

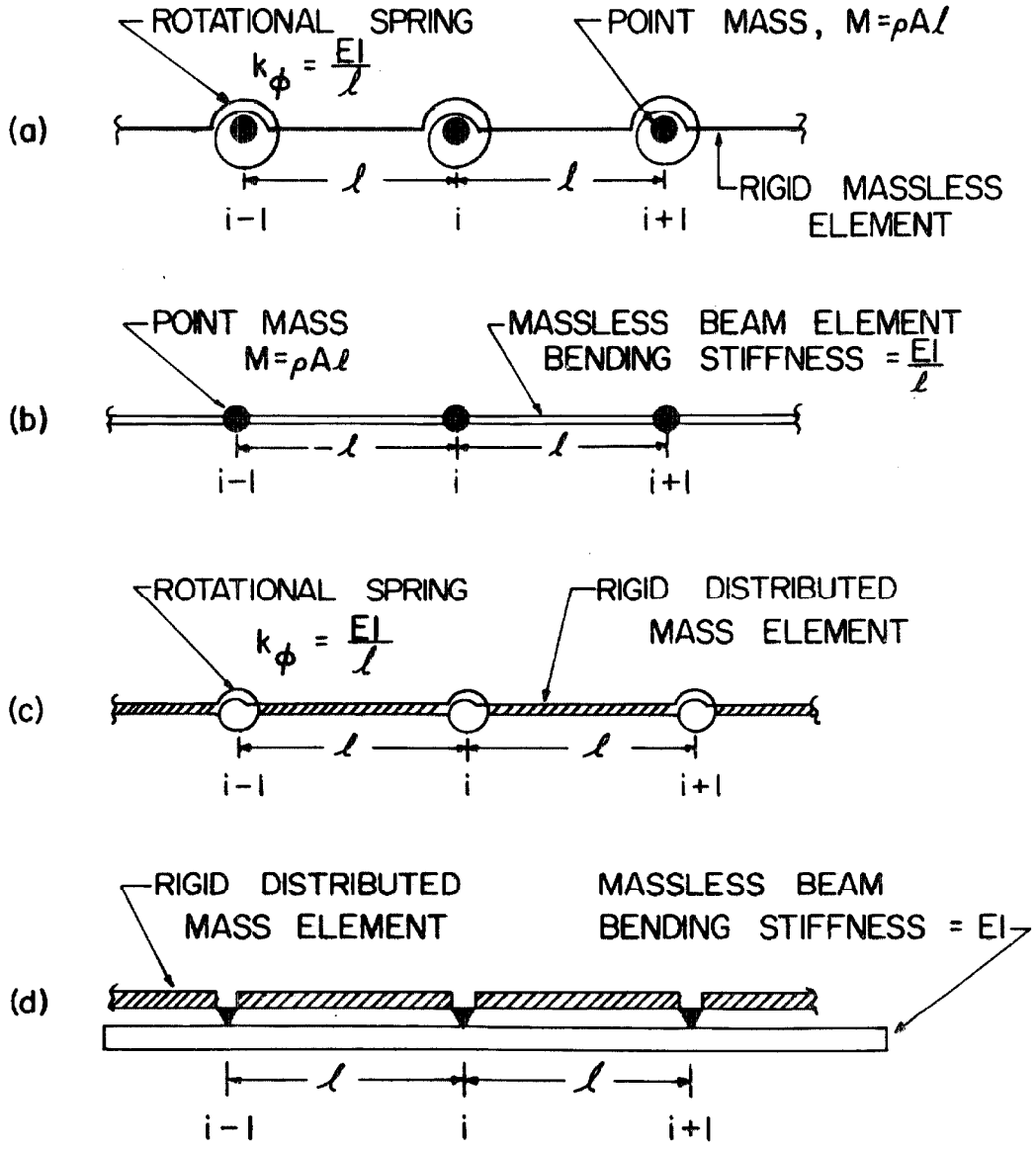

LUMPED PARAMETER MODELS FOR UNIFORM BEAMS

FIG. 4.1.2

model. Because the error behaves as $1/N^4$ for some boundary conditions and only $1/N^2$ for others, Lindberg and Leckie have attempted to derive a new model which will give more consistent results. They have succeeded in finding an improved model which does exhibit frequency root errors proportional to $1/N^4$, for large N, with all boundary conditions. To achieve this result, they have eliminated the concentrated mass points and have distributed the inertia force of the mass along the increment in proportion to the static deflection shape for a massless beam. By using the principle of virtual work they have obtained a stiffness matrix relating forces to displacements which is a function of frequency, ω, and has been designated a "dynamic stiffness" matrix. Lindberg[21] has also applied this model to a group of linearly tapered beam elements which have exhibited the same error behavior, $e_{\nu N} \sim 1/N^4$.

Archer[22] has also modeled continuous beams using a first order approximation for the distributed inertia forces as does the dynamic stiffness matrix used by Lindberg and Leckie. The matrix formulation of the general structural dynamic response problem results in the equation:

$$[m_{ij}]\{\ddot{x}_i\} + [k_{ij}]\{x_i\} = \{Q_i\} \qquad (4.1.1)$$

in which k_{ij} is a stiffness matrix whose coefficients represent the elastic restraining force at coordinate i developed by a unit displacement $x_j = 1$ with other coordinate displacements zero. When using lumped parameter models, such as those in Fig. (4.1.1), the mass

matrix in Eq.(4.1.1) becomes a simple diagonal matrix as all mass is lumped at the coordinate points. Archer uses a technique whereby the mass is not lumped and inertia force is distributed according to the static deflection shapes of massless beams similar to the method used by Lindberg and Leckie. This produces a non-diagonal mass matrix which is designated a "consistent mass" matrix where m_{ij} is the mass inertia force effective at point i resulting from a unit acceleration of coordinate j. This mass matrix is then used in conjunction with the standard stiffness matrix. Using this approach to model uniform beams, Archer has shown that it does give improved results which are consistent with those of Lindberg and Leckie previously discussed. In Chapter V another method is given for obtaining a consistent mass matrix.

A dynamic stiffness matrix, because of its frequency dependence, is essentially the same type of matrix as the transmission matrix. The equations which define a dynamic stiffness matrix for a beam element can be written in partitioned matrix form as:

$$\begin{Bmatrix} -V_i \\ -M_i \\ V_{i-1} \\ M_{i-1} \end{Bmatrix} = \left[\begin{array}{c|c} A & B \\ \hline C & D \end{array}\right] \begin{Bmatrix} w_i \\ \phi_i \\ w_{i-1} \\ \phi_{i-1} \end{Bmatrix} \qquad (4.1.2)$$

where [A], [B], [C], and [D] are (2×2) submatrices. These equations can be rearranged and cast into the same form as the

transmission matrix which is :

$$\begin{Bmatrix} V \\ M \\ w \\ \phi \end{Bmatrix}_{i-1} = \left[\begin{array}{c|c} -DB^{-1} & -DBA^{-1} + C \\ \hline -B^{-1} & -BA^{-1} \end{array}\right] \begin{Bmatrix} V \\ M \\ w \\ \phi \end{Bmatrix}_{i} \quad . \qquad (4.1.3)$$

In other words, a comparable dynamic stiffness matrix contains the same information as a transmission matrix and eigenvalue solutions utilizing this stiffness matrix must yield equivalent results, and will require a similar iterative procedure. Because the static deflection shape for a massless beam was used in its derivation, the dynamic stiffness matrix of Lindberg and Leckie can not give exact representation of the continuous beam. It does, however, give better results than the lumped parameter models because a first order approximation of distributed mass is used. A transmission matrix can, however, give exact representation of a continuous beam element within the limitations of the theory, i.e. Bernoulli-Euler, used in its derivation. Consequently, the transmission matrix provides the more favorable basis for this type of approach. The goal in the next section is to derive transmission matrices for a group of commonly used non-uniform beam elements using the Bernoulli-Euler theory.

4.2 Transmission Matrices for Non-uniform Continuous Beams

The transmission matrix for a simple transverse bending beam is a fourth order (4 X 4) matrix. When using the Bernoulli-

Euler elementary theory, the governing [A] matrix can be shown to be (see Appendix D):

$$[A] = \begin{bmatrix} 0 & 0 & \omega^2 \rho A(x) & 0 \\ -1 & 0 & 0 & 0 \\ 0 & 0 & 0 & 1 \\ 0 & -\frac{1}{EI(x)} & 0 & 0 \end{bmatrix} \qquad (4.2.1)$$

In deriving the T_{ij} elements for the transmission matrix, four, similar, fourth-order, variable coefficient, differential equations must be solved. These equations are of the form:

$$T_{i_1}'''' + 2\,\frac{(EI(x))'}{EI(x)}\,T_{i_1}''' + \frac{(EI(x))''}{EI(x)}\,T_{i_1}'' - \frac{\rho A(x)\omega^2}{EI(x)}\,T_{i_1} = 0 \qquad (4.2.2)$$

where

$$i = 1, 2, 3, 4$$

and

$$(') \text{ denotes } \frac{d}{dx} \quad .$$

The twelve remaining $T_{ij}(x)$ terms can be obtained by using the following expressions once the solutions for $T_{i_1}(x)$ are available.

$$\left.\begin{aligned} T_{i_1}'(x) &= -\,T_{i_2}(x) \\ T_{i_2}'(x) &= T_{i_4}(x)\,\frac{1}{EI(x)} \quad . \\ T_{i_4}'(x) &= T_{i_3}(x) \end{aligned}\right\} \qquad (4.2.3)$$

Equation (4.2.2) and expressions (4.2.3) are obtained directly from:

$$\frac{d}{dx}\,[T] = -\,[T][A]$$

which is the differential equation that defines the transmission matrix, see Appendix D.

From inspection of Eq. (4.2.2) it is not obvious what types of functions can be chosen to describe $A\rho(x)$ and $EI(x)$ and still obtain closed form solutions. Cranch and Adler[23], however, simplified problems of this type when studying the following fourth-order differential equation:

$$\frac{d^2}{dx^2}\left[EI(x)\ \frac{d^2W}{dx^2}\right] - \rho A(x)\omega^2 W = 0 \qquad (4.2.4)$$

where

$W(x)$ = mode shape, and

$w(x,t) = W(x)e^{i\omega t}$.

This equation describes the normal modes of a simple non-uniform bending beam and in expanded form it is identical to Eq. (4.2.2) when $W(x)$ is replaced by $T_{i_1}(x)$. By reducing this fourth-order equation to a simpler form which has been more thoroughly studied, Cranch and Adler have determined several suitable functions for $A\rho(x)$ and $EI(x)$ which do result in closed formed solutions. Consequently, the procedures used by Cranch and Adler can be applied here to obtain solutions for $T_{i_1}(x)$ from Eq. (4.2.2) which ultimately determines the entire transmission matrix.

To simplify Eq. (4.2.2) Cranch and Adler have shown that

this type of fourth-order differential equation can be written as the product of two second-order linear differential operators as follows:

$$\left[\frac{1}{R}\frac{d}{dx}\left(S\frac{d}{dx}\right)+\Omega\right]\left[\frac{1}{R}\frac{d}{dx}\left(S\frac{d}{dx}\right)-\Omega\right]T_{i_1}=0 \quad . \tag{4.2.5}$$

Expanding Eq. (4.2.5) and equating the coefficients of the same order terms with those of Eq. (4.2.2) gives the following relationships:

$$R = \rho A(x) \tag{4.2.6}$$

$$S^2 = [\rho A(x)][EI(x)] \tag{4.2.7}$$

$$\frac{dS}{dx} = \bar{C}R \quad \text{when} \quad \frac{dS}{dx} \neq 0 \tag{4.2.8}$$

$$S = \bar{C} \quad \text{when} \quad \frac{dS}{dx} = 0 \tag{4.2.9}$$

where $\bar{C}$ is a constant. The expressions above give the important and necessary relationships which must exist between $\rho A(x)$ and $EI(x)$ if Eq. (4.2.2) is to be written in the form of Eq. (4.2.5). These relationships in a more explicit form are:

$$EI(x) = \frac{\left[\bar{C}\int \rho A(x)dx\right]^2}{\rho A(x)} \quad \text{when} \quad \frac{dS}{dx} \neq 0 \tag{4.2.10}$$

$$EI(x) = \frac{\bar{C}^2}{\rho A(x)} \quad \text{when} \quad \frac{dS}{dx} = 0 \quad . \tag{4.2.11}$$

Consequently, if $\rho A(x)$ and $EI(x)$ are related by Eqs. (4.2.10) or (4.2.11) then the differential equation for $T_{i_1}(x)$ can be written as:

$$[D_1(x)]\ [D_2(x)]\ T_{i_1} = 0 \tag{4.2.12}$$

where:

$$D_1(x) = \left[\frac{1}{\rho A(x)} \frac{d}{dx}\left(\sqrt{(\rho A)(EI)}\frac{d}{dx}\right) + \omega\right] \qquad (4.2.13)$$

$$D_2(x) = \left[\frac{1}{\rho A(x)} \frac{d}{dx}\left(\sqrt{(\rho A)(EI)}\ \frac{d}{dx}\right) - \omega\right] . \qquad (4.2.14)$$

Since the four-order differential equation has been rewritten as the repeated operation of two commutable, second-order operators, the total solution to Eq. (4.2.2) will be the sum of the solutions, which are assumed to be independent, to the two second-order operators given in expressions (4.2.13) and (4.2.14).

It has been shown[24] that operators $D_1(x)$ and $D_2(x)$ have Bessel function solutions if $R \sim x^n$ and $S \sim x^m$ where $m \neq n + 2$. In the case of $m = n + 2$, Eq. (4.2.5) reduces to a differential equation with constant coefficients if a suitable change in variable is used. For $R \sim x^n$ the variable area can be written as:

$$\rho A(x) = \rho_o A_o \left(\frac{x}{\ell}\right)^n \qquad (4.2.15)$$

and the required $EI(x)$ as determined by Eq. (4.2.10) is:

$$EI(x) = E_o I_o \left(\frac{x}{\ell}\right)^{n+2} . \qquad (4.2.16)$$

To define a general beam element as shown in Fig. (4.2.1) where the area at the input end is not zero Eqs. (4.2.15) and (4.2.16) must be changed to the following form:

$$EA(x) = \rho_o A_o \left(1 + \frac{\xi x}{\ell}\right)^n \qquad (4.2.17)$$

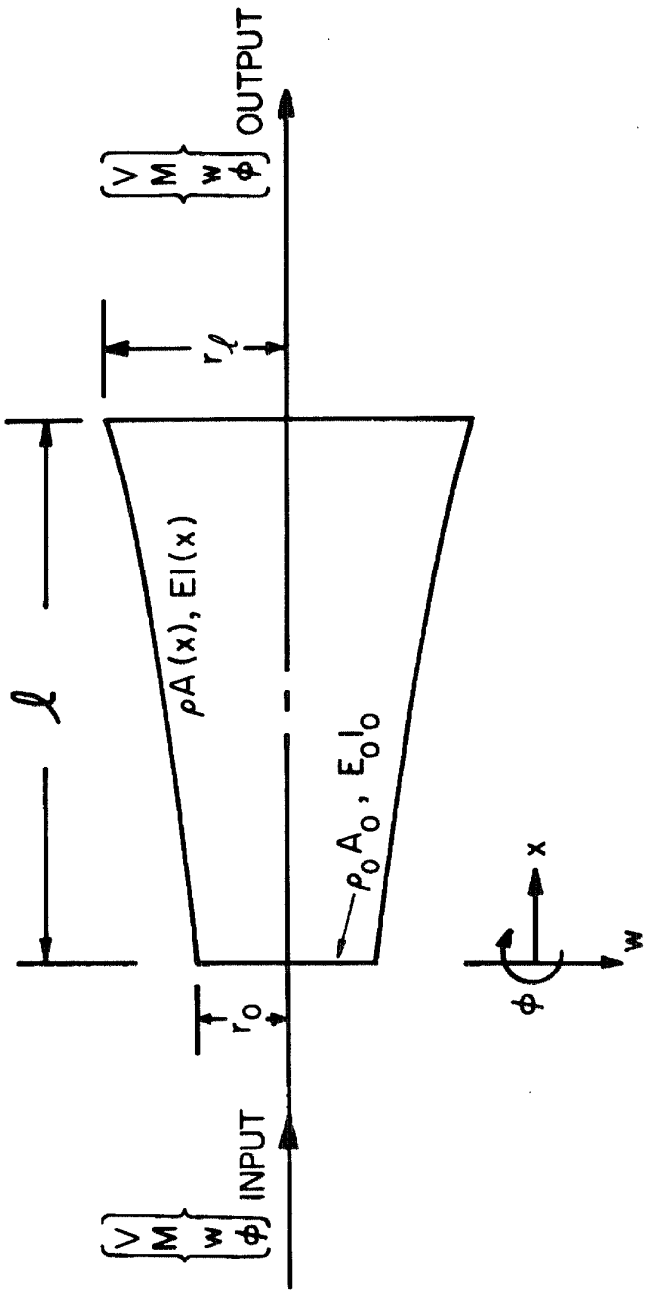

NON-UNIFORM ELASTIC BEAM ELEMENT

FIG. 4.2.1

$$EI(x) = E_o I_o \left(1 + \frac{\xi x}{\ell}\right)^{n+2} \quad . \qquad (4.2.18)$$

Setting $z = (1+\xi x/\ell)$, and using the above expressions, Eqs. (4.2.13) and (4.2.14) when set equal to zero become:

$$D_1(z) = d^2/dz^2 + \frac{(n+1)}{z}\frac{d}{dz} + \frac{1}{z}\sqrt{\frac{\rho_o A_o}{E_o I_o}}\left(\frac{\ell}{\xi}\right)^2 \omega = 0 \qquad (4.2.19)$$

$$D_2(z) = d^2/dz^2 + \frac{(n+1)}{z}\frac{d}{dz} - \frac{1}{z}\sqrt{\frac{\rho_o A_o}{E_o I_o}}\left(\frac{\ell}{\xi}\right)^2 \omega = 0 \quad . \qquad (4.2.20)$$

In Appendix D the solutions to Eqs. (4.2.19) and (4.2.20) and subsequently to Eq. (4.2.2) for T_{i_1} are given for the two cases where:

1. $n = 0$ or an integer, and
2. $n \neq$ an integer.

Through the use of appropriate initial conditions and expressions (4.2.3) the solution for the entire transmission matrix for case one has been completed in Appendix D.

Case one, n = an integer, describes several interesting and useful cross sectional variations. Considering E and ρ to be constant and using Eqs. (4.2.17) and (4.2.18) three specific groups of non-uniform cross sections can be defined as follows:

Group I — Rectangular Cross Sections

$$b = b_o z^{n-1} \qquad (4.2.21)$$

$$h = h_o z \qquad (4.2.22)$$

where

$A_o = b_o h_o$

$I_o = \frac{1}{12} b_o h_o^3$

b = width and

h = height

Group II Elliptical Cross Sections

$$b = b_o z^{n-1} \qquad (4.2.23)$$

$$h = h_o z \qquad (4.2.24)$$

where

$A_o = \frac{\pi}{4} b_o h_o$

$I_o = \frac{\pi}{64} b_o h_o^3$

b = width and

h = height

Group III Circular Cross Sections

$$r = r_o z \qquad (4.2.25)$$

where

n = 1 only

$A_o = \pi r_o^2$, and

r = radius.

The following two expressions apply to all three groups (see Fig. 4.2.1):

$$z = 1 + \frac{\xi x}{\ell} \quad \text{and} \quad \xi = \frac{r_\ell - r_o}{r_o} \quad .$$

In Groups I and II the height of the cross section varies linearly and by chosing n properly several choices of width variation are available, i.e. constant width with $n = 1$, linear width variation with $n = 2$, etc. Group III is actually only one single case where the radius of a circular cross section varies linearly. The T_{ij} elements of the transmission matrix for beam segments of length ℓ whose cross sections are described by these three groups are:

$$T_{i_1}(\ell) = a_1 \{C_1^i J_n(\hat{\mu}) + C_2^i Y_n(\hat{\mu}) + C_3^i I_n(\hat{\mu}) + C_4^i K_n(\hat{\mu})\} \tag{4.2.26}$$

$$T_{i_2}(\ell) = -a_2 \{C_1^i J_{n+1}(\hat{\mu}) + C_2^i Y_{n+1}(\hat{\mu}) - C_3^i I_{n+1}(\hat{\mu}) + C_4^i K_{n+1}(\hat{\mu})\} \tag{4.2.27}$$

$$\begin{aligned} T_{i_3}(\ell) = [a_3 \{&C_1^i J_{n+3}(\hat{\mu}) + C_2^i Y_{n+3}(\hat{\mu}) - C_3^i I_{n+3}(\hat{\mu}) + C_4^i K_{n+3}(\hat{\mu})\} \\ &- a_4 \{C_1^i J_{n+2}(\hat{\mu}) + C_2^i Y_{n+2}(\hat{\mu}) + C_3^i I_{n+2}(\hat{\mu}) + C_4^i K_{n+2}(\hat{\mu})\}] \end{aligned} \tag{4.2.28}$$

$$T_{i_4}(\ell) = a_5 \{C_1^i J_{n+2}(\hat{\mu}) + C_2^i Y_{n+2}(\hat{\mu}) + C_3^i I_{n+2}(\hat{\mu}) + C_4^i K_{n+2}(\hat{\mu})\} \tag{4.2.29}$$

where:

$$i = 1, 2, 3, \quad \text{and} \quad 4$$

$$a_1 = \left(\frac{g}{f}\right)^{-n/2}$$

$$a_2 = \frac{\mu\xi}{2\ell} \left(\frac{g}{f}\right)^{-\left(\frac{n+1}{2}\right)}$$

$$a_3 = \left(\frac{\mu\xi}{2}\right)^3 \frac{EI_o}{\ell^3} \left(\frac{g}{f}\right)^{\left(\frac{n+1}{2}\right)}$$

$$a_4 = (n+2) \frac{EI_o}{\ell^3} \left(\frac{\mu\xi}{2}\right)^2 \xi \left(\frac{g}{f}\right)^{n/2}$$

$$a_5 = \left(\frac{\mu\xi}{2}\right)^2 \frac{EI_o}{\ell^2} \left(\frac{g}{f}\right)^{-\left(\frac{n+2}{2}\right)}$$

$$\frac{g}{f} = (1+\xi)$$

$$\mu = 2\left(\frac{\ell}{\xi}\right)\left[\frac{\omega^2 \rho A_o}{EI_o}\right]^{\frac{1}{4}}$$

$$\hat{\mu} = \mu\sqrt{g/f} \quad , \qquad \text{and}$$

the constants C_1^i, C_2^i, C_3^i, and C_4^i are given by Eqs. (D.11) and (D.14) in Appendix D. The validity of the $T_{ij}(\ell)$ expressions has been checked by examining the limiting case of the uniform beam, $\xi \to 0$. As $\xi \to 0$ in the limit $\mu\sqrt{g/f} \to \infty$ and the asymptotic expansions for Bessel and modified Bessel functions of large arguments can be used in Eqs. (4.2.26) through (4.2.29). The expansion of Eq. (4.2.28) for the particular term $T_{43}(\ell)$ has been completed in Appendix D for this limiting case.

To utilize these groups of transmission matrices the recommendation made previously for the one dimensional systems in Section 3.4 is again applicable. To represent non-uniform continuous beams, exact or best fitting variable cross sectional segments which have transmission matrices defined by Groups I, II, or III should

be employed. The product of the transmission matrices for the segments is the transmission matrix for the total non-uniform beam from which normal mode frequencies and mode shapes can be determined. It is anticipated that the use of best fitting linear taper segments will give greatly improved results as compared to the piecewise uniform segment approximation which is commonly used to represent non-uniform beams. Although the types of cross sectional variations available from Groups I, II, and III are still very limited others can be derived. In addition to case two, $n \neq$ integer, which was not completed herein, several other forms of sectional variation which can be solved in closed form are outlined by Cranch and Adler[23].

CHAPTER V

POWER SERIES EXPANSION OF TRANSMISSION MATRICES

5.1 Method Description

In previous chapters transmission matrices have been derived in closed form for various non-uniform systems, i.e., rods and beams. In addition, there are several ways to obtain approximate transmission matrices to describe non-uniform systems which can not be solved in closed form. The first, which has been mentioned previously is to use best fitting variable cross section segments which are described by transmission matrices belonging to the groups derived in Chapters III and IV. The second is to obtain approximate transmission matrices directly. Pestel and Leckie[10] briefly describe how the Runge-Kutta and Picard Iteration methods can be employed to numerically integrate the following differential equation for the state vector,

$$\frac{d\psi}{dx} = [A(x)]\psi \quad , \tag{5.1.1}$$

which results in a transmission matrix. Another suggested method[14] is to use a Maclaurin series expansion which utilizes the following differential equation:

$$\frac{d}{dx}[M] = -[M][A(x)] \quad . \tag{5.1.2}$$

This approach appears attractive as it utilizes the known variables $\rho A(x)$, $EI(x)$, etc. which appear in the governing $[A]$ matrix and it eliminates the need to make equivalent uniform cross sections which

are required in the more standard methods of piecewise uniform segmenting or lumped parameter approximations. It can also be organized into a very simple, straightforward form which is easy to apply and one which is independent of matrix size. These attributes will be demonstrated in the following section by an illustrative example.

Expanding $[M(x)]$ in a Maclaurin series about the origin of the segment gives:

$$[M(x)] = [M(0)] + x[M'(0)] + \frac{x^2}{2!}[M''(0)] + \frac{x^3}{3!}[M'''(0)] + \ldots$$

$$\text{higher order terms} \qquad (5.1.3)$$

where:

$$(') \text{ denotes } d/dx \ .$$

The condition for the Maclaurin series that the function be piecewise analytic in this case requires through Eq. (5.1.2) that the variables in $[A(x)]$ be piecewise analytic. In particular they must be analytic in the region between points i and $i+1$ for which the transmission matrix is desired. By definition:

$$[M(0)] = I \ , \quad \text{the identity matrix.} \qquad (5.1.4)$$

Using Eqs. (5.1.4) and (5.1.2) the first three derivatives of $[M(x)]$ evaluated at the origin are found to be:

$$\left.\begin{aligned} [M'(0)] &= -[A(0)] \\ [M''(0)] &= [A(0)]^2 - [A'(0)] \\ [M'''(0)] &= -[A(0)]^3 + [A'(0)][A(0)] + 2[A(0)][A'(0)] - [A''(0)] \end{aligned}\right\} \quad (5.1.5)$$

Using the above expressions, the series for $[M(x)]$ becomes:

$$[M(x)] = [I] - x[A(0)] + \frac{x^2}{2!}\{[A(0)]^2 - [A'(0)]\}$$

$$+ \frac{x^3}{3!}\{-[A(0)]^3 + [A'(0)][A(0)] + 2[A(0)][A'(0)] - [A''(0)]\} + \ldots \quad (5.1.6)$$

It can be noted that if $[A]$ is a constant matrix then Eq. (5.1.6) reduces to:

$$[M(x)] = [I] - x[A(0)] + \frac{\{x[A(0)]\}^2}{2!} - \frac{\{x[A(0)]\}^3}{3!} + \ldots \quad \text{or}$$

$$[M(x)] = e^{-[A]x}$$

which is the known solution[10] for a uniform system.

The transmission matrix obtained from Eq. (5.1.6) is a low frequency approximation for the system. For a segment of length ℓ the variable x is replaced by ℓ in Eq. (5.1.6) and the parameter of interest in each of the terms of the series becomes β or some power of β. The condition discussed earlier in Section 3.3.1 which leads to good low frequency approximations applies here also; β must be small, which means the product of $\omega\ell$ must be small. The results found in Chapters III and IV can serve as general guide lines for the

magnitude of error to be expected for any given N, the number of segments used to represent the system, and the transmission matrices can be obtained for each of the N segments using the series expansion method.

5.2 Illustration

To illustrate the series expansion method, the transmission matrix will be found for one non-uniform segment of a rod for which the closed form solution has been given previously in Section 3.2. In general, a non-uniform system will be described by piecewise analytic functions for the spatial variables occurring in the [A] matrix. When several variables are required to describe a system, e.g., $A\rho(x)$ and $EI(x)$ in the beam, it will be assumed for simplicity that these functions become non-analytic at the same position in the system. The number of segments used to represent the system will be determined by the number of non-analytic points in these functions. This insures that [A(x)] is analytic in the segment being described by a transmission matrix. The final transmission matrix for the overall system is the product of the transmission matrices for the segments. If greater accuracy is desired, the segments can be subdivided further to increase N.

A linearly tapered segment of a solid, circular, cross

sectional rod will be used for this example. The transmission matrix describing this segment in closed form is given in Section 3.4 and the $T_{ij}(\ell)$ elements of this matrix are given in series form in Eqs. (3.4.10) through (3.4.13). The [A] matrix for this segment, given in the form where the accompanying state vector is defined by force and displacement, is given by:

$$[A(x)] = \begin{bmatrix} 0 & -\bar{Z}(x) \\ -\bar{Y}(x) & 0 \end{bmatrix} = \begin{bmatrix} 0 & \rho\omega^2 A_o (1+ax)^2 \\ -\dfrac{(1+ax)^{-2}}{EA_o} & 0 \end{bmatrix} \qquad (5.2.1)$$

Forms of [A(0)] required by the first few terms of the series for [M(x)] in Eq. (5.1.6) are:

$$[A(0)]^2 = \left.\begin{bmatrix} \bar{Z}(0)\bar{Y}(0) & 0 \\ 0 & \bar{Z}(0)\bar{Y}(0) \end{bmatrix}\right\} \qquad (5.2.2)$$

$$
\left.
\begin{aligned}
[A(0)]^3 &= \begin{bmatrix} 0 & -\bar{Z}^2(0)\bar{Y}(0) \\ -\bar{Z}(0)\bar{Y}^2 & 0 \end{bmatrix} \\
[A'(0)][A(0)] &= \begin{bmatrix} \bar{Z}'(0)\bar{Y}(0) & 0 \\ 0 & \bar{Z}(0)\bar{Y}'(0) \end{bmatrix} \\
[A(0)][A'(0)] &= \begin{bmatrix} \bar{Z}(0)\bar{Y}'(0) & 0 \\ 0 & \bar{Z}'(0)\bar{Y}(0) \end{bmatrix}
\end{aligned}
\right\} \quad (5.2.2)
$$

where:

$$
\left.
\begin{aligned}
\bar{Z}(x) &= -\rho\omega^2 A_o(1+ax)^2 \quad , \\
\bar{Y}(x) &= (1+ax)^{-2}/EA_o \quad ,
\end{aligned}
\right\} \quad (5.2.3)
$$

and

$$a = \xi/\ell \quad .$$

Substituting expressions (5.2.2) into Eq. (5.1.6) and writing the matrix elements $M_{ij}(x)$ separately results in:

$$M_{11}(x) = 1 + \frac{x^2}{2}\{\bar{Z}(0)\bar{Y}(0)\} + \frac{x^3}{6}\{2\bar{Z}(0)\bar{Y}'(0) + \bar{Z}'(0)\bar{Y}(0)\}$$

$$+O(x^4) + \ldots .$$

$$M_{12}(x) = x\{\bar{Z}(0)\} + \frac{x^2}{2}\{\bar{Z}'(0)\} + \frac{x^3}{6}\{\bar{Z}''(0) + \bar{Z}^2(0)\bar{Y}(0)\}$$

$$+ O(x^4) + \ldots .$$

$$M_{21}(x) = x\{\bar{Y}(0)\} + \frac{x^2}{2}\{\bar{Y}'(0)\} + \frac{x^3}{6}\{\bar{Y}''(0) + \bar{Z}(0)\bar{Y}^2(0)\}$$

$$+O(x^4) + \ldots .$$

$$M_{22}(x) = 1 + \frac{x^2}{2}\{\bar{Z}(0)\bar{Y}(0)\} + \frac{x^3}{6}\{2\bar{Z}'(0)\bar{Y}(0)+\bar{Z}(0)\bar{Y}'(0)\}$$

$$+O(x^4) + \ldots .$$

Rewriting these expressions for a segment of length ℓ using $\bar{Z}(0)$, $\bar{Y}(0)$, and derivatives of these functions evaluated from expressions (5.2.3) gives:

$$M_{11}(\ell) = 1 - \left[\frac{1}{2} - \frac{\xi}{3}\right]\beta^2 + O(x^4) + \ldots \qquad (5.2.4)$$

$$M_{12}(\ell) = \frac{EA_o}{\ell}\left[1 + \xi + \frac{\xi^2}{3}\right]\beta^2 + O(x^4) + \ldots \qquad (5.2.5)$$

$$M_{21}(\ell) = \frac{\ell}{EA_o}\left[1 - \xi + \xi^2 - \frac{\beta^2}{6}\right] + O(x^4) + \ldots \qquad (5.2.6)$$

$$M_{22}(\ell) = 1 - \left[\frac{1}{2} + \frac{\xi}{3}\right]\beta^2 + O(x^4) + \ldots . \qquad (5.2.7)$$

Comparing the above expressions for $M_{ij}(\ell)$ to those for $T_{ij}(\ell)$, which are given in Eqs. (3.4.10) through (3.4.13), indicates

close agreement for the first few terms in each series. Through the $O(\beta^2)$ term $M_{12}(\ell)$ is the same as $T_{12}(\ell)$ and $M_{22}(\ell)$ is the same as $T_{22}(\ell)$. In both the $M_{12}(\ell)$ and $M_{22}(\ell)$ expressions, the $O(x^4)$ term reduces to $O(\beta^4)$ only. In comparing $M_{11}(\ell)$ to $T_{11}(\ell)$ and $M_{21}(\ell)$ to $T_{21}(\ell)$, however, there is a consistent discrepancy as the $O(\beta^2)$ terms in these expressions do not appear equal. By inspection of Eqs. (3.4.10) and (3.4.12) it can be seen that a factor of $(1/1+\xi)$ appears in both $T_{11}(\ell)$ and $T_{21}(\ell)$. From expressions (5.2.3) it can be seen that in evaluating $\bar{Z}(0)$, $\bar{Y}(0)$, and derivatives of these functions ξ will never appear in the denominator of any $M_{ij}(\ell)$ expression as it does for $T_{11}(\ell)$ and $T_{21}(\ell)$. If, however, the $O(\beta^2)$ term in $T_{11}(\ell)$ and $T_{21}(\ell)$ is expanded by using the Binomial expansion for $(1/1+\xi)$ with the assumption that $\xi \ll 1$, then $T_{11}(\ell)$ and $T_{21}(\ell)$ become:

$$T_{11}(\ell) = 1 - \left[\frac{1}{2} - \frac{\xi}{3} + \frac{\xi^2}{3} + O(\xi^3) + \ldots\right]\beta^2 + O(\beta^4) \qquad (5.2.8)$$

$$T_{21}(\ell) = \frac{\ell}{A_o E}\left[(1-\xi+\xi^2+O(\xi^3)+\ldots) - (1-\xi+\xi^2+O(\xi^3)+\ldots)\frac{\beta^2}{6}\right]$$

$$+ O(\beta^4) \quad . \qquad (5.2.9)$$

With the assumption that ξ is small for the segment and of the same order of magnitude as β, then $T_{21}(\ell)$ and $M_{21}(\ell)$ are the same through the $O(\beta^2)$ term when given by Eqs. (5.2.6) and (5.2.9).

Likewise, $T_{11}(\ell)$ and $M_{11}(\ell)$ agree in the $O(\beta^2)$ term within this same level of accuracy. Evaluation of the $O(x^4)$ term in Eqs. (5.2.4) and (5.2.6) gives terms of $\xi^2\beta^2/6$ in $M_{11}(\ell)$,

$\frac{\ell}{A_o E}\left(\frac{\xi\beta^2}{6}\right)$ in $M_{21}(\ell)$, and $O(\beta^4)$ terms in both $M_{11}(\ell)$ and $M_{21}(\ell)$. Moreover, it is expected that higher orders of $(\beta^2\xi)$ are contributed throughout the series for $M_{11}(\ell)$ and $M_{21}(\ell)$ by $O(x^5)$ and higher order terms in Eq. (5.1.6). The transmission matrix for another case of the non-uniform rod, $p = 1.0$, has also been obtained using the Maclaurin series expansion and the same difference occurs between the $M_{ij}(\ell)$ and $T_{ij}(\ell)$ expressions where $(1/1+\xi)$ is a factor in the closed form solution. With the assumption that $\xi \ll 1$ for any given segment, however, exact agreement between the $M_{ij}(\ell)$ and $T_{ij}(\ell)$ expressions through $O(\beta^2\xi)$ can be achieved for this case also.

The example outlined in this section indicates the simplicity of the Maclaurin series expansion method. The application is straightforward utilizing the governing [A] matrix for any order system directly, i.e., rods, beams, etc. In the example of the linearly tapered rod with $\xi \ll 1$ for any given segment all elements of the approximate transmission matrix agree with the $T_{ij}(\ell)$ elements within $O(\beta^2\xi)$ which is approximately the same as the governing criterion for selecting the parameters in the linear taper lumped parameter model derived in Section 3.4. This assumption, $\xi \ll 1$ for the segments, is not very restrictive when considering the number of segments required to give a reasonable error of 2 - 5% for the first and second normal mode frequencies. Hence, by using the first four terms of the power series in Eq. (5.1.6), which only requires the values for $[A(0)]$, $[A'(0)]$, and $[A''(0)]$ for the segment, a transmission matrix comparable to that for the improved lumped

parameter model of Section 3.4 can be found directly without any calculation of mass or stiffness of the segment. It is anticipated that the advantages of this method will become even more attractive in obtaining low frequency approximations for more complicated, higher-order, non-uniform systems, i.e., Bernoulli-Euler beam, Timoshenko beam, etc., where closed form solutions are very difficult to find and standard approximations are still uncertain. In addition, it has been shown[14] for the uniform Bernoulli-Euler beam that this method can be used to obtain the consistent mass matrix which was previously discussed in Section 4.1.

CHAPTER VI

SUMMARY AND CONCLUSIONS

The objective of this study has been to evaluate the use of transmission matrices and lumped parameter models in describing continuous systems. These approaches have been applied to individual segments which constitute an entire system. This type of representation can be exact or approximate.

In Chapter II a description of transmission matrices and a new systematic approach for their derivation are presented. In Chapter III the physical properties of vibration systems obeying the one dimensional wave equation are presented. Transmission matrices exact within the assumptions of the elementary theory used are given for three classes of non-uniform continuous one dimensional systems. These matrices can be employed at the segment level to describe a system composed of N segments. This type of representation will be exact or approximate depending upon whether the individual segments can be matched exactly or whether they must be approximated on a best fit basis by the segments which are described in closed form. The latter process is expected to give much better results than the usual recommendation of using a piecewise uniform segment approximation.

Three types of lumped parameter models (see Fig. 3.3.1) were evaluated in Chapter III on the basis of the uniform one dimensional system. On the basis of this investigation several conclusions are drawn concerning uniform one dimensional models:

1. Model (a) (mass-spring-mass) and model (b) (spring-mass-spring) produce essentially equivalent frequency root errors. For large N the errors behave as $1/N^2$ for all four combinations of fixed and free boundary conditions.
2. Model (c) (spring-mass) is less consistent than models (a) and (b) under the same comparison. For free-free or fixed-fixed ends the error behavior is $1/N^2$ for large N. However, for free-fixed or fixed-free boundary conditions the error behaves as $1/N$.
3. Model (d), N equal masses and N-1 or N + 1 equal springs, produces errors which behave as $1/N$ for large N with boundary conditions of free-free and fixed-fixed ends.
4. Because models (a) and (b) display more consistent error behavior for all of the elementary boundary conditions used, it is expected that they would be better for arbitrary boundary conditions also.
5. The models whose transmission matrices best fit the exact transmission matrix for the uniform increment were found to be superior in representing the entire uniform system.

The above results led to the formation of a new lumped parameter model (see Fig. 3.4.3) for representation of non-uniform segments. This model is defined on the basis of achieving a best low frequency approximation to the exact transmission matrix. In addition, the effect of unequal segment lengths was investigated. Conclusions from this part of the study are:

1. Evaluation of the non-uniform model for systems with quadratic and linear area variation indicates the error behavior when N is large to be $1/N^2$ for all boundary conditions used. This model shows improved results when compared to Duncan's model and the uniform segment approximation. Also evidence suggests better error behavior under arbitrary boundary conditions when this model is used.
2. From a study of variation of segment lengths it was found that equal length segments give errors which are not much larger than the best obtainable by linear variations.

In Chapter IV a brief summary of various approaches which have been used to model uniform Bernoulli-Euler beams has been given. Most models are inconsistent in that the frequency root errors behave as $1/N^2$ for some boundary conditions and as $1/N^4$ for others when N is large. In an attempt to eliminate this inconsistency

several investigators have used an approximate dynamic stiffness matrix which is based upon a first order approximation of the inertia forces. A dynamic stiffness matrix contains the same type of information and can be transformed into the same form as the transmission matrix. Exact transmission matrices for several types of non-uniform Bernoulli- Euler beam elements are derived. These transmission matrices can be applied on an exact or best fit piecewise basis for describing compound tapered beams. This can be viewed as an extension to the previously used dynamic stiffness matrix approach.

A power series expansion method has been presented in Chapter V for determining approximate transmission matrices for segments of non-uniform systems independently of the availability of closed form solutions. The method holds for any order transmission matrix. The following two conclusions have been formed:

1. The method is direct requiring only the values of the functions and derivatives of the functions contained in the [A] matrix, which characterizes the system, evaluated at the origin of the segment. Calculations of mass, equivalent cross sections, stiffnesses, etc. are eliminated.
2. Based on a comparison with the closed form solution for a linearly tapered segment of a one dimensional system, the series method was found to produce a low frequency approximation

comparable to the best lumped parameter model when ξ, the slope parameter, is small and the first four terms of the series, which require the values of $[A(0)]$, $[A'(0)]$, and $[A''(0)]$, are used.

The work presented here has by no means completed the study of lumped parameter models or exhausted the possibilities of transmission matrices for non-uniform continuous systems which could be applied in practical vibration problems. One area stemming from this work which needs further investigation is the application of the power series method to beams, in particular non-uniform beams. Another important problem, which is a natural continuation of this study, is the efficient modeling of structures which are composed of many elements like those treated herein, i.e., rods, beams, etc. Because of the different mass and stiffness distributions among the elements in the structure, some elements should be represented by more segments than others in order to best approximate the overall structure. Efficient usage of a minimum number of segments for this problem requires guide lines which have not been completely established.

APPENDIX A

DERIVATION OF THE GOVERNING [A] MATRIX FOR SEVERAL ONE DIMENSIONAL SYSTEMS

A.1 Longitudinal Rod

Assumptions (see Figure A.1):

1. ρ and E are assumed to be constants.
2. Area, $A(x)$, is variable.
3. Plane sections remain plane.

Summing forces on the dx element gives (see Figure A.1):

$$\sum \text{forces} = \text{mass} \cdot \text{acceleration, or}$$

$$-\frac{\partial F}{\partial x}\,dx = \rho A(x)\left(\frac{\partial v}{\partial t}\right)dx \quad .$$

For sinusodial, steady state motion:

$$\frac{\partial v}{\partial t} = i\omega v$$

$$\therefore \quad \frac{dF}{dx} = -i\omega\rho A(x)v \quad . \tag{A.1}$$

Using Hooke's law gives:

$$\text{Force} = -\sigma A(x) = -\frac{\partial u}{\partial x}\,EA(x) \quad , \text{ and}$$

$$u = \frac{v}{i\omega}$$

$$\therefore \quad \frac{dv}{dx} = -\left(\frac{i\omega}{EA(x)}\right)F \quad . \tag{A.2}$$

Casting Eq. (A.1) and (A.2) into the state vector form to determine the [A] matrix gives:

$$\frac{d}{dx}\begin{Bmatrix} F \\ v \end{Bmatrix} = [A]\begin{Bmatrix} F \\ v \end{Bmatrix} \tag{A.3}$$

where:

$$[A] = \begin{bmatrix} 0 & -i\omega\rho A(x) \\ -\frac{i\omega}{EA(x)} & 0 \end{bmatrix} .$$

A.2 Torsional Bar

Assumptions (see Figure A.2):

1. ρ and G are assumed to be constants.
2. Area, A(x), is variable.
3. Each section rotates about its center of gravity and plane sections remain plane.
4. The shape of a general cross section does not depart greatly from a circle.

Summing moments on the dx element gives (see Figure A.2):

$$-\frac{\partial T}{\partial x}\,dx = \bar{r}^2\rho A(x)\left|\frac{\partial \dot{\theta}}{\partial t}\right|dx \quad .$$

For sinusodial, steady state motion:

$$\frac{\partial \dot{\theta}}{\partial t} = i\omega\dot{\theta}$$

$$\therefore \quad \frac{dT}{dx} = -i\omega\rho\bar{r}^2 A(x)\dot{\theta} \quad . \tag{A.4}$$

From elastic properties:

$$T = -\frac{\partial \theta}{\partial x} G\bar{r}^2 A(x) \quad , \quad \text{and}$$

$$\theta = \frac{\dot{\theta}}{i\omega}$$

$$\therefore \qquad \frac{d\theta}{dx} = -\left(\frac{i\omega}{G\bar{r}^2 A(x)}\right) T \quad . \qquad (A.5)$$

Casting Eqs. (A.4) and (A.5) into the matrix form to determine the [A] matrix gives:

$$\frac{d}{dx}\begin{Bmatrix} T \\ \dot{\theta} \end{Bmatrix} = \begin{bmatrix} 0 & -i\omega\rho\bar{r}^2 A(x) \\ -\dfrac{i\omega}{G\bar{r}^2 A(x)} & 0 \end{bmatrix} \begin{Bmatrix} T \\ \dot{\theta} \end{Bmatrix} . \qquad (A.6)$$

A.3 Acoustical Tube

Assumptions (see Figure A.3):

1. Vibrating medium is a homogeneous, isotropic, ideal gas.
2. Plane waves exist or plane sections remain plane.
3. Container walls are perfectly rigid.
4. Areas, A(x), are slowly varying functions of the spatial variable.

From the continuity equation[25]:

$$\frac{\Delta V}{V} = \frac{\partial \xi}{\partial x} \quad ,$$

where:

V = volume
ξ = particle displacement
v = particle velocity .

For the ideal gas[25]:

$$\frac{\Delta V}{V} = - \frac{p}{\rho_o c^2}$$

where:

$$p = F/A(x) = \text{pressure.}$$

$$\therefore \quad \frac{dv}{dx} = - \frac{i\omega}{\rho_o c^2} p = - \frac{i\omega}{\rho_o c^2 A(x)} F \quad . \tag{A.7}$$

Summing forces on a dx element gives (see Figure A.3):

$$\frac{dF}{dx} = -i\omega\rho_o A(x)v \quad . \tag{A.8}$$

Putting Eqs. (A.7) and (A.8) into matrix form gives the following result for the [A] matrix:

$$\frac{d}{dx}\begin{Bmatrix} F \\ v \end{Bmatrix} = \begin{bmatrix} 0 & -i\omega\rho_o A(x) \\ -\dfrac{i\omega}{\rho_o c^2 A(x)} & 0 \end{bmatrix} \begin{Bmatrix} F \\ v \end{Bmatrix} \quad . \tag{A.9}$$

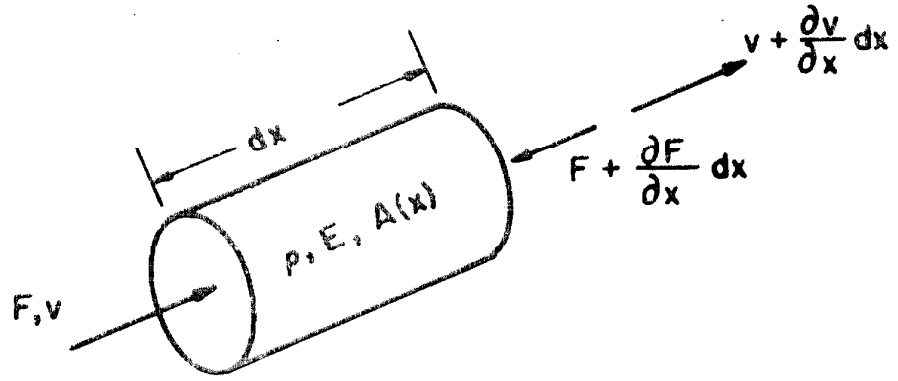

FIG. A.1

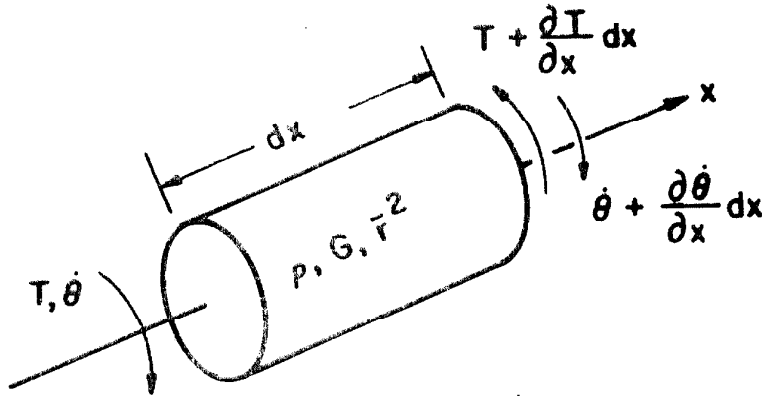

FIG. A.2

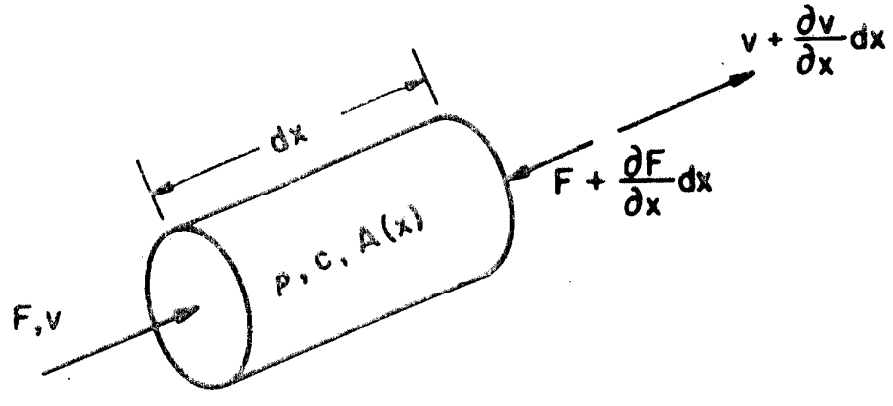

FIG. A.3

APPENDIX B

DERIVATION OF TRANSMISSION MATRICES

(ONE DIMENSIONAL SYSTEMS)

The differential equation defining the transmission matrix is (see Section 2.2):

$$\frac{d[T]}{dx} = -[T][A(x)] \quad , \tag{2.2.4}$$

where:

$$[A] = \begin{bmatrix} 0 & -\bar{Z}(x) \\ -\bar{Y}(x) & 0 \end{bmatrix} \quad .$$

Consequently:

$$\begin{bmatrix} T'_{11} & T'_{12} \\ T'_{21} & T'_{22} \end{bmatrix} = \begin{bmatrix} T_{12}\bar{Y}(x) & T_{11}\bar{Z}(x) \\ T_{22}\bar{Y}(x) & T_{21}\bar{Z}(x) \end{bmatrix}$$

where:

$$T'_{ij} \quad \text{denotes} \quad \frac{dT_{ij}}{dx} \quad .$$

Expanding the above gives:

$$T'_{11} = T_{12}\bar{Y}(x) \tag{B.1}$$

$$T'_{12} = T_{11}\bar{Z}(x) \tag{B.2}$$

$$T'_{21} = T_{22}\bar{Y}(x) \tag{B.3}$$

$$T'_{22} = T_{21}\bar{Z}(x) \qquad (B.4)$$

and the necessary initial conditions are:

$$[T(0)] = [I] \quad , \text{ the identity matrix}$$

$$[T'(0)] = -[A(0)] \quad .$$

Using Eqs. (B.1) and (B.2) gives,

$$T''_{11}(x) - \left[\frac{\bar{Y}'(x)}{\bar{Y}(x)}\right] T'_{11}(x) - \bar{Y}(x)\bar{Z}(x)T_{11}(x) = 0 \quad . \qquad (B.5)$$

From Eqs. (B.3) and (B.4) results:

$$T''_{22}(x) - \left[\frac{\bar{Z}'(x)}{\bar{Z}(x)}\right] T'_{22}(x) - \bar{Y}(x)\bar{Z}(x)T_{22}(x) = 0 \quad . \qquad (B.6)$$

Providing solutions can be found for $T_{11}(x)$ and $T_{22}(x)$, the determination of $[T(x)]$ can be completed by using the initial conditions and Eqs. (B.1) and (B.4).

Case I

$$A(x) = A_o(1+ax)^{2p-1} \qquad p = 0 \text{ or an integer}$$

$$\bar{Z}(x) = i\omega\rho A_o(1+ax)^{2p-1}$$

$$\bar{Y}(x) = \frac{i\omega}{EA_o}(1+ax)^{1-2p} \quad .$$

For this case Eqs. (B.5) and (B.6) become:

$$(1+ax)T''_{11}(x)+(2p-1)aT'_{11}(x)+\beta_1^2(1+ax)T_{11}(x) = 0 \qquad (B.7)$$

$$(1+ax)T''_{22}(x)-(2p-1)aT'_{22}(x)+\beta_1^2(1+ax)T_{22}(x) = 0 \qquad (B.8)$$

where

$$\beta_1 = \beta/\ell \quad .$$

A convenient coordinate transformation is:

$$\theta = \alpha(1+ax) \quad ,$$

where:

$$\alpha = \beta_1/a \quad ,$$

$$\frac{d}{dx} = \frac{d}{d\theta}\frac{d\theta}{dx} = a\alpha\frac{d}{d\theta} \quad ,$$

$$\frac{d^2}{dx^2} = a^2\alpha^2\frac{d^2}{d\theta^2} \quad .$$

As a result of this change in variables, Eqs. (B.7) and (B.8) become:

$$\theta^2\frac{d^2T_{11}(\theta)}{d\theta^2} + (2p-1)\theta\frac{dT_{11}(\theta)}{d\theta} + \theta^2T_{11}(\theta) = 0 \qquad (B.9)$$

$$\theta^2\frac{d^2T_{22}(\theta)}{d\theta^2} - (2p-1)\theta\frac{dT_{22}(\theta)}{d\theta} + \theta^2T_{22}(\theta) = 0 \quad . \qquad (B.10)$$

Equations (B.9) and (B.10) are of the standard form whose solutions are Bessel functions. Also (B.10) follows from (B.9) if $p \longrightarrow (1-p)$; hence,

$$T_{11}(\theta) = \theta^{1-p}\{\tilde{D}_1 J_{1-p}(\theta) + \tilde{D}_2 Y_{1-p}(\theta)\} \qquad (B.11)$$

$$T_{22}(\theta) = \theta^p\{D_1 J_p(\theta) + D_2 Y_p(\theta)\} \quad . \qquad (B.12)$$

The initial conditions are:

$$T_{11}(x)\Big|_{x=o} = T_{11}(\theta)\Big|_{\theta=\alpha} = T_{11}(\alpha) = 1$$

$$\left.\frac{dT_{11}(x)}{dx}\right|_{x=o} = a\alpha \left.\frac{dT_{11}(\theta)}{d\theta}\right|_{\theta=\alpha} = 0 \quad .$$

Likewise, for T_{22}

$$T_{22}(x)\Big|_{x=o} = T_{22}(\theta)\Big|_{\theta=\alpha} = 1$$

$$\left.\frac{dT_{22}(x)}{dx}\right|_{x=o} = a\alpha \left.\frac{dT_{22}(\theta)}{d\theta}\right|_{\theta=\alpha} = 0 \quad .$$

Using the above initial conditions with Eqs. (B.11) and (B.12) gives:

$$\tilde{D}_1 = \frac{\alpha^{(p-1)} Y_{-p}(\alpha)}{\tilde{X}}$$

$$\tilde{D}_2 = -\frac{\alpha^{(p-1)} J_{-p}(\alpha)}{\tilde{X}}$$

where:

$$\tilde{X} = J_{1-p}(\alpha) Y_{-p}(\alpha) - Y_{1-p}(\alpha) J_{-p}(\alpha) \quad .$$

The form of $\tilde{X}$ is commonly called the Wronskian determinant[26] and its value is:

$$\tilde{X} = W\{J_{-p}(\alpha),\ Y_{-p}(\alpha)\} = 2/\pi\alpha \quad .$$

Likewise,

$$D_1 = + \frac{\alpha^{-p} Y_{p-1}(\alpha)}{X}$$

$$D_2 = - \frac{\alpha^{-p} J_{p-1}(\alpha)}{X}$$

where:

$$X = J_p(\alpha)Y_{p-1}(\alpha) - Y_p(\alpha)J_{p-1}(\alpha) = \frac{2}{\pi\alpha} \quad .$$

Therefore, the solutions for $T_{11}(\theta)$ and $T_{22}(\theta)$ become:

$$T_{11}(\theta) = \left(\frac{\theta}{\alpha}\right)^{1-p} \left(\frac{\pi\alpha}{2}\right) \{Y_{-p}(\alpha)J_{1-p}(\theta) - J_{-p}(\alpha)Y_{1-p}(\theta)\} \qquad (B.13)$$

$$T_{22}(\theta) = \left(\frac{\theta}{\alpha}\right)^{p} \left(\frac{\pi\alpha}{2}\right) \{Y_{p-1}(\alpha)J_p(\theta) - J_{p-1}(\alpha)Y_p(\theta)\} \quad . \qquad (B.14)$$

To determine the two remaining matrix terms, T_{12} and T_{21}, requires using Eqs. (B.1) and (B.4) as follows:

$$T_{12}(x) = \frac{dT_{11}(x)}{dx} \frac{1}{\bar{Y}(x)} \quad \text{or} \quad T_{12}(\theta) = \frac{1}{\bar{Y}(\theta)} a\alpha \frac{dT_{11}(\theta)}{d\theta}$$

$$T_{21}(x) = \frac{1}{Z(x)} \frac{dT_{22}(x)}{dx} \quad \text{or} \quad T_{21}(\theta) = \frac{1}{Z(\theta)} a\alpha \frac{dT_{22}(\theta)}{d\theta} \quad .$$

Completing these operations gives;

$$T_{12}(\theta) = \frac{\beta}{i\omega} \left(\frac{EA_o}{\ell}\right) \left(\frac{\theta}{\alpha}\right)^{p} \left(\frac{\pi\alpha}{2}\right) \{Y_{-p}(\alpha)J_{-p}(\theta) - J_{-p}(\alpha)Y_{-p}(\theta)\} \qquad (B.15)$$

$$T_{21}(\theta) = - \frac{i\omega}{\beta} \left(\frac{\ell}{EA_o}\right) \left(\frac{\theta}{\alpha}\right)^{1-p} \left(\frac{\pi\alpha}{2}\right) \{Y_{p-1}(\alpha)J_{p-1}(\theta) - J_{p-1}(\alpha)Y_{p-1}(\theta)\} \quad ,$$

(B.16)

and when $x \to \ell$; $\theta \to g\beta$ and $\alpha \to f\beta$

where:

$$g = f+1 \quad , \quad f = 1/\xi \quad , \quad \xi = \frac{\sqrt{A_\ell} - \sqrt{A_o}}{\sqrt{A_o}} \text{ , and } a = \xi/\ell \quad .$$

To check the validity of the above expressions, the limiting case of a uniform rod is useful. For the uniform rod,

$$\xi = \frac{\sqrt{A_\ell} - \sqrt{A_o}}{\sqrt{A_o}} \to 0 \quad \therefore \quad f \to \infty \quad \text{and} \quad g \to \infty \quad .$$

Therefore, the arguments of the Bessel functions, which are all $f\beta$ or $g\beta$, all become infinitely large as the uniform case is approached in the limit. The common Bessel function expansions for large agruments are:

$$J_p(f\beta) \sim \sqrt{\frac{2}{\pi f\beta}} \cos\left(f\beta - \pi/4 - \frac{p\pi}{2}\right)$$

$$Y_p(f\beta) \sim \sqrt{\frac{2}{\pi f\beta}} \sin\left(f\beta - \frac{\pi}{4} - \frac{p\pi}{2}\right)$$

also for p = an integer $Y_{-p} = (-1)^p Y_p$ and $J_{-p} = (-1)^p J_p$. Using the above expansions and checking the $T_{12}(\theta)$ term in the limit requires the following expansion.

$$\left\{ Y_{-p}(f\beta)J_{-p}(g\beta) - J_{-p}(f\beta)Y_{-p}(g\beta) \right\} \xrightarrow[o]{\xi}$$

$$\xrightarrow[o]{\xi} (-1)^{2p} \frac{2}{\pi\beta} \left(\frac{1}{gf}\right)^{\frac{1}{2}} \begin{Bmatrix} +a_1 & +a_2 & +a_3 & +a_4 \\ +a_5 & +a_6 & +a_7 & +a_8 \end{Bmatrix}$$

where:

$$a_1 = -\sin(g\beta)\cos(f\beta)\cos^2(\epsilon)$$

$$a_2 = -\sin(f\beta)\sin(g\beta)\cos(\epsilon)\sin(\epsilon)$$

$$a_3 = \cos(f\beta)\cos(g\beta)\cos(\epsilon)\sin(\epsilon)$$

$$a_4 = \sin(f\beta)\cos(g\beta)\sin^2(\epsilon)$$

$$a_5 = \cos(g\beta)\sin(f\beta)\cos^2(\epsilon)$$

$$a_6 = \sin(f\beta)\sin(g\beta)\cos(\epsilon)\sin(\epsilon)$$

$$a_7 = -\cos(f\beta)\cos(g\beta)\sin(\epsilon)\cos(\epsilon)$$

$$a_8 = -\sin(g\beta)\cos(f\beta)\sin^2(\epsilon)$$

$$\epsilon = \frac{\pi}{4}(1-2p) \quad .$$

In the above, the a_2 and a_6 terms and the a_3 and a_7 terms cancel. Then by using the trigonometric identity $\cos^2\epsilon + \sin^2\epsilon = 1$ and the fact that $(-1)^{2p}$ is always equal to $+1$ for p = an integer, the above expression reduces to:

$$\longrightarrow -\frac{2}{\pi\beta}\left(\frac{1}{\sqrt{gf}}\right)\{\sin(g\beta)\cos(f\beta) - \cos(g\beta)\sin(f\beta)\}$$

which is independent of p. Further reduction gives:

$$\longrightarrow -\frac{2}{\pi\beta}\left(\frac{1}{\sqrt{gf}}\right)\sin(g-f)\beta \quad .$$

But $(g-f) = f+1-f = 1$ and $(g/f) = 1+\xi \xrightarrow[o]{\xi} 1$. Therefore, $T_{12}(\ell)$ goes in the limit to:

$$T_{12}(\ell) \xrightarrow[o]{\xi} \frac{\beta}{i\omega}\left(\frac{EA_o}{\ell}\right)\left(\frac{g}{f}\right)^p \frac{\pi f\beta}{2}\left[-\frac{2}{\pi\beta}\frac{1}{\sqrt{gf}}\sin\beta\right]$$

$$T_{12} \xrightarrow[o]{\xi} -\frac{1}{i\omega}\left(\frac{EA_o}{\ell}\right)\beta\sin\beta \quad . \qquad \text{(B.17)}$$

For the sign convention and form of state vector used here, Pestel[10]

gives for the uniform rod:

$$T_{12}(\text{uniform rod}) = -\frac{1}{i\omega}\left(\frac{EA_o}{\ell}\right)\beta \sin\beta$$

which agrees exactly with the limiting value obtained above. The same procedure has been used to extend $T_{11}(\ell)$, $T_{21}(\ell)$, and $T_{22}(\ell)$ to the limiting case which also resulted in expressions identical to those for the uniform rod.

$$T_{11}(\ell) \xrightarrow[o]{\xi} \cos\beta$$

$$T_{21}(\ell) \xrightarrow[o]{\xi} i\omega\left(\frac{\ell}{A_o E}\right)\frac{\sin\beta}{\beta}$$

$$T_{22}(\ell) \xrightarrow[o]{\xi} \cos\beta \quad .$$

Case II

$$A(x) = A_o(1+ax)^{2p-1} \qquad p \neq 0 \text{ or an integer}$$

Equations (B.9) and (B.10) apply here just as in Case I. However, the solutions for $T_{11}(\theta)$ and $T_{22}(\theta)$ now become:

$$T_{11}(\theta) = \theta^{1-p}\{\tilde{C}_1 J_{1-p}(\theta) + \tilde{C}_2 J_{p-1}(\theta)\} \tag{B.18}$$

$$T_{22}(\theta) = \theta^{p}\{C_1 J_p(\theta) + C_2 J_{-p}(\theta)\} \quad . \tag{B.19}$$

Imposing the same initial conditions as before gives:

$$\tilde{C}_1 = \frac{\alpha^{p-1}J_p(\alpha)}{\tilde{U}}$$

$$\tilde{C}_2 = \frac{\alpha^{p-1} J_{-p}(\alpha)}{\tilde{U}}$$

$$C_1 = \frac{\alpha^{-p} J_{1-p}(\alpha)}{U}$$

$$C_2 = \frac{\alpha^{-p} J_{p-1}(\alpha)}{U}$$

where:

$$\tilde{U} = J_{1-p}(\alpha)J_p(\alpha)+J_{-p}(\alpha)J_{p-1}(\alpha)$$

and

$$U = J_p(\alpha)J_{1-p}(\alpha)+J_{p-1}(\alpha)J_{-p}(\alpha) \quad .$$

It can also be shown that

$$\tilde{U} = U = \left(\frac{2}{\pi\alpha}\right) \sin(p\pi) \quad ;$$

and if

$$p = n/2 \, , \; \tilde{U} = U = (-1)^n \frac{2}{\pi\alpha} \quad .$$

Therefore, the solutions for $T_{11}(\theta)$ and $T_{22}(\theta)$ become:

$$T_{11}(\theta) = \left(\frac{\theta}{\alpha}\right)^{1-p} \frac{1}{\tilde{U}} \{J_p(\alpha)J_{1-p}(\theta)+J_{-p}(\alpha)J_{p-1}(\theta)\} \qquad \text{(B.20)}$$

$$T_{22}(\theta) = \left(\frac{\theta}{\alpha}\right)^{p} \frac{1}{U} \{J_{1-p}(\alpha)J_p(\theta)+J_{p-1}(\alpha)J_{-p}(\theta)\} \quad . \qquad \text{(B.21)}$$

Following the same approach as in Case I using Eqs. (B.1) and (B.4) gives:

$$T_{12}(\theta) = \frac{1}{\bar{Y}(\theta)} a\alpha \frac{dT_{11}(\theta)}{d\theta}$$

$$T_{21}(\theta) = \frac{1}{\bar{Z}(\theta)} a\alpha \frac{dT_{22}(\theta)}{d\theta} \quad .$$

Hence,

$$T_{12}(\theta) = \frac{\beta}{i\omega}\left(\frac{EA_o}{\ell}\right)\left(\frac{\theta}{\alpha}\right)^p \frac{1}{U}\{J_p(\alpha)J_{-p}(\theta)-J_{-p}(\alpha)J_p(\theta)\} \qquad (B.22)$$

$$T_{21}(\theta) = -\frac{i\omega}{\beta}\left(\frac{\ell}{A_o E}\right)\left(\frac{\theta}{\alpha}\right)^{1-p} \frac{1}{U}\{J_{1-p}(\alpha)J_{p-1}(\theta)-J_{p-1}(\alpha)J_{1-p}(\theta)\} \; . \qquad (B.23)$$

Using the large agrument expansions, as in Case I, in Eqs. (B.20), (B.21), (B.22), and (B.23) for the limiting case again gives the uniform rod expressions for the T_{ij} elements in the limit.

Case III

$$A(x) = A_o e^{2(x/x_o)}$$

Equations (B.5) and (B.6) reduce in this case to the following second order differential equation with constant coefficients.

$$T''_{11}(x) + \left(\frac{2}{x_o}\right) T'_{11}(x) + \beta_1^2 T_{11}(x) = 0 \qquad (B.24)$$

$$T''_{22}(x) - \left(\frac{2}{x_o}\right) T'_{22}(x) + \beta_1^2 T_{22}(x) = 0 \quad . \qquad (B.25)$$

Assuming exponential solutions gives:

$$T_{11}(x) = C_1 e^{d_1 x} + C_2 e^{d_2 x}$$

$$d_{1,2} = -x_o \pm i\sqrt{\beta_1^2 - 1/x_o^2} \quad . \tag{B.26}$$

Two solutions are possible from Eq. (B.26):

1. $\beta_1^2 < 1/x_o^2 \sim$ non-oscillatory hyperbolic functions
2. $\beta_1^2 > 1/x_o^2 \sim$ oscillatory trigonometric functions.

The solution of interest here is the second; hence,

$$T_{11}(x) = e^{-x/x_o}\{E_1 \cos \gamma x + E_2 \sin \gamma x\}$$

$$T_{22}(x) = e^{x/x_o}\{\tilde{E}_1 \cos \gamma x + \tilde{E}_2 \sin \gamma x\} \quad .$$

Using the same initial conditions as before gives:

$$E_1 = 1 \quad , \qquad E_2 = 1/x_o\gamma \quad ;$$

$$\tilde{E}_1 = 1 \quad , \quad \text{and} \quad \tilde{E}_2 = -1/x_o\gamma \quad .$$

Using the above constants and Eqs. (B.1) and (B.4), all four T_{ij} elements can be determined.

$$T_{11}(x) = e^{-x/x_o}\left(\cos(\gamma x) + \frac{1}{\gamma x_o}\sin(\gamma x)\right) \tag{B.27}$$

$$T_{12}(x) = -\frac{e^{x/x_o}}{i\omega}\left(EA_o\right)\left(\frac{\beta_1^2}{\gamma}\right)\sin(\gamma x) \tag{B.28}$$

$$T_{21}(x) = -\frac{e^{-x/x_o}}{i\omega}\left(\frac{\beta_1^2}{\rho A_o \gamma}\right)\sin(\gamma x) \tag{B.29}$$

$$T_{22}(x) = e^{x/x_o}\left[\cos(\gamma x) - \frac{1}{\gamma x_o}\sin(\gamma x)\right] \qquad (B.30)$$

where

$$\gamma = \sqrt{\beta_1^2 - 1/x_o^2} \quad .$$

To take this system to the limiting case of the uniform rod requires $x_o \to \infty$. Imposing this limit gives,

$$x_o \to \infty \ , \quad \gamma \to \beta_1 \ , \quad A(x) = A_o \quad ,$$

and

$$T_{11}(\ell) \xrightarrow[\infty]{x_o} \cos\beta$$

$$T_{12}(\ell) \xrightarrow[\infty]{x_o} -\frac{1}{i\omega}\left(\frac{A_o E}{\ell}\right)\beta\sin\beta$$

$$T_{21}(\ell) \xrightarrow[\infty]{x_o} i\omega\left(\frac{\ell}{A_o E}\right)\frac{\sin\beta}{\beta}$$

$$T_{22}(\ell) \xrightarrow[\infty]{x_o} \cos\beta \quad .$$

These expressions also agree with those for the uniform rod.

APPENDIX C

DERIVATION OF SPRING CONSTANTS FOR LINEARLY TAPERED SEGMENTS (ONE DIMENSIONAL SYSTEMS)

In the following, spring constants are found for the linearly tapered segments belonging to Groups I and II which are described in Chapter III.

Summing forces on the dx element in Fig. C.1 gives:

$$\frac{\partial}{\partial x}\left[\frac{\partial u}{\partial x}\,EA(x)\right] = 0 \qquad \text{(C.1)}$$

where:

$A(x) = A_o(1+ax)^2$ for Group I ,

$A(x) = A_o(1+ax)$ for Group II, and

u = displacement.

Because u and A(x) are functions only of x $\frac{\partial}{\partial x} \longrightarrow \frac{d}{dx}$ and Eq. (C.1) becomes:

$$\frac{du}{dx}\,EA(x) = C_1 \text{ (a constant)} \quad .$$

Using the coordinate transformation $Z = (1+ax)$ gives:

$$\frac{d}{dx} = a\,\frac{d}{dZ}$$

$$\therefore \quad aZ^2\,\frac{du}{dZ} = \frac{C_1}{EA_o} \quad \text{for Group I} \qquad \text{(C.2)}$$

$$aZ\,\frac{du}{dZ} = \frac{\tilde{C}_1}{EA_o} \quad \text{for Group II} \quad . \tag{C.3}$$

Solving Eqs. (C.2) and (C.3) for $u(Z)$ gives:

$$u(Z) = -\left(\frac{\ell}{EA_o}\right)\frac{C_1}{\xi Z} + C_2 \quad \text{for Group I} \tag{C.4}$$

and

$$u(Z) = \left(\frac{\ell}{EA_o}\right)\frac{\tilde{C}_1}{\xi}\,\ell n(Z) + \tilde{C}_2 \quad \text{for Group II} \quad . \tag{C.5}$$

For a force, F_o, applied to an element of length ℓ, appropriate boundary conditions at $x = 0$ and $x = \ell$ are:

$$-\frac{du(0)}{dx}\,EA_o = F_o \tag{C.6}$$

$$u(\ell) = 0 \quad .$$

Applying the boundary conditions to Eqs. (C.4) and (C.5) and finding the displacement $u(0)$ at $x = 0$ gives:

$$\delta = u(0) = F_o\left(\frac{\ell}{EA_o}\right)\frac{1}{1+\xi} \quad \text{for Group I} \tag{C.7}$$

$$\delta = u(0) = \frac{F_o}{\xi}\left(\frac{\ell}{EA_o}\right)\ell n(1+\xi) \quad \text{for Group II} \quad . \tag{C.8}$$

Hence, the spring constants, $k = F_o/\delta$, are:

$$k = \left(\frac{A_o E}{\ell}\right)(1+\xi) \quad \text{for Group I} \tag{C.9}$$

$$k = \left(\frac{A_o E}{\ell}\right)\frac{\xi}{\ell n(1+\xi)} \quad \text{for Group II.} \tag{C.10}$$

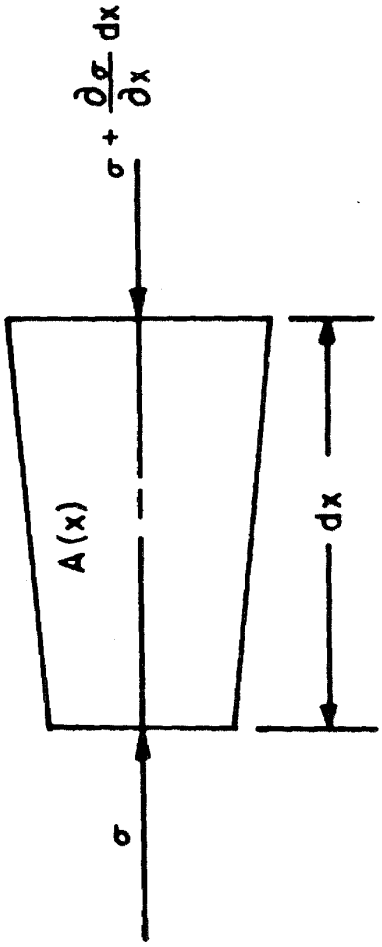

ELASTIC NON-UNIFORM ROD INCREMENT

FIG. C.1

APPENDIX D

DERIVATION OF TRANSMISSION MATRICES FOR NON-UNIFORM CONTINUOUS BEAMS

Assumptions (see Figure D.1):

1. Shear deflection and rotatory inertia effects are small and negligible, i.e., Bernoulli-Euler beam.
2. ρ and E are assumed to be constants.
3. Area, $A(x)$, and stiffness, $EI(x)$, are variables.

The differential equation for the state vector is:

$$\frac{d}{dx}\{\psi(x)\} = [A(x)]\{\psi(x)\} \quad . \tag{D.1}$$

Summing forces on the dx increment gives(see Figure D.1):

$$V - V - \frac{\partial V}{\partial x}\,dx + \rho A(x)\omega^2 w\,dx = 0$$

$$\therefore \quad \frac{dV}{dx} = \rho A(x)\omega^2 w \quad .$$

Summing moments on the increment gives:

$$M + \rho A(x)\omega^2 w\,dx\left(\frac{dx}{2}\right) - M - \frac{\partial M}{\partial x}\,dx + V\,dx + \frac{\partial V}{\partial x}(dx)^2 = 0$$

and neglecting $O(dx)^2$ terms reduces this to:

$$\frac{dM}{dx} = V \quad .$$

By definition:

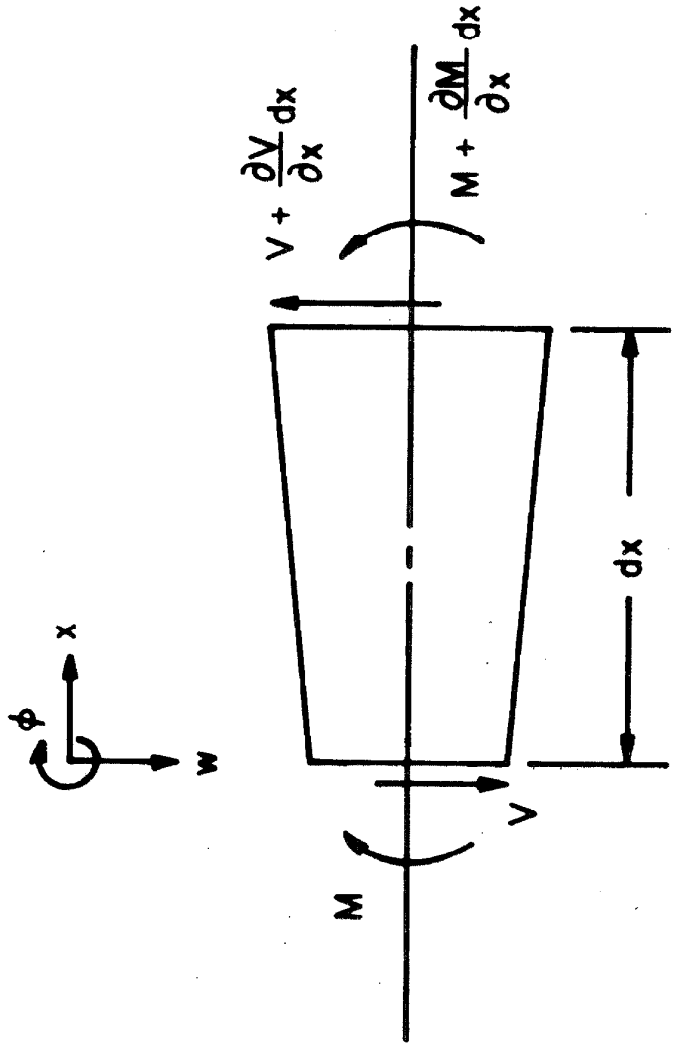

ELASTIC BEAM INCREMENT

FIG. D.1

$$\frac{dw}{dx} = \phi \quad , \quad \frac{d^2w}{dx^2} = \frac{d\phi}{dx} \quad , \quad EI(x)\ \frac{d^2w}{dx^2} = -M$$

$$\therefore \quad \frac{d\phi}{dx} = -\ \frac{M}{EI(x)} \quad .$$

Casting these terms into the form of Eq. (D.1) gives:

$$\frac{d}{dx}\{\psi(x)\} = \begin{bmatrix} 0 & 0 & +\rho A(x)\omega^2 & 0 \\ -1 & 0 & 0 & 0 \\ 0 & 0 & 0 & +1 \\ 0 & -1/EI(x) & 0 & 0 \end{bmatrix} \{\psi(x)\}$$

where:

$$\{\psi(x)\} = \begin{Bmatrix} V \\ M \\ w \\ \phi \end{Bmatrix} \quad .$$

Using the notation $\overline{Z}(x) = \rho A(x)\omega^2$ and $\overline{Y}(x) = 1/EI(x)$ reduces the governing $[A]$ matrix for the beam to:

$$[A] = \begin{bmatrix} 0 & 0 & \overline{Z}(x) & 0 \\ -1 & 0 & 0 & 0 \\ 0 & 0 & 0 & 1 \\ 0 & -\overline{Y}(x) & 0 & 0 \end{bmatrix} \quad . \qquad (D.2)$$

Expanding the differential equation which defines the transmission matrix, $\frac{d}{dx}[T] = -[T][A(x)]$, gives four sets of equations of the following form:

$$\left.\begin{aligned} T'_{i1} &= -T_{i2} \\ T'_{i2} &= -T_{i4}\,\bar{Y}(x) \\ T'_{i3} &= T_{i1}\,\bar{Z}(x) \\ T'_{i4} &= T_{i3} \end{aligned}\right\} \quad (D.3)$$

where $i = 1, 2, 3, 4$ and T'_{ij} denotes $\frac{dT_{ij}}{dx}$. The necessary initial conditions are:

$$\left.\begin{aligned} &[T(0)] = I \quad , \text{ the unity matrix} \\ &[T'(0)] = -[A(0)] \\ &[T''(0)] = -[A(0)]^2 - [A'(0)] \\ &[T'''(0)] = -[A(0)]^3 + [A'(0)][A(0)] + 2[A(0)][A'(0)] - [A''(0)] \end{aligned}\right\} \quad (D.4)$$

Using higher derivatives and rearranging terms in expressions (D.3) gives:

$$T''''_{i1} - 2\left(\frac{\bar{Y}'}{\bar{Y}}\right)T'''_{i1} - \left[2\left(\frac{\bar{Y}'}{\bar{Y}}\right)^2 - \left(\frac{\bar{Y}''}{\bar{Y}}\right)\right] T''_{i1} - \bar{Z}\bar{Y}\, T_{i1} = 0 \quad .$$

Substituting for $\bar{Y}(x)$ and $\bar{Z}(x)$ gives one general fourth-order differential equation for $T_{i1}(x)$ as follows:

$$T''''_{i1} + \frac{2(EI(x))'}{EI(x)}\, T'''_{i1} + \frac{(EI(x))''}{EI(x)}\, T''_{i1} - \frac{\rho A(x)\omega^2}{EI(x)}\, T_{i1} = 0 \quad . \quad (D.5)$$

In Chapter IV Eq. (D.5) has been rewritten as a product of two second-order differential operators with a coordinate transformation.

These operators are given in Eqs. (4.2.19) and (4.2.20) and the resulting solutions for $T_{i1}(z)$ are:

Case 1 $\qquad n = 0$ or an integer

$$T_{i1}(z) = z^{-n/2}\{C_1^i J_n(\kappa)+C_2^i Y_n(\kappa) + C_3^i I_n(\kappa)+C_4^i K_n(\kappa)\} \quad . \qquad (D.6)$$

Case 2 $\qquad n \neq$ an integer

$$T_{i1}(z) = z^{-n/2}\{C_1^i J_n(\kappa)+C_2^i J_{-n}(\kappa)+C_3^i I_n(\kappa)+C_4^i I_{-n}(\kappa)\} \qquad (D.7)$$

where:

$$\rho A = \rho A_o (z)^n$$

$$EI = EI_o (z)^{n+2}$$

$$\kappa = \mu z^{\frac{1}{2}} = 2\omega^{\frac{1}{2}} \left(\frac{\ell}{\xi}\right)\left[\frac{\rho A_o}{EI_o}\right]^{\frac{1}{4}} z^{\frac{1}{2}}$$

$$z = \left(1+ \frac{\xi x}{\ell}\right) \quad \text{and} \quad \frac{d}{dx} = \frac{\xi}{\ell}\frac{d}{dx} \quad .$$

The transmission matrix will be derived only for Case One in the following; however, Case Two follows by using the same procedures. An additional coordinate transformation, $y = z^{\frac{1}{2}}$, is required to make the variable in the arguments of the Bessel functions in Eq. (D.6) be of the first power; thus, allowing standard recurrence relationships to be used in taking derivatives of T_{i1}. Changing Eq. (D.6) gives:

$$T_{i_1}(y) = y^{-n}\{C_1^i J_n(\mu y)+C_2^i Y_n(\mu y)+C_3^i I_n(\mu y)+C_4^i (\mu y)\} \quad . \qquad (D.8)$$

Taking derivatives of T_{i1} for application of initial conditions gives:

$$\frac{dT_{i1}}{dz} = \frac{1}{2y}\frac{dT_{i1}}{dy} \quad ; \quad \frac{d^2T_{i1}}{dz^2} = \frac{1}{2y}\left[\frac{d}{dy}\left(\frac{1}{2y}\frac{dT_{i1}}{dy}\right)\right]$$

and

$$\frac{d^3T_{i1}}{dz^3} = \frac{1}{2y}\left[\frac{d}{dy}\left(\frac{d^2T_{i1}}{dz^2}\right)\right] .$$

Applying these to Eq. (D.8) gives:

$$\left.\begin{aligned}
T_{i1}(1) &= C_1^i J_n(\mu)+C_2^i Y_n(\mu)+C_3^i I_n(\mu)+C_4^i K_n(\mu) \\
\frac{2}{\mu}\frac{dT_{i1}(1)}{dz} &= -\{C_1^i J_{n+1}(\mu)+C_2^i Y_{n+1}(\mu)-C_3^i I_{n+1}(\mu)+C_4^i K_{n+1}(\mu)\} \\
\left(\frac{2}{\mu}\right)^2\frac{d^2T_{i1}(1)}{dz^2} &= \{C_1^i J_{n+2}(\mu)+C_2^i Y_{n+2}(\mu)+C_3^i I_{n+2}(\mu)+C_4^i K_{n+2}(\mu)\} \\
\left(\frac{2}{\mu}\right)^3\frac{d^3T_{i1}(1)}{dz^3} &= -\{C_1^i J_{n+3}(\mu)+C_2^i Y_{n+3}(\mu)-C_3^i I_{n+3}(\mu)+C_4^i K_{n+3}(\mu) .
\end{aligned}\right\} \quad (D.9)$$

The initial conditions for $T_{i1}(z)$ and derivatives of $T_{i1}(z)$ at $z = 1$ or $x = 0$ are evaluated by using expressions (D.4) and the values of $[A(0)]$, $[A(0)]^2$, $[A(0)]^3$, $\frac{d}{dz}[A(0)]$, and $\frac{d^2}{dz^2}[A(0)]$ which are obtained from expression (D.2). Upon evaluation, the initial conditions become:

$$\{v^1\} = \begin{Bmatrix} 1 \\ 0 \\ 0 \\ 0 \end{Bmatrix} \qquad \{v^2\} = \begin{Bmatrix} 0 \\ \frac{2}{\mu}\frac{\ell}{\xi} \\ 0 \\ 0 \end{Bmatrix}$$

$$\{v^3\} = \begin{Bmatrix} 0 \\ 0 \\ 0 \\ -\left(\frac{2\ell}{\mu\xi}\right)^3 \overline{Y}_o \end{Bmatrix} \qquad \{v^4\} = \begin{Bmatrix} 0 \\ 0 \\ \left(\frac{2\ell}{\mu\xi}\right)^2 \overline{Y}_o \\ -\left(\frac{\ell}{\xi}\right)^2 \left(\frac{2}{\mu}\right)^3 (n+2)\overline{Y}_o \end{Bmatrix}$$

where:

$$\overline{Y}_o = \frac{1}{EI_o} \quad ,$$

and

$$\{v^i\} = \begin{Bmatrix} T_{i_1}(1) \\ \frac{2}{\mu}\frac{dT_{i_1}(1)}{dz} \\ \left(\frac{2}{\mu}\right)^2 \frac{d^2T_{i_1}(1)}{dz^2} \\ \left(\frac{2}{\mu}\right)^3 \frac{d^3T_{i_1}(1)}{dz^3} \end{Bmatrix} \qquad \text{(D.10)}$$

Equating expressions (D.9) for the derivatives of $T_{i_1}(1)$ to the above expressions for $\{v^i\}$ determines the 16 constants

$(C_k^i;\ i,k = 1,2,3,4)$ required to define $T_{i1}(y)$. Abbreviating the above process by using matrix notation gives:

$$\{v^i\} = [B]\{C_k^i\} \tag{D.11}$$

Inspection of expression (D.9) shows:

$$[B] = \begin{bmatrix} J_n(\mu) & Y_n(\mu) & I_n(\mu) & K_n(\mu) \\ -J_{n+1}(\mu) & -Y_{n+1}(\mu) & I_{n+1}(\mu) & -K_{n+1}(\mu) \\ J_{n+2}(\mu) & Y_{n+2}(\mu) & I_{n+2}(\mu) & K_{n+2}(\mu) \\ -J_{n+3}(\mu) & -Y_{n+3}(\mu) & I_{n+3}(\mu) & -K_{n+3}(\mu) \end{bmatrix} . \tag{D.12}$$

Consequently, the constants C_k^i are given by:

$$\{C_k^i\} = [B]^{-1}\{v^i\} \tag{D.13}$$

or

$$C_k^i = \text{Det.} \begin{Vmatrix} B_{11} & \cdots & v_1^i & \cdots & B_{14} \\ \vdots & & \vdots & & \vdots \\ B_{41} & \cdots & v_4^i & \cdots & B_{44} \end{Vmatrix} \times \overline{B} \tag{D.14}$$

where the determinant in Eq. (D.14) has the i^{th} column replaced by

the column vector $\{v^i\}$ and $\overline{B} = 1/\det ||B||$.

Having determined the C_k^i constants, the remaining T_{ij} elements can be determined by using expressions (D.3) and Eq. (D.8) as follows:

$$T_{i1} = -\frac{d}{dx} T_{i1} = -\left(\frac{\xi}{\ell}\right)\frac{d}{dz} T_{i1} = \frac{\xi}{\ell}\left(\frac{1}{2y}\right)\frac{dT_{i1}}{dy}$$

$$\therefore T_{i2}(y) = -\left(\frac{\xi}{\ell}\right)\left(\frac{\mu}{2}\right) y^{-(n+1)} \{C_1^i J_{n+1}(\mu y)+C_2^i Y_{n+1}(\mu y)-C_3^i I_{n+1}(\mu y) + C_4^i K_{n+1}(\mu y)\} \qquad (D.15)$$

$$T_{i4} = -\frac{1}{\overline{Y}(x)}\frac{d}{dx} T_{i2} = \frac{1}{\overline{Y}(z)}\left(\frac{\xi}{\ell}\right)^2 \frac{d^2 T_{i1}}{dz^2} = \frac{1}{\overline{Y}(y)}\left(\frac{\xi}{\ell}\right)^2 \frac{1}{2y}\left[\frac{d}{dy}\left(\frac{1}{2y}\frac{dT_{i1}}{dy}\right)\right]$$

$$\therefore T_{i4}(y) = \frac{1}{\overline{Y}(y)}\left(\frac{\xi}{\ell}\frac{\mu}{2}\right)^2 y^{-(n+2)} \{C_1^i J_{n+2}(\mu y)+C_2^i Y_{n+2}(\mu y) + C_3^i I_{n+2}(\mu y)+C_4^i K_{n+2}(\mu y)\} \qquad (D.16)$$

$$T_{i3} = \frac{d}{dx} T_{i4} = -\left(\frac{\xi}{\ell}\right)^3\left[\frac{1}{\overline{Y}(z)}\frac{d^3 T_{i1}}{dz^3} - \frac{1}{\overline{Y}^2(z)}\frac{d\overline{Y}}{dz}\frac{d^2 T_{i1}}{dz^2}\right]$$

where:

$$\frac{d^2 T_{i1}}{dz^2} = \frac{1}{2y}\left[\frac{d}{dy}\left(\frac{1}{2y}\frac{dT_{i1}}{dy}\right)\right]$$

and

$$\frac{d^3 T_{i1}}{dz^3} = \frac{1}{2y}\left[\frac{d}{dy}\left(\frac{1}{2y}\frac{d^2 T_{i1}}{dz^2}\right)\right] .$$

Hence, the final expression for $T_{i3}(y)$ becomes:

$$T_{i3}(y) = \frac{1}{\bar{Y}_o}\left[\frac{\xi\mu}{2\ell}\right]^3 y^{(n+1)}\{A_1\} - \frac{(n+2)}{\bar{Y}_o}\left[\frac{\xi\mu}{2\ell}\right]^2\left[\frac{\xi}{\ell}\right] y^n\{A_2\} \qquad (D.17)$$

where:

$$A_1 = C_1^i J_{n+3}(\mu y)+C_2^i Y_{n+3}(\mu y)-C_3^i I_{n+3}(\mu y)+C_4^i K_{n+3}(\mu y)$$

$$A_2 = C_1^i J_{n+2}(\mu y)+C_2^i Y_{n+2}(\mu y)+C_3^i I_{n+2}(\mu y)+C_4^i K_{n+2}(\mu y) \quad .$$

The complete transmission matrix for the transverse bending beam element is given by the above expressions for $T_{ij}(y)$ and C_j^i where $i,j = 1, 2, 3, 4$.

To check the validity of the $T_{ij}(y)$ expressions the limiting condition of the uniform beam can be employed. For an element of length ℓ:

$$z = (1 + \xi) = (g/f)$$

$$y = (1+\xi)^{\frac{1}{2}} = \sqrt{g/f} \quad .$$

Consequently, when $\xi \to 0$ in the limit, which describes the uniform beam, the argument $\mu y \to \infty$ as:

$$\mu y\Big|_{y=\ell} \xrightarrow[0]{\xi} 2\omega^{\frac{1}{2}}(1+\xi)^{\frac{1}{2}}\left[\frac{\ell}{\xi}\right]\left[\frac{\rho A_o}{EI}\right]^{\frac{1}{4}} \longrightarrow \infty \quad .$$

Likewise,

$$\mu \xrightarrow[0]{\xi} 2\omega^{\frac{1}{2}}\left[\frac{\ell}{\xi}\right]\left[\frac{\rho A_o}{EI_o}\right]^{\frac{1}{4}} \longrightarrow \infty \quad .$$

The fact that μ and μy both tend to infinity as $\xi \to 0$ justifies the use of the following asymptotic expansions for J_n, Y_n, I_n, and K_n

which appear in the $T_{ij}(y)$ and C^i_j expressions.

$$J_n(x) \approx \sqrt{\frac{2}{\pi x}} \cos\left(x - \pi/4 - \frac{n\pi}{2}\right)$$

$$Y_n(x) \approx \sqrt{\frac{2}{\pi x}} \sin\left(x - \pi/4 - \frac{n\pi}{2}\right)$$

$$I_n(x) \approx \frac{e^x}{\sqrt{2\pi x}} \quad \text{and} \quad K_n \approx \sqrt{\frac{\pi}{2x}}\, e^{-x} \quad .$$

Using the above expressions and checking $T_{43}(\ell)$ from Eq. (D.17), which checks all the basic steps in the derivation because of the ordering in expression (D.3), as $\xi \to 0$ gives:

$$\begin{aligned} T_{43}(\ell) \xrightarrow[0]{\xi} \quad & C^4_1\{b_1 J_{n+3} - b_2 J_{n+2}\} + \\ & C^4_2\{b_1 Y_{n+3} - b_2 Y_{n+2}\} - \\ & C^4_3\{b_1 I_{n+3} + b_2 I_{n+2}\} + \\ & C^4_4\{b_1 K_{n+3} - b_2 K_{n+2}\} \end{aligned} \tag{D.18}$$

where:

$$b_1 = \left(\frac{\Omega}{\ell}\right)^3 \frac{1}{\bar{Y}_o} \quad , \quad b_2 = \frac{(n+2)}{\bar{Y}_o}\left(\frac{\xi}{\ell}\right)\left(\frac{\Omega}{\ell}\right)^2 \quad , \quad \Omega = \frac{\xi}{2}\,\mu$$

and the undesignated argument of the Bessel functions in Eq. (D.18) is:

$$\bar{\mu} = 2\omega^{\frac{1}{2}}(1+\xi)^{\frac{1}{2}}\left(\frac{\ell}{\xi}\right)\left[\frac{\rho A_o}{EI_o}\right]^{\frac{1}{4}} \quad . \tag{D.19}$$

The constants C_k^4 are evaluated from Eq. (D.14) and as $\xi \to 0$ they reduce to:

$$C_1^4 = \frac{\overline{B}}{\mu}\{a_1(Y_{n+3} - Y_{n+1}) + a_2(Y_{n+2} + Y_n)\}$$

$$C_2^4 = -\frac{\overline{B}}{4\mu}\{a_1(J_{n+3} - J_{n+1}) + a_2(J_{n+2} - J_n)\}$$

$$C_3^4 = -\frac{2\overline{B}}{\pi\mu}\{a_1(K_{n+3} + K_{n+1}) + a_2(K_{n+2} + K_n)\}$$

$$C_4^4 = -\frac{2\overline{B}}{\pi\mu}\{a_1(I_{n+3} + I_{n+1}) - a_2(I_n + I_{n+2})\}$$

where:

$$\overline{B} \xrightarrow[0]{\xi} -\frac{\pi\mu^2}{8} \qquad a_1 = \left(\frac{\ell}{\Omega}\right)^2 \overline{Y}_o \quad , \quad a_2 = \left(\frac{\xi}{\ell}\right)\left(\frac{\ell}{\Omega}\right)^3 (n+2)\overline{Y}_o$$

and the undesignated argument in the Bessel functions for the constants C_k^4 is:

$$\mu = 2\omega^{\frac{1}{2}}\left(\frac{\ell}{\xi}\right)\left[\frac{\rho A_o}{EI_o}\right]^{\frac{1}{4}} \quad . \tag{D.20}$$

Substituting the expressions for constants C_k^4 into Eq. (D.18) gives the following:

$$\frac{\mu}{\overline{B}} T_{43}(\ell) \xrightarrow[0]{\xi} \sum_{m=1}^{16} d_m$$

where:

$$d_1 = a_1 b_1 J_{n+3}(\bar{\mu}) \{Y_{n+3} - Y_{n+1}\}$$

$$d_2 = a_2 b_1 J_{n+3}(\bar{\mu}) \{Y_{n+2} - Y_n\}$$

$$d_3 = -a_1 b_2 J_{n+2}(\bar{\mu}) \{Y_{n+3} - Y_{n+1}\}$$

$$d_4 = -a_2 b_2 J_{n+2}(\bar{\mu}) \{Y_{n+2} - Y_n\}$$

$$d_5 = -a_1 b_1 Y_{n+3}(\bar{\mu}) \{J_{n+3} - J_{n+1}\}$$

$$d_6 = -a_2 b_1 Y_{n+3}(\bar{\mu}) \{J_{n+2} - J_n\}$$

$$d_7 = a_1 b_2 Y_{n+2}(\bar{\mu}) \{J_{n+3} - J_{n+1}\}$$

$$d_8 = a_2 b_2 Y_{n+2}(\bar{\mu}) \{J_{n+2} - J_n\}$$

$$d_9 = \frac{2}{\pi} a_1 b_1 I_{n+3}(\bar{\mu}) \{K_{n+3} + K_{n+1}\}$$

$$d_{10} = \frac{2}{\pi} a_2 b_1 I_{n+3}(\bar{\mu}) \{K_{n+2} + K_n\}$$

$$d_{11} = \frac{2}{\pi} a_1 b_2 I_{n+2}(\bar{\mu}) \{K_{n+3} + K_{n+1}\}$$

$$d_{12} = \frac{2}{\pi} a_2 b_2 I_{n+2}(\bar{\mu}) \{K_{n+2} + K_n\}$$

$$d_{13} = -\frac{2}{\pi} a_1 b_1 K_{n+3}(\bar{\mu}) \{I_{n+3} + I_{n+1}\}$$

$$d_{14} = \frac{2}{\pi} a_2 b_1 K_{n+3}(\bar{\mu}) \{I_{n+2} + I_n\}$$

$$d_{15} = \frac{2}{\pi} a_1 b_2 K_{n+2}(\bar{\mu}) \{I_{n+3} + I_{n+1}\}$$

$$d_{16} = -\frac{2}{\pi} a_2 b_2 K_{n+2}(\bar{\mu}) \{I_{n+2} + I_n\}$$

and the undesignated arguments are μ. From the asymptotic expansions

for I_n and K_n:

$$K_{n+k}(\bar{\mu})\ \{I_{n+i}(\mu) + I_{n+j}(\mu)\} \xrightarrow[0]{\xi} \frac{}{\sqrt{\bar{\mu}\mu}}\ e^{+(\mu-\bar{\mu})}$$

and

$$I_{n+k}(\bar{\mu})\ \{K_{n+i}(\mu) + K_{n+j}(\mu)\} \xrightarrow[0]{\xi} \frac{1}{\sqrt{\bar{\mu}\mu}}\ e^{-(\mu-\bar{\mu})} \quad .$$

These results are independent of the dummy subscripts i, j, and k. Therefore the last 8 terms in the previous expression for $T_{43}(\ell)$ can be reduced to :

$$A_4 = \frac{4}{\pi}\frac{1}{\sqrt{\bar{\mu}\mu}}\left(\frac{\Omega}{\ell}\ \sinh\Omega\right) \quad . \tag{D.21}$$

Expanding the first 8 terms of $T_{43}(\ell)$ into trigonometric terms by using the asymptotic expansions for J_n and Y_n and reducing for $\xi \to 0$ gives:

$$A_3 = -\frac{4}{\pi}\frac{1}{\sqrt{\mu\bar{\mu}}}\left(\frac{\Omega}{\ell}\ \sin\Omega\right) \quad .$$

Hence, the final result is:

$$T_{43}(\ell) \xrightarrow[0]{\xi} \frac{\bar{B}}{\mu}\,[A_3 + A_4] \longrightarrow -\frac{1}{2}\,\frac{\Omega}{\ell}\,[\sinh\Omega - \sin\Omega] \quad . \tag{D.22}$$

For the uniform beam with the sign convention used herein, the transmission matrix is known to be[13]:

$$[E]= \begin{bmatrix} C_o & \frac{\Omega}{\ell} C_3 & -\left(\frac{\Omega}{\ell}\right)^3 \bar{Y}_o C_1 & \left(\frac{\Omega}{\ell}\right)^2 \bar{Y}_o C_2 \\ \frac{\ell}{\Omega} C_1 & C_o & -\left(\frac{\Omega}{\ell}\right)^2 \bar{Y}_o C_2 & \frac{\Omega}{\ell} C_3 \bar{Y}_o \\ -\left(\frac{\ell}{\Omega}\right)^3 \frac{1}{\bar{Y}_o} C_3 & -\left(\frac{\ell}{\Omega}\right)^2 \frac{C_2}{\bar{Y}_o} & C_o & -\frac{\ell}{\Omega} C_1 \\ \left(\frac{\ell}{\Omega}\right)^2 \frac{1}{\bar{Y}_o} C_2 & \frac{\ell}{\Omega} \frac{C_1}{\bar{Y}_o} & -\frac{\Omega}{\ell} C_3 & C_o \end{bmatrix} \qquad (D.23)$$

where:

$$C_o = \frac{1}{2}[\cos\Omega + \cosh\Omega]$$

$$C_1 = \frac{1}{2}[\sin\Omega + \sinh\Omega]$$

$$C_2 = \frac{1}{2}[\cosh\Omega - \cos\Omega]$$

$$C_3 = \frac{1}{2}[\sinh\Omega - \sin\Omega]$$

and

$$\Omega = \omega^{\frac{1}{2}} \ell \left[\frac{\rho A_o}{EI_o}\right]^{\frac{1}{4}} .$$

Therefore, the $E_{43}(\ell)$ term for the uniform beam agrees exactly with the limiting case of $T_{43}(\ell)\Big|_{\xi \to o}$ as given in Eq. (D.22). Other terms, not recorded here, have been reduced and they also check with the

uniform case in the limit.

REFERENCES

1. Lagrange, J. L., Mechanique Analytique, (1788).

2. Strutt, J. W., Baron Rayleigh, The Theory of Sound, Volume I; 2d ed. rev.; Dover Publications, New York, 1945, pp. 172-177.

3. Duncan, W. J., "A Critical Examination of the Representation of Massive and Elastic Bodies by Rigid Masses Elastically Connected," Quarterly Journal of Mechanics and Applied Mathematics, Vol. 5 (1952), pp. 97-108.

4. Livesley, R. K., "The Equivalence of Continuous and Discrete Mass Distributions in Certain Vibration Problems," Quarterly Journal of Mechanics and Applied Mathematics, Vol. 8 (1955), pp. 353-360.

5. Gladwell, G. M. L., "The Approximation of Uniform Beams in Transverse Vibration by Sets of Masses Elastically Connected," Proceedings, 4th U. S. National Congress of Applied Mechanics (A.S.M.E. 1962), pp. 169-176.

6. Leckie, F. A. and Lindberg, G. M., "The Effect of Lumped Parameters on Beam Frequencies," Aeronautical Quarterly, Vol. 14 (1963), pp. 224-240.

7. Wen, R. D., "Dynamic Response of Beams with Lumped Parameters," Journal of Applied Mechanics, Trans. A.S.M.E., June 1965, pp. 453-454.

8. Fowler, J., "Accuracy of Lumped System Approximations for Lateral Vibrations of a Free-Free Uniform Beam," Report No. EM 9-12, Engineering Mechanics Department, Space Technology Laboratories, Inc., Los Angeles, Calif., July, 1959.

9. Molloy, C. T., "Four Pole Parameters in Vibration Analysis," Colloquim on Mechanical Impedance Methods for Mechanical Vibrations, Edited by R. Plunket, Applied Mechanics Division A.S.M.E. (Shock and Vibration Committee) (1958), pp. 43-68.

10. Pestel, E. C. and Leckie, F. A., Matrix Methods in Elastomechanics, McGraw-Hill Book Company, Inc., New York (1963), pp. 51-152.

11. Rubin, S., "Transmission Matrices for Vibration and Their Relation to Admittance and Impedance," Journal of Engineering of Industry, Trans. A.S.M.E., Vol. 86 (1964), Series B, Number 1, pp. 9-21.

12. Rubin, S., "Longitudinal Instability of Liquid Rockets Due to Propulsion Feedback (POGO)," A.I.A.A. Symposium on Structural Dynamics and Aeroelasticity, Boston, Mass., Aug. 30, 1965, pp. 543-554.

13. Rubin, S., "On the Use of Eight-Pole Parameters for the Analysis of Beam Systems," SAE Paper No. 925F, National Aeronautic and Space Engineering and Manufacturing Meeting, Los Angeles, Calif., October, 1964.

14. Rubin, S., "Unpublished Notes on Transmission Matrices," 1965.

15. Pipes, L. A., "The Matrix Theory of Four Terminal Networks," Philosophical Magazine, Vol. 30 (1940), p. 370.

16. Pipes, L.A., "Direct Computation of Transmission Matrices of Electrical Transmission Lines," Unpublished Notes at Aerospace Corporation, El Segundo, Calif., 1965.

17. Pipes, L.A., Matrix Methods for Engineering, Prentice-Hall, Inc., Englewood Cliffs, N. J. (1963), pp. 337-364.

18. Bishop, R.E.D., Gladwell, G.M. L., and Michaelson, S., The Matrix Analysis of Vibration, Cambridge University Press, London (1965), pp. 212-224.

19. Frazer, R. A., Duncan, W. J., and Collar, A. R., Elementary Matrices, Cambridge University Press, London (1938), pp. 70-73.

20. Hildebrand, F. B., Introduction to Numerical Analysis, McGraw-Hill Book Company, Inc., New York (1956), pp. 49.

21. Lindberg, G. M., "Vibration of Non-Uniform Beams," Aeronautical Quarterly, Vol. 14 (1963), pp. 387-395.

22. Archer, J. S., "Consistent Mass Matrix for Distributed Mass Systems," Journal of the Structural Division, A.S.C.E., Vol. 89, No. ST4, Aug., 1963, pp. 161-178.

23. Cranch, E. T. and Adler, A. A., "Bending Vibration of Variable Section Beams," Journal of Applied Mechanics, Trans. A.S.M.E., Vol. 78 (1956), pp. 103-108.

24. von Karman, T. and Biot, M. A., Mathematical Methods in Engineering, McGraw-Hill Book Company, Inc., New York (1940), pp. 66.

25. Morse, P. M., Vibration and Sound, 2d ed., McGraw-Hill Book Company, Inc., New York (1948), pp. 217-222.

26. U.S., National Bureau of Standards, Handbook of Mathematical Functions, edited by M. Abramowitz and I. A. Stegun, A.M.S. 55 (1965) pp. 360.

27. Pipes, L. A., "Matrix Treatment of Waves in Mechanical Systems," S.A.E. Paper No. 650822, National Aeronautic and Space Engineering and Manufacturing Meeting, Los Angeles, Calif., October, 1965.

28. O'Kelly, M. E. J., "Vibration of Viscously Damped Linear Dynamic Systems," Ph.D. Thesis, California Institute of Technology (1964), pp. 200-210.

29. Housner, G. W. and Keightley, W. D., "Vibration of Linearly Tapered Cantilever Beams," Journal of the Engineering Mechanics Division, A. S. C. E., Vol. 88, No. EM2, April 1962, pp. 95-126.

30. Lanczos, C., Applied Analysis, Prentice Hall, Inc., Englewood Cliffs, N. J. (1961).

31. McCann, G. D. and Braham, H. S., "A Study of the Accuracy of Lumped Parameter and Analog Computer Representation of Cantilevered Beams Under Conditions of Static Stress and Dynamic Vibrations, "Technical Report No. 3, Contract No. AF 18(600)-669, Project No. R-354-30-1, California Institute of Technology, Pasadena, Calif., April, 1955.

32. Wylie, C. R., Jr., Advanced Engineering Mathematics, McGraw-Hill Book Company, Inc., New York (1960), pp. 345-357.

33. Marguerre, K., "Matrices of Transmission in Beam Problems," Chapter II of, Progress in Applied Mechanics, by Sneddon and Hill, John Wiley and Sons, Inc., New York (1960), Vol. 1, pp. 61-82.